

STUDY OF TETRAQUARK SPECTROSCOPY IN GROUP THEORY AND  
QUARK MODEL



A Thesis Submitted in Partial Fulfillment of the Requirements for the  
Degree of Doctor of Philosophy in Physics  
Suranaree University of Technology  
Academic Year 2021

การศึกษาสเปกโทรสโกปีของเตตระควาร์กในทฤษฎีกลุ่ม  
และแบบจำลองควาร์ก



วิทยานิพนธ์นี้เป็นส่วนหนึ่งของการศึกษาตามหลักสูตรปริญญาวิทยาศาสตรดุษฎีบัณฑิต  
สาขาวิชาฟิสิกส์  
มหาวิทยาลัยเทคโนโลยีสุรนารี  
ปีการศึกษา 2564

# STUDY OF TETRAQUARK SPECTROSCOPY IN GROUP THEORY AND QUARK MODEL

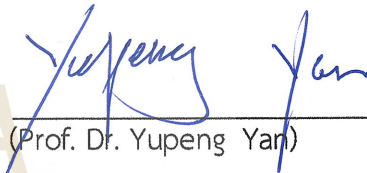
Suranaree University of Technology has approved this thesis submitted in partial fulfillment of the requirements for the Degree of Doctor of Philosophy.

Thesis Examining Committee



(Assoc. Prof. Dr. Panomsak Meemon)

Chairperson



(Prof. Dr. Yupeng Yan)

Member (Thesis Advisor)



(Asst. Prof. Dr. Ayut Limphirat)

Member (Thesis Co-advisor)



(Assoc. Prof. Dr. Sorakrai Srisuphaphon)

Member

*Member.*

(Asst. Prof. Dr. Khanchai Khosonthongkee)

Member



(Assoc. Prof. Dr. Chatchai Jothityangkoon)

Vice Rector for Academic Affairs  
and Quality Assurance



(Prof. Dr. Santi Maensiri)

Dean of Institute of Science

เจิ้ง จ้าว : การศึกษาสเปกโทรสโกปีของเตตระควาร์กในทฤษฎีกลุ่มและแบบจำลองควาร์ก (STUDY OF TETRAQUARK SPECTROSCOPY IN GROUP THEORY AND QUARK MODEL) อาจารย์ที่ปรึกษา : ศาสตราจารย์ ดร.ยูเบ็ง แยน, 71 หน้า

คำสำคัญ: ทฤษฎีกลุ่ม, แบบจำลองควาร์ก, เตตระควาร์ก

งานวิจัยนี้ได้ศึกษามวลของเตตระควาร์กที่มีองค์ประกอบควาร์กคล้ายชาร์โมเนียมและองค์ประกอบควาร์กที่เป็นควาร์กมวลเบาทั้งหมดในสถานะพื้นและสถานะกระตุ้นที่ 1 และศึกษามวลของเตตระควาร์กที่มีองค์ประกอบควาร์กเป็นควาร์กชาร์มทั้งหมดในสถานะพื้นและสถานะกระตุ้นเชิงรัศมีที่ 1 และ 2 ซึ่งในการคำนวณได้ใช้แบบจำลองควาร์กที่มีอันตรกิริยาจากศักย์คล้ายคอร์เนล การแลกเปลี่ยนกลูออนหนึ่งตัว และการคู่ควบระหว่างสปิน พารามิเตอร์ทั้งหมดที่ใช้ในการศึกษา เช่น พารามิเตอร์ในศักย์คล้ายคอร์เนล พารามิเตอร์ในการแลกเปลี่ยนกลูออนหนึ่งตัว พารามิเตอร์ในการคู่ควบสปิน เป็นต้น ได้กำหนดมาจากการศึกษาเมซอนมวลเบา เมซอนที่มีควาร์กชาร์ม และเมซอนที่มีควาร์กบอททอม

นอกจากนี้ได้ทำนายผลทางทฤษฎีของสถานะเตตระควาร์กและเปรียบเทียบกับข้อมูลของสถานะเมซอน โดยสถานะที่มีองค์ประกอบควาร์กคล้ายชาร์โมเนียมและควาร์กมวลเบาทั้งหมดจะเปรียบเทียบกับข้อมูลของสถานะ XYZ และสถานะเมซอนประหลาดชนิดไม่มีเพลเวอร์ตามลำดับ พร้อมทั้งระบุสถานะของอนุภาค โดยงานวิจัยนี้ได้เสนอว่าสถานะ X(6900) ซึ่งสังเกตพบโดย LHCb นั้นมีลักษณะอยู่ในสถานะกระตุ้นเชิงรัศมีที่ 1 และเป็นสถานะเตตระควาร์กที่มีองค์ประกอบเป็นชาร์มควาร์กทั้งหมด มีเลขควอนตัมคือ  $J=1$  และมีโครงสร้างส่วนสี่เป็นแอนติทริปเพิลท์-ทริปเพิลท์

สาขาวิชาฟิสิกส์

ปีการศึกษา 2564

ลายมือชื่อนักศึกษา

Zheng Zhao

ลายมือชื่ออาจารย์ที่ปรึกษา

Yupeng Yan

ลายมือชื่ออาจารย์ที่ปรึกษาร่วม

[Signature]

ZHENG ZHAO : STUDY OF TETRAQUARK SPECTROSCOPY IN GROUP THEORY  
AND QUARK MODEL. THESIS ADVISOR : PROF. YUPENG YAN, Ph.D. 71 PP.

Keyword: Group theory/ Quark model/ Tetraquark

The charmonium-like and fully-light tetraquark masses of the ground and first radial excited states, and the fully-charm tetraquark masses of ground, first and second radial excited states are evaluated in a constituent quark model where the Cornell-like potential and one-gluon exchange spin-spin coupling are employed. The three coupling parameters for the Cornell-like potential and one-gluon exchange spin-spin coupling are proposed mass-dependent, and all model parameters are predetermined by studying light, charmed and bottom mesons.

The theoretical predictions of the charmonium-like and fully-light tetraquarks are compared with the observed XYZ states and the observed exotic meson states in the light-unflavored meson sector respectively, and tentative assignments are suggested. The work suggests that the X(6900) observed by LHCb is likely to be the first radial excited fully-charm tetraquark state with  $J = 1$  in the color antitriplet-triplet configuration.



School of Physics  
Academic Year 2021

Student's Signature Zheng Zhao  
Advisor's Signature Yupeng Yan  
Co-Advisor's Signature [Signature]

## ACKNOWLEDGEMENTS

I would like to thank a lot of people for their encouragement, help, and support in helping me finish my Ph.D. studies.

First and foremost, I would want to express my gratitude to my thesis advisor Prof. Dr. Yupeng Yan, for his unwavering support, patient guidance, consideration, and assistance throughout the study. I would want to express my gratitude to Asst. Prof. Dr. Ayut Limphirat for all of his assistance and advice regarding my living and work.

I would like to express my gratitude to Assoc. Prof. Dr. Panomsak Meemon, Assoc. Prof. Dr. Sorakrai Srisuphaphon, and Asst. Prof. Dr. Khanchai Khosonthongkee for serving as my committee, despite the fact that we could only hold an online thesis exam due to the COVID-19 epidemic.

Then I would want to express my gratitude to my seniors, Dr. Kai Xu and Dr. Attaphon Kaewsnod, for all their assistance and suggestions on my calculations and programming. This work would not be possible without their assistance.

I would like to express my gratitude for the SUT-OROG Ph.D. scholarship under Contract No. 62/2559 of Suranaree University of Technology and Center of Excellence in High Energy Physics and Astrophysics (COE). Thank you also to our Suranaree University of Technology theoretical physics group, as well as the teachers and members of the group, for the great teachings, discussions, and ideas.

Last but not least, I would want to express my immense gratitude to my family for their continuous love, understanding, encouragement, and support throughout the progress and for giving me the motivation to complete my study.

Zheng Zhao

# CONTENTS

	Page
ABSTRACT IN THAI . . . . .	I
ABSTRACT IN ENGLISH . . . . .	II
ACKNOWLEDGEMENTS . . . . .	III
CONTENTS . . . . .	V
LIST OF TABLES . . . . .	VI
LIST OF FIGURES . . . . .	VII
<b>CHAPTER</b>	
<b>I INTRODUCTION . . . . .</b>	<b>1</b>
<b>II CONSTRUCTION OF TETRAQUARK WAVE FUNCTIONS . . . . .</b>	<b>13</b>
2.1 Tetraquark Color Wave Functions . . . . .	13
2.2 Spatial-spin-flavor configurations of tetraquark . . . . .	15
2.3 Spatial Wave Function . . . . .	17
<b>III THEORETICAL MODEL ESTABLISHMENT . . . . .</b>	<b>20</b>
3.1 Constituent quark model . . . . .	20
3.2 Fixing model parameters . . . . .	22
<b>IV PREDICTION OF TETRAQUARK MASSES . . . . .</b>	<b>25</b>
<b>V ASSIGNMENTS OF TETRAQUARK STATES . . . . .</b>	<b>28</b>
5.1 Tentative assignments of $qc\bar{q}\bar{c}$ tetraquark . . . . .	28
5.2 Tentative assignments of $qq\bar{q}\bar{q}$ tetraquark . . . . .	34
5.3 The first $cc\bar{c}\bar{c}$ tetraquark candidate: $X(6900)$ . . . . .	40
<b>VI CONCLUSIONS . . . . .</b>	<b>43</b>
REFERENCES . . . . .	45
<b>APPENDICES</b>	
APPENDIX A GROUP THEORY APPROACH . . . . .	60
APPENDIX B COLOR-SPIN WAVE FUNCTIONS . . . . .	62
APPENDIX C SPATIAL WAVE FUNCTION . . . . .	68
CURRICULUM VITAE . . . . .	71

## LIST OF TABLES

Table		Page
3.1	Spin-averaged masses $M_k^{ave}$ for various kinds of mesons. . . . .	20
3.2	Color matrix elements of tetraquarks. . . . .	22
3.3	Spin matrix elements of $qc\bar{q}\bar{c}$ and $qq\bar{q}\bar{q}$ tetraquark states. . . . .	22
3.4	Spin matrix elements of $cc\bar{c}\bar{c}$ tetraquark states. . . . .	23
3.5	Meson states applied to fit the model parameters. . . . .	23
4.1	1S and 2S $qc\bar{q}\bar{c}$ tetraquark masses. . . . .	25
4.2	1S and 2S $qq\bar{q}\bar{q}$ tetraquark masses. . . . .	26
4.3	1S, 2S, and 3S $cc\bar{c}\bar{c}$ tetraquark masses. . . . .	26
5.1	Masses, widths and $J^{PC}$ of $X$ and $Z_c$ states in the $c\bar{c}$ region. . . . .	29
5.2	Tentative assignments of 1S and 2S $qc\bar{q}\bar{c}$ tetraquark states. . . . .	30
5.3	Masses, widths and $J^{PC}$ of the $qq\bar{q}\bar{q}$ tetraquark candidates. . . . .	35
5.4	Tentative assignments of 1S and 2S $qq\bar{q}\bar{q}$ tetraquark states. . . . .	36
5.5	Present predictions of 1S state $cc\bar{c}\bar{c}$ tetraquark masses compared with others. . . . .	42
C.1	The complete bases of tetraquark with $N = 2n$ , $L = 0$ , and $N \leq 14$ . . . . .	68

## LIST OF FIGURES

Figure		Page
1.1	Charmonium meson spectrums include some XYZ states (Olsen, 2015). . . . .	2
1.2	Tentative $q\bar{q}$ mass spectrum for the three light quarks (Amsler and Tornqvist, 2004). . . . .	9
5.1	The distributions of $M_{max}[\pi^\pm\psi(2S)]$ from Belle (Wang et al., 2015). . . . .	32
5.2	The distributions of $M[\pi^\pm\psi(2S)]$ at $\sqrt{s} = 4.416$ GeV from BESIII (Ablikim et al., 2017a). . . . .	33
5.3	Invariant mass spectra of weighted di- $J/\psi$ candidates (Aaij et al., 2020). . . . .	41



# CHAPTER I

## INTRODUCTION

Over the last half-century, hundreds of hadrons have been observed while these established hadrons are classified as mesons and baryons easily by the naive quark model. In the past two decades, after the discovery of  $X(3872)$  in 2003 (Choi et al., 2003), over 20 charmonium-like and bottomonium-like  $XYZ$  states have been observed (Brambilla et al., 2020), which can not be classified by the naive quark model easily. Because of the observations of these  $XYZ$  states, the discovery of the underlying structures of the  $XYZ$  states has attracted the curiosity of many theorists. Instead of using the latest naming scheme suggested by Particle Data Group (PDG) (Zyla et al., 2020), throughout this thesis,  $X$  represents neutral states,  $Z_c$  represents charged states, and  $Y$  represents  $J^{PC} = 1^{--}$  states, for the convenience of referring to other works.

In Figure 1.1, some charmonium-like  $XYZ$  states are indicated as red and purple rectangles aligned, which do not match the expectations for the currently unassigned charmonium states (Olsen, 2015).

Obviously, the charged states observed in the charmonium meson mass region are beyond the conventional  $c\bar{c}$  meson picture and are good tetraquark candidates with quark contents  $c\bar{c}u\bar{d}$  and  $c\bar{c}d\bar{u}$  because of taking a charge. These observed charged  $XYZ$  states provide a good place for testing various phenomenological methods of hadron physics. Eight charged charmonium-like resonances  $Z_c(4430)$ ,  $Z_c(4250)$ ,  $Z_c(4200)$ ,  $Z_c(4100)$ ,  $Z_c(4055)$ ,  $Z_c(4050)$ ,  $Z_c(4020)$  and  $Z_c(3900)$  have been successively observed by experimental collaborations (Brambilla et al., 2020). The multiquark study is applied to understand these exotic states in quark models.

The possible existence of multiquarks was suggested at the birth of the quark model (Gell-Mann, 1964), such as, tetraquark consisting of two quarks and two antiquarks ( $q^2\bar{q}^2$ ), pentaquark consisting of four quarks and one antiquark ( $q^4\bar{q}$ ), dibaryon consisting of six quarks ( $q^6$ ), and baryonium consisting of three quarks and three antiquarks ( $q^3\bar{q}^3$ ). A systematic study of the charged  $Z_c$  states' internal structure would bring fresh insights into multiquark system dynamics and provide information for future experimental searches for the  $Z_c$  missing higher excitations.

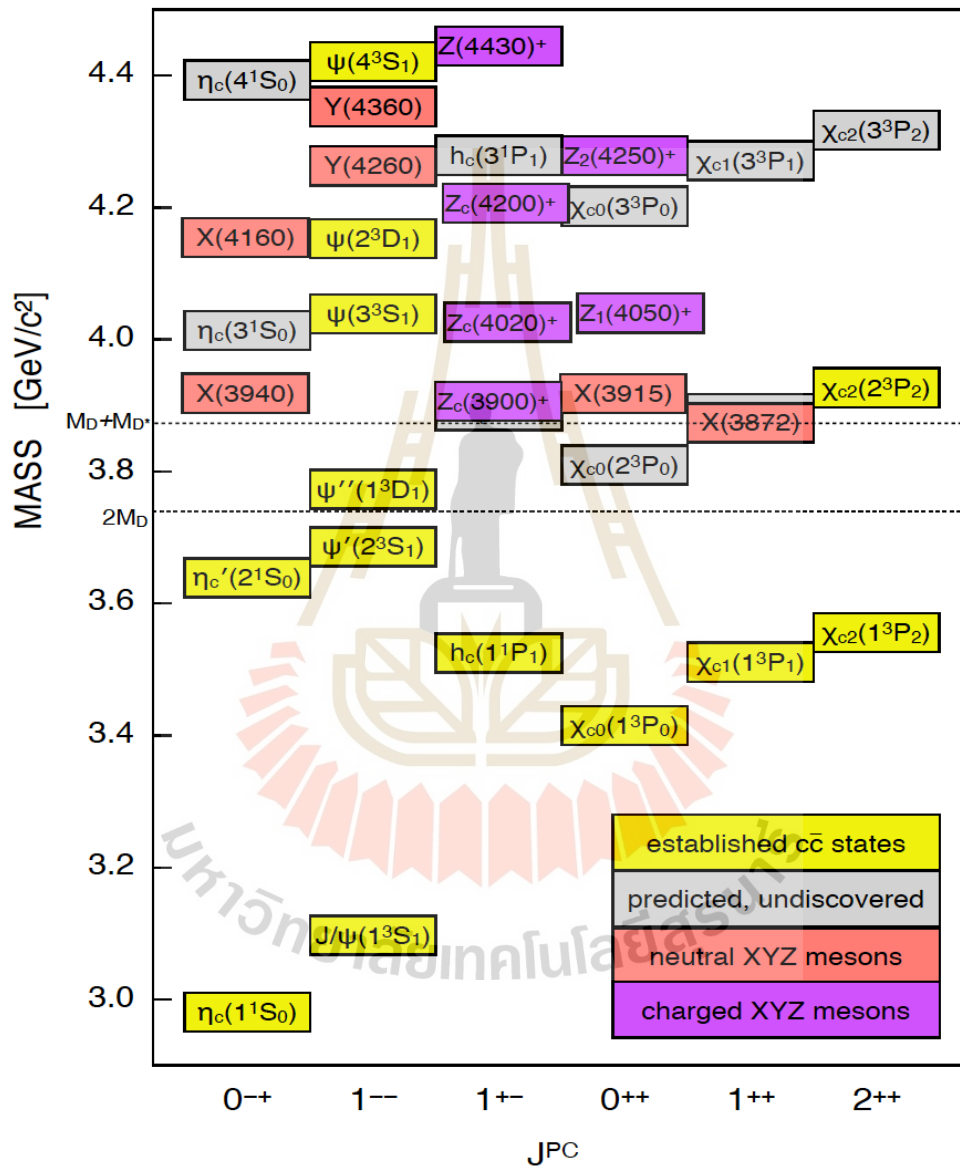


Figure 1.1 Charmonium meson spectrums include some XYZ states (Olsen, 2015).

The newest experimental evidences for eight  $Z_c$  states from the major collaborations are collected as follows:

**a.  $Z_c(3900)$ :** The charged  $Z_c(3900)$  is first observed in the  $J/\psi\pi^\pm$  invariant mass distribution in the  $e^+e^- \rightarrow J/\psi\pi^+\pi^-$  process by BESIII Collaboration (Ablikim et al., 2013a). In the same production channel, a charged  $Z_c(3900)$  structure is also reported by Belle Collaboration (Liu et al., 2013).

The quantum number  $J^P$  of the charged  $Z_c^+(3900)$  is determined to be  $1^+$  in a partial wave analysis of the process  $e^+e^- \rightarrow J/\psi\pi^+\pi^-$  by BESIII (Ablikim et al., 2017b). The measured mass and width of the charged  $Z_c^+(3900)$  are  $(3881 \pm 4 \pm 53)$  MeV and  $(52 \pm 5 \pm 36)$  MeV respectively. The neutral state  $Z_c^0(3900)$  is observed in  $\pi^0 J/\psi$  invariant mass spectrum while studying the process  $e^+e^- \rightarrow J/\psi\pi^0\pi^0$  by BESIII (Ablikim et al., 2020), and the  $J^P$  of the  $Z_c^0(3900)$  is determined to be  $1^+$ . The measured mass and width of the neutral  $Z_c^0(3900)$  are  $(3893 \pm 2 \pm 20)$  MeV and  $(44 \pm 5 \pm 9)$  MeV respectively.

The open-charm decays  $e^+e^- \rightarrow (D\bar{D}^*)^\pm\pi^\mp$  and  $e^+e^- \rightarrow (D\bar{D}^*)^0\pi^0$  are also studied by BESIII, and charged structures are found in the  $(D\bar{D}^*)^\pm$  and  $(D\bar{D}^*)^0$  invariant mass spectrum (Ablikim et al., 2014b; Ablikim et al., 2015c). Because the measured mass is lower than that of the  $Z_c(3900)$  in the  $J/\psi\pi$  channel by BESIII and Belle, the resonance is named as  $Z_c(3885)$  by BESIII. The mass and width of the  $Z_c(3885)$ , on the other hand, are compatible with the  $Z_c(3900)$  state obtained by Xiao (Xiao et al., 2013). Nowadays, the  $Z_c(3900)$  and  $Z_c(3885)$  are thought to be related (Zyla et al., 2020). The  $Z_c(3900) / Z_c(3885)$  may be seen in both the hidden-charm  $J/\psi\pi$  and open-charm  $D\bar{D}^*$  decay channels if the  $Z_c(3900)$  and  $Z_c(3885)$  are considered the same state.

**b.  $Z_c(4020)$ :** The charged charmonium-like  $Z_c^\pm(4020)$  and neutral  $Z_c^0(4020)$  in the  $\pi^\pm h_c(1P)$  and  $\pi^0 h_c(1P)$  invariant mass distribution are reported while studying the processes of  $e^+e^- \rightarrow h_c(1P)\pi^\pm\pi^\mp$  and  $e^+e^- \rightarrow h_c(1P)\pi^0\pi^0$  by BESIII (Ablikim et al., 2013c; Ablikim et al., 2014a), respectively. The mass and width are measured to be  $(4023 \pm 1 \pm 3)$  MeV and  $(8 \pm 3 \pm 3)$  MeV for charged  $Z_c^\pm(4020)$ .

The charged and neutral  $Z_c(4020)$  in the  $(D^*\bar{D}^*)^\pm$  and  $(D^*\bar{D}^*)^0$  invariant mass distributions are also reported by BESIII (Ablikim et al., 2014c; Ablikim et al., 2015b) while studying the processes of  $e^+e^- \rightarrow (D^*\bar{D}^*)^\pm\pi^\mp$  and  $e^+e^- \rightarrow (D^*\bar{D}^*)^0\pi^0$ , respectively. The charged and neutral  $Z_c(4020)$  are grouped together due to their comparable production rates and mass values (Zyla et al., 2020).

**c.  $Z_c(4050)$  and  $Z_c(4250)$ :** The two charged states,  $Z_c^+(4050)$  and  $Z_c^+(4250)$ , are first observed by Belle in 2008 (Mizuk et al., 2008) while studying the  $\pi^+\chi_{c1}(1P)$  invariant mass distribution in the exclusive  $B \rightarrow K^-\pi^+\chi_{c1}(1P)$  decay. The masses and widths of the  $Z_c^+(4050)$  and  $Z_c^+(4250)$  are determined to be  $(4051 \pm 14_{-41}^{+20})$  MeV and  $(82_{-17}^{+21+47})$  MeV, and  $(4248_{-29}^{+44+180})$  MeV and  $(177_{-39}^{+54+316})$  MeV, respectively.

**d.  $Z_c(4055)$ :** The charged  $Z_c(4055)$  is first observed in the process  $e^+e^- \rightarrow \gamma\pi^+\pi^-\psi(2S)$  with a significance of  $3.5\sigma$  by Belle (Wang et al., 2015). The mass and width are measured to be  $(4054 \pm 3 \pm 1)$  MeV and  $(45 \pm 11 \pm 6)$  MeV respectively.

Later, the charged and neutral  $Z_c(4055)$  in the  $\pi^\pm\psi(2S)$  and  $\pi^0\psi(2S)$  invariant mass distribution are reported while studying the processes of  $e^+e^- \rightarrow \pi^+\pi^-\psi(2S)$  and  $e^+e^- \rightarrow \pi^0\pi^0\psi(2S)$  with significances of  $9.2\sigma$  and  $5.9\sigma$  by BESIII (Ablikim et al., 2017a; Ablikim et al., 2018), respectively. The mass and width are measured to be  $(4032 \pm 2)$  MeV and  $(26 \pm 5)$  MeV for charged  $Z_c(4055)$ , and  $(4039 \pm 6)$  MeV and  $(32 \pm 15)$  MeV for neutral  $Z_c(4055)$ .

**e.  $Z_c(4100)$ :** The charged  $Z_c^-(4100)$  is observed in the  $\eta_c(1S)\pi^-$  invariant mass distribution in  $B^0 \rightarrow \eta_c(1S)K^+\pi^-$  decay process with a significance  $3.4\sigma$  by LHCb Collaboration (Aaij et al., 2018). The mass and width are measured to be  $(4096 \pm 20_{-22}^{+18})$  MeV and  $(152 \pm 58_{-35}^{+60})$  MeV respectively.

**f.  $Z_c(4200)$ :** A charged charmonium-like structure  $Z_c^+(4200)$  which decays into  $\pi^+J/\psi$  is observed by Belle (Chilikin et al., 2014) in the  $\bar{B}^0 \rightarrow K^-\pi^+J/\psi$  decay process with a significance of  $6.2\sigma$ . The measured mass and width of the  $Z_c^+(4200)$  are  $(4196_{-29}^{+31+17})$  MeV and  $(370_{-70}^{+70+70})$  MeV respectively while the quantum number  $J^P$  is assigned as  $1^+$ . In addition, the evidence of  $Z^+(4430) \rightarrow \pi^+J/\psi$  is found during studying the same process.

**g.  $Z_c(4430)$ :** The charged charmonium-like state  $Z_c^+(4430)$  is first observed by Belle in the  $\pi^+\psi(2S)$  invariant mass distribution in  $B^+ \rightarrow K\pi^+\psi(2S)$  decay process in 2007 (Choi et al., 2008) with a significance of  $6.5\sigma$ . The mass and width are measured to be  $(4433 \pm 4 \pm 2)$  MeV and  $(45_{-13}^{+18+30})$  MeV, respectively. A year later, a signal for  $Z_c^+(4430) \rightarrow \pi^+\psi(2S)$  is also observed during performing a Dalitz plot analysis of  $B^+ \rightarrow K\pi^+\psi(2S)$  by Belle with a significance of  $6.4\sigma$  (Mizuk et al., 2009). The existence of  $Z_c^-(4430)$  is confirmed by LHCb in  $B \rightarrow K^+\pi^-\psi(2S)$  decays with a model-independent approach (Aaij et al., 2014; Aaij et al., 2015). The

quantum number  $J^P$  is determined unambiguously to be  $1^+$ , and the mass and width are measured to be  $(4475 \pm 7_{-25}^{+15})$  MeV and  $(172 \pm 13_{-34}^{+37})$  MeV by LHCb (Aaij et al., 2014), and  $(4485 \pm 22_{-11}^{+28})$  MeV and  $(200_{-46}^{+41+26}_{-35})$  MeV by Belle (Chilikin et al., 2013), respectively.

Except for these  $Z_c$  states listed above, recently, while studying the process of  $e^+e^- \rightarrow K^+D_s^-D^{*0}$  and  $K^+D_s^{*-}D^0$ , the first candidate of the charged charmonium-like tetraquark with strangeness with a quark content  $c\bar{c}s\bar{u}$  named  $Z_{cs}(3985)^-$  is observed by BESIII with a significance of  $5.3\sigma$  (Ablikim et al., 2021). The mass and width are measured to be  $(3982.5_{-2.0}^{+2.1} \pm 1.7)$  MeV and  $(13.8_{-5.2}^{+8.1} \pm 4.9)$  MeV, respectively.

Four exotic states, the  $Z_{cs}(4000)^+$  and  $Z_{cs}(4220)^+$  with a quark content  $c\bar{c}u\bar{s}$ , and the  $X(4630)$  and  $X(4685)$  with a quark content  $c\bar{c}s\bar{s}$ , are reported by LHCb in the  $J/\psi K^+$  invariant mass spectrum with high significance (Aaij et al., 2021). The mass, width, and quantum number of  $Z_{cs}(4000)^+$  are measured to be  $(4003 \pm 6_{-14}^{+4})$  MeV,  $(131 \pm 15 \pm 26)$ , and  $J^P = 1^+$  with the highest significance  $15\sigma$  in these four exotic states. The  $Z_{cs}(4000)^+$  is not related to the  $Z_{cs}(3985)^-$  observed by BESIII due to their significantly different decay widths.

In the mass spectrum of  $J/\psi$  pair, the first fully-heavy tetraquark candidates  $X(6900)$  with a quark content  $c\bar{c}c\bar{c}$  is observed by LHCb with a significance around  $5\sigma$  (Aaij et al., 2020).

Due to the discovery of these tetraquark candidates, many phenomenological methods of hadron physics can be tested. A systematic study for tetraquark mass spectrum would provide information for future experimental searches for the undiscovered higher excitations. Some representative models and improved pictures proposed to study the tetraquark states are briefly reviewed here and later in Chapter V.

The charmonium-like tetraquark mass spectrum has been studied in diquark-antidiquark model (Maiani et al., 2005; Maiani et al., 2013; Maiani et al., 2014), non-relativistic potential model (Silvestre-Brac and Semay, 1993; Patel et al., 2014), chromomagnetic interaction model (Zhao et al., 2014a; Wu et al., 2019), color flux-tube model (Deng et al., 2015; Deng et al., 2018), and relativized diquark model (Anwar et al., 2018b). These theoretical works of charmonium-like tetraquark are briefly reviewed as follows:

- a. **Diquark-antidiquark model:** After the discovery of  $X(3872)$ , a

charmonium-like tetraquark mass spectrum is derived, and the  $X(3872)$  is taken as an input in a diquark-antidiquark model named “Type-I” model. In this model, the  $X(3872)$  is assumed as a diquark-antidiquark charmonium-like tetraquark state (Maiani et al., 2005), and the parameters of diquark and quark-antiquark pairs are fixed by the conventional baryon and meson mass spectra respectively. The constituent quark mass of diquark is fixed by taking the  $X(3872)$  state as an input. After the discovery of the  $Z_c(3900)$ , the  $Z_c(3900)$  is also interpreted as a tetraquark state. The decay modes were investigated in the “Type-I” model (Maiani et al., 2013). Later, the “Type-I” model was further developed to be “Type-II” diquark-antidiquark model where more complicated spin-spin interactions are employed (Maiani et al., 2014).

**b. Non-relativistic potential model:** In a non-relativistic quark model, the S-wave tetraquark states are systematically studied with all quark configurations. The Bhaduri potential is employed (Silvestre-Brac and Semay, 1993). The parameters are fitted by reproducing charmonium mesons. The constituent quark mass  $m_{u,d}$  is chosen by reproducing the magnetic moments of nucleons, and other masses are fixed by reproducing conventional  $\phi$ ,  $J/\psi$  and  $\Upsilon$  mesons.

The  $Z_c(3885)/Z_c(3900)$  and  $Z_c(4025)/Z_c(4020)$  states are studied in a diquark-antidiquark non-relativistic potential model. The Cornell potential is employed and the parameters are fitted by taking the mass of  $X(3823)$ ,  $Z_c(3885)$ , and  $Z_c(3900)$  states as inputs (Patel et al., 2014). The  $Z_c(3885)$  is assigned as a diquark-antidiquark tetraquark state while the  $Z_c(3900)$  and  $Z_c(4025)$  are assigned as  $Q\bar{q} - \bar{Q}q$  molecularlike tetraquark states.

**c. chromomagnetic interaction model:** The  $c\bar{c}q\bar{q}$  and  $b\bar{b}q\bar{q}$  tetraquark states are studied in a chromomagnetic interaction model where the color-magnetic interaction is employed (Zhao et al., 2014a). The constituent quark masses are extracted by fitting seven conventional meson masses, and the other parameters are extracted by fitting the observed  $Z_c(4200)$ ,  $Z_c(4025)$ , and  $Z_c(3900)$  states.

The charmonium-like, bottomonium-like, and  $B_c$ -like tetraquark states are studied in a chromomagnetic interaction model where both parameters and constituent quark masses are extracted from eight conventional mesons and nine conventional baryons (Wu et al., 2019). Assignments of tetraquark states are suggested.

**d. color flux-tube model:** The charmonium-like tetraquark states are

studied in a color flux-tube model where a multi-body confinement potential is employed (Deng et al., 2015). The parameters and constituent quark masses are determined by reproducing the nineteen ground state meson masses except for  $m_\pi$ ,  $m_K$ , and  $m_\eta$  which are fixed by experimental data. The ground state meson mass spectrum is obtained by solving the two-body Schrödinger equation. Assignments are suggested after comparing theoretical results and experimental data. Later, based on this color flux-tube model, all  $X$ ,  $Y$ , and  $Z_c$  hidden-charm tetraquark states are studied, and assignments for all  $X$ ,  $Y$ , and  $Z_c$  states are suggested (Deng et al., 2018).

**e. relativized diquark model:** The hidden-charm  $qc\bar{q}\bar{c}$  and  $sc\bar{s}\bar{c}$  tetraquarks are studied in a relativized diquark model where one gluon exchange plus confining potential are employed. Most of parameters are extracted from previous meson mass spectrum studies (Anwar et al., 2018b). After comparing theoretical results and experimental data of  $X$ ,  $Y$ , and  $Z_c$  states, assignments are provided for both  $qc\bar{q}\bar{c}$  and  $sc\bar{s}\bar{c}$  tetraquarks.

Fully-heavy tetraquark mass spectrum has also been studied in non-relativistic potential model (Silvestre-Brac and Semay, 1993; Berezhnoy et al., 2012; Wang et al., 2019; Liu et al., 2019; Debastiani and Navarra, 2019), non-relativistic effective field theory (Anwar et al., 2018a), chromomagnetic interaction model (Wu et al., 2018), and QCD sum rules (Wang, 2017; Wang and Di, 2019). The theoretical works of fully-charm tetraquark  $cc\bar{c}\bar{c}$  in potential models are briefly reviewed as follows:

All tetraquark configurations, including fully-charm tetraquark  $cc\bar{c}\bar{c}$ , are studied in a non-relativistic potential model systematically (Silvestre-Brac and Semay, 1993). Bhaduri potential is employed, and charmonium mesons are chosen for fitting the parameters. The experimental data of magnetic moments of nucleons, conventional  $\phi$ ,  $J/\psi$ , and  $\Upsilon$  meson masses are chosen for fitting the constituent quark masses  $m_{u,d}$ ,  $m_s$ ,  $m_c$ , and  $m_b$  respectively.

In a diquark-antidiquark picture, the S-wave mass spectra of fully-heavy tetraquark  $cc\bar{c}\bar{c}$ ,  $bbb\bar{b}$ , and  $bb\bar{c}\bar{c}$  are calculated in two non-relativistic potential models simultaneously while considering  $\bar{3}_c \otimes 3_c$ ,  $6_c \otimes \bar{6}_c$ , and mixture color configurations (Wang et al., 2019). The potential of the first quark model adopted from the work (Wong et al., 2002) contains Coulomb plus linear confinement interactions, spin-spin interactions, and a constant, and the potential of the second quark

model is adopted from the work (Silvestre-Brac, 1996). The model parameters are extracted from 9 conventional heavy meson states.

Similar with the work reviewed above, the mass spectra of fully-heavy tetraquarks are studied in a potential model where the potential contains the linear confining potential, Coulomb potential, and spin-spin interactions (Liu et al., 2019). 10 bottomonium and bottom-charm meson states are chosen for fitting the model parameters.

The ground state mass spectra of fully-heavy tetraquark  $cc\bar{c}\bar{c}$ ,  $bb\bar{b}\bar{b}$ , and  $bc\bar{b}\bar{c}$  are studied in a non-relativistic quark model where the OGE spin-spin interaction is considered (Berezhnoy et al., 2012). The wave function is formed in a diquark-antidiquark picture, but only  $\bar{\mathbf{3}}_c \otimes \mathbf{3}_c$  color configuration is considered.

The fully-charm  $cc\bar{c}\bar{c}$  tetraquark mass spectrum is calculated in a Cornell-inspired potential model (Debastiani and Navarra, 2019), but only  $\bar{\mathbf{3}}_c \otimes \mathbf{3}_c$  color configuration is considered. The parameters are extracted by reproducing all charmonium meson  $c\bar{c}$  mass spectrum, and 14 recent experimental data of charmonium states are selected. The masses of  $cc\bar{c}\bar{c}$  tetraquark are lighter than other works in potential model.

In the framework of the color-magnetic interaction, the fully-heavy tetraquark mass spectrum is studied where the Hamiltonian contains only effective mass and OGE interaction (Wu et al., 2018). The parameters of OGE interactions are fixed by mass splittings between pseudoscalar and vector mesons from experimental data, the effective masses are adopted from their previous charmonium-like tetraquark and pentaquark calculations.

For the light-unflavored mesons, the experimental status is shown in Figure 1.2, where the mesons of an isovector, a strange isodoublet and two isoscalars are grouped together to represent a flavor nonet, and the clear and definitive assignments are shaded. The states are classified by their total angular momentum  $J$ , orbital angular momentum  $L$ , spin multiplicity  $2S + 1$ , and radial excitation  $n$  while the vertical scale is  $v = n + L - 1$ , and the horizontal scale is the orbital excitation  $L$ . Even though the ground state pseudoscalars ( $J^{PC} = 0^{-+}$ ) and vectors ( $1^{--}$ ) are well established, a number of predicted radial excitations ( $n > 1$ ) and orbital excitations ( $L > 0$ ) are still missing and some observed meson candidates do not fit into quark model conventional meson mass spectra easily (Amsler and Tornqvist, 2004).

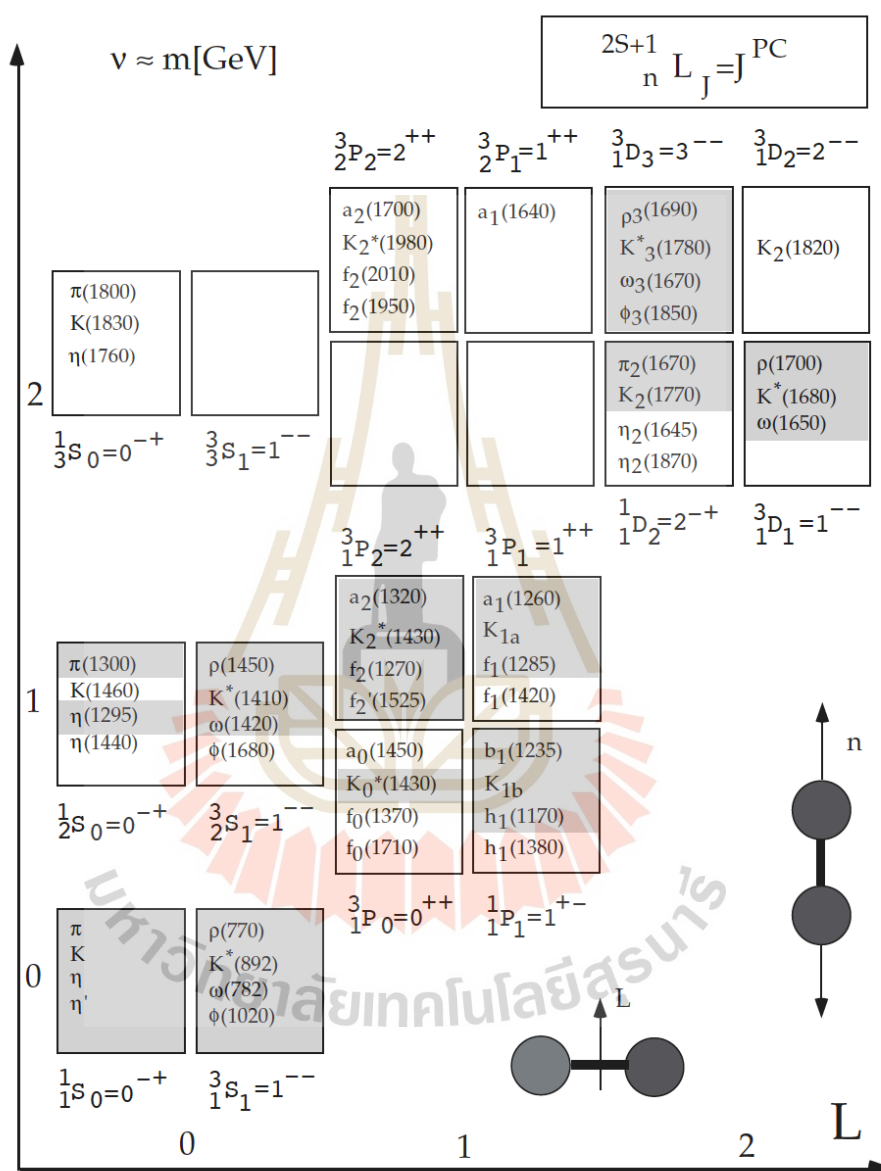


**Figure 1.2** Tentative  $q\bar{q}$  mass spectrum for the three light quarks (Amsler and Tornqvist, 2004).

The researches on conventional  $q\bar{q}$  meson states have conducted for more than a half century, and the light-unflavored meson mass spectrum has been studying in various quark models, which provide us with a good knowledge to understand their underlying structures. Theoretical predictions of conventional  $q\bar{q}$  meson states can be found in some works (Godfrey and Isgur, 1985; Vijande et al., 2005; Ebert et al., 2009; Xiao et al., 2019; Li et al., 2021).

The meson mass spectra from the  $\pi$  to  $\Upsilon$  are studied systematically in a relativized quark model with chromodynamics (Godfrey and Isgur, 1985). The potential motivated by QCD contains linear confinement, Coulomb-type interaction, OGE hyperfine interaction, and spin-orbital interaction.

Similar as the one above, a study of meson spectra from the light meson states to the  $b\bar{b}$  states are performed in the constituent quark model (Vijande et al., 2005). Goldstone-boson exchanges are considered, and parameters of  $\pi$ ,  $\sigma$ ,  $\eta$ , and  $K$  are fixed separately with other mesons. After comparing theoretical results and experimental data, assignments and discussions are performed.

The mass spectrum of strangeonium  $s\bar{s}$  up to 3D multiplet within a non-relativistic linear potential model where Cornell-like potential, spin-spin contact hyperfine potential, spin-orbit interaction, and tensor potential are employed (Li et al., 2021). Detail discussions for assigning states of experimental data are performed and classified by quantum number  $J^{PC}$ , and assignments are suggested.

With reasonable flavor symmetry breaking and binding assumptions, the well established experimental candidates can be easily assigned to the theoretical predictions of  $L = 0$  and 1 ground state meson nonets except for the scalar  $^3P_0$  nonet due to too many observed candidates (Hagiwara et al., 2002).

Exotic meson states such as glueballs, tetraquarks, and hybrids have been widely studied in the past two decades, especially focusing on the states having same quantum numbers as conventional  $q\bar{q}$  systems.

Hybrids might come with exotic quantum numbers which are different with quantum numbers of conventional  $q\bar{q}$  mesons, and the main assumption of hybrid states is that meson-meson interactions are dominated by s-channel resonances. Some  $J^{PC} = 1^{-+}$  exotics may have properties consistent with the interpretation, the quark-antiquark bound by a gluon string, in flux tube model (Klempt and Zaitsev, 2007).

Glueballs are bound states of gluons without valence quarks, which is

guided by quantum chromodynamics (QCD). However, glueballs have not been observed and identified with certainty so far, and may be mixed with conventional  $q\bar{q}$  mesons while particles are identified in accelerators (Ochs, 2013). In QCD, the ground state scalar glueball with quantum number  $0^{++}$  is estimated in the mass range from 1000 to 1800 MeV, the ground state mass of tensor glueball  $2^{++}$  is higher than the scalar glueball (Klempt and Zaitsev, 2007). In lattice gauge theories, the lowest mass of  $0^{++}$  and  $2^{++}$  glueballs are estimated to be  $1710 \pm 50 \pm 80$  and  $2390 \pm 30 \pm 120$  respectively (Chen et al., 2006).

Two typical exotic light mesons  $f_0(1500)$  and  $f_0(1710)$  which can not be fitted into conventional  $q\bar{q}$  meson mass spectrum easily, and the  $f_0(1370)$  which might be a conventional  $q\bar{q}$  meson, are reviewed as follows:

a.  $f_0(1370)$ : The mass and decay width averaged by PDG of the very broad  $f_0(1370)$  states are 1200 to 1500 MeV and 200 to 500 MeV respectively (Zyla et al., 2020). According to the partial decay width, the  $f_0(1370)$  decays mostly into  $4\pi$  channel within four main decay modes  $4\pi$ ,  $2\pi$ ,  $\eta\eta$ , and  $K\bar{K}$ . Branching fraction  $\Gamma_{4\pi}/\Gamma_{total}$  is measured to be  $(80 \pm 5)\%$  from  $p\bar{p}$  annihilation (Gaspero, 1993).

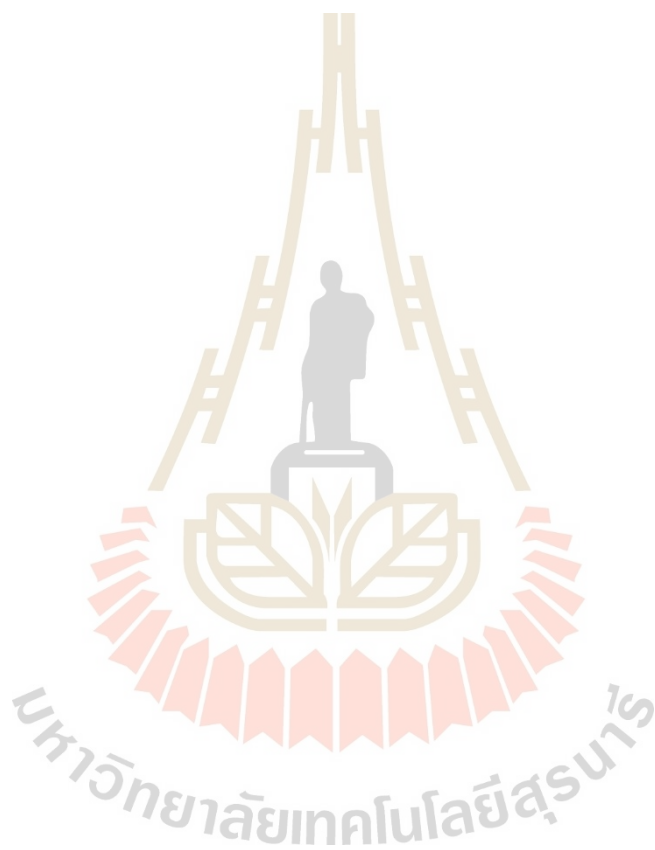
b.  $f_0(1500)$ : The averaged mass and decay width of the  $f_0(1500)$  are  $1506 \pm 6$  MeV and  $112 \pm 9$  respectively (Zyla et al., 2020), which are significantly accurate comparing with the  $f_0(1370)$ . The  $f_0(1500)$  decays mostly into  $2\pi$  and  $4\pi$  within four main decay modes  $4\pi$ ,  $2\pi$ ,  $\eta\eta$ , and  $K\bar{K}$ . Branching fractions  $\Gamma_{2\pi}/\Gamma_{total}$  and  $\Gamma_{4\pi}/\Gamma_{total}$  are  $(34.5 \pm 2.2)\%$  and  $(48.9 \pm 3.3)\%$  respectively (Zyla et al., 2020).

c.  $f_0(1710)$ : The mass and decay width are averaged to be  $1704 \pm 12$  MeV and  $123 \pm 18$  respectively (Zyla et al., 2020). The  $f_0(1710)$  is observed from five main decay channels  $K\bar{K}$ ,  $\eta\eta$ ,  $\pi\pi$ ,  $\gamma\gamma$ , and  $\omega\omega$ . Branching fractions  $\Gamma_{K\bar{K}}/\Gamma_{total}$  and  $\Gamma_{\eta\eta}/\Gamma_{total}$  are  $(36 \pm 12)\%$  and  $(22 \pm 12)\%$  respectively from a coupled channel study (Albaladejo and Oller, 2008).

We do not focus on repeating the tetraquark mass by applying a huge number of parameters, instead establishing a simplified model. In this model, we predetermine the model parameters by fitting the believed normal meson mass spectrum, and apply these predetermined parameters as imported parameters to predict the mass of all possible tetraquark configurations.

This thesis is organized as follows. The construction of tetraquark wave function is in Chapter II and the details are presented in Appendix B and C. The constituent quark model is introduced in Chapter III. Fixing model parameters

by calculating meson mass spectrum is also in this section. The prediction of tetraquark masses is displayed in Chapter IV. After comparing theoretical results and experimental data of exotic states, tentative assignments with discussions are given in Chapter V. Finally, the conclusions are summarized in Chapter VI.



## CHAPTER II

### CONSTRUCTION OF TETRAQUARK WAVE FUNCTIONS

#### 2.1 Tetraquark Color Wave Functions

A tetraquark state must be a color singlet, which means that the tetraquark color wave function must be a  $[222]_1$  singlet of the  $SU_c(3)$  group. The Young tabloid construction of the  $q_1q_2\bar{q}_3\bar{q}_4$  configuration is shown as,

$$\begin{array}{l}
 \begin{array}{|c|c|} \hline \square & \square \\ \hline \square & \square \\ \hline \end{array} (q_1q_2\bar{q}_3\bar{q}_4) = \begin{array}{|c|c|} \hline \square & \square \\ \hline \end{array} (q_1q_2) \otimes \begin{array}{|c|c|} \hline \square & \square \\ \hline \square & \square \\ \hline \end{array} (\bar{q}_3\bar{q}_4), \\
 \begin{array}{|c|c|} \hline \square & \square \\ \hline \square & \square \\ \hline \end{array} (q_1q_2\bar{q}_3\bar{q}_4) = \begin{array}{|c|} \hline \square \\ \hline \square \\ \hline \end{array} (q_1q_2) \otimes \begin{array}{|c|c|} \hline \square & \square \\ \hline \square & \square \\ \hline \end{array} (\bar{q}_3\bar{q}_4).
 \end{array}$$

The Young tabloids  $[11]_{\bar{3}}$  and  $[2]_6$  of the  $SU_c(3)$  group characterize the permutation symmetry of the two-quark cluster ( $q_1q_2$ ) of tetraquark state, while the color part of the two-antiquark cluster is a  $[211]_3$  triplet and  $[22]_{\bar{6}}$  antisextet. Thus, a  $[222]_1$  color singlet of tetraquark state demands the following configurations:

$$[11]_{\bar{3}}(q_1q_2) \otimes [211]_3(\bar{q}_3\bar{q}_4), \quad [2]_6(q_1q_2) \otimes [22]_{\bar{6}}(\bar{q}_3\bar{q}_4). \quad (2.1)$$

The general color wave function of  $\bar{3}_c \otimes 3_c$  and  $6_c \otimes \bar{6}_c$  color configurations may be written as follows:

$$\begin{aligned}
 \psi_{[11]_{\bar{3}}^c [211]_3^c}^{q_1q_2\bar{q}_3\bar{q}_4} &= \frac{1}{\sqrt{3}} \sum_{i=1}^3 \psi_{[11]_{\bar{3}}^c i}^{q_1q_2} \psi_{[211]_3^c i}^{\bar{q}_3\bar{q}_4}, \\
 \psi_{[2]_6^c [22]_{\bar{6}}^c}^{q_1q_2\bar{q}_3\bar{q}_4} &= \frac{1}{\sqrt{6}} \sum_{i=1}^6 \psi_{[2]_6^c i}^{q_1q_2} \psi_{[22]_{\bar{6}}^c i}^{\bar{q}_3\bar{q}_4}.
 \end{aligned} \quad (2.2)$$

Three quark configurations, charmonium-like ( $qc\bar{q}\bar{c}$ ), fully-light ( $qq\bar{q}\bar{q}$ ) and fully-charm ( $cc\bar{c}\bar{c}$ ) tetraquark, are considered in this work. The explicit color wave

functions are listed as follows:

$$\begin{aligned}
\psi_{[2]_6^c[22]_6^c}^{q_1 q_2 \bar{q}_3 \bar{q}_4} &= \frac{1}{\sqrt{6}} [R_1 R_2 \bar{R}_3 \bar{R}_4 + G_1 G_2 \bar{G}_3 \bar{G}_4 + B_1 B_2 \bar{B}_3 \bar{B}_4 \\
&\quad + \frac{1}{2} (R_1 G_2 + G_1 R_2) (\bar{R}_3 \bar{G}_4 + \bar{G}_3 \bar{R}_4) \\
&\quad + \frac{1}{2} (B_1 R_2 + R_1 B_2) (\bar{B}_3 \bar{R}_4 + \bar{R}_3 \bar{B}_4) \\
&\quad + \frac{1}{2} (G_1 B_2 + B_1 G_2) (\bar{G}_3 \bar{B}_4 + \bar{B}_3 \bar{G}_4)] \\
&= \frac{1}{\sqrt{6}} [RR\bar{R}\bar{R} + GG\bar{G}\bar{G} + BB\bar{B}\bar{B} \\
&\quad + \frac{1}{2} (RG\bar{R}\bar{G} + GR\bar{R}\bar{G} + RG\bar{G}\bar{R} + GR\bar{G}\bar{R}) \\
&\quad + \frac{1}{2} (BR\bar{B}\bar{R} + RB\bar{B}\bar{R} + BR\bar{R}\bar{B} + RB\bar{R}\bar{B}) \\
&\quad + \frac{1}{2} (GB\bar{G}\bar{B} + BG\bar{G}\bar{B} + GB\bar{B}\bar{G} + BG\bar{B}\bar{G})], \\
\psi_{[11]_3^c[211]_3^c}^{q_1 q_2 \bar{q}_3 \bar{q}_4} &= \frac{1}{\sqrt{3}} \left[ \frac{1}{2} (R_1 G_2 - G_1 R_2) (\bar{R}_3 \bar{G}_4 - \bar{G}_3 \bar{R}_4) \right. \\
&\quad + \frac{1}{2} (B_1 R_2 - R_1 B_2) (\bar{B}_3 \bar{R}_4 - \bar{R}_3 \bar{B}_4) \\
&\quad + \frac{1}{2} (G_1 B_2 - B_1 G_2) (\bar{G}_3 \bar{B}_4 - \bar{B}_3 \bar{G}_4) \\
&= \frac{1}{\sqrt{3}} \left[ \frac{1}{2} (RG\bar{R}\bar{G} - GR\bar{R}\bar{G} - RG\bar{G}\bar{R} + GR\bar{G}\bar{R}) \right. \\
&\quad + \frac{1}{2} (BR\bar{B}\bar{R} - RB\bar{B}\bar{R} - BR\bar{R}\bar{B} + RB\bar{R}\bar{B})
\end{aligned}$$

$$+\frac{1}{2}(GB\bar{G}\bar{B} - BG\bar{G}\bar{B} - GB\bar{B}\bar{G} + BG\bar{B}\bar{G}).$$

## 2.2 Spatial-spin-flavor configurations of tetraquark

For charmonium-like tetraquark states,  $q_1$  and  $q_2$  are light quark  $q$  and charm quark  $c$  respectively, and  $q_3$  and  $q_4$  are light antiquark  $\bar{q}$  and charm antiquark  $\bar{c}$  respectively. The possible spin combinations are:

$$\left[ \psi_{[s=1]}^{qc} \otimes \psi_{[s=1]}^{\bar{q}\bar{c}} \right]_{S=0,1,2}, \quad \psi_{[s=1]}^{qc} \otimes \psi_{[s=0]}^{\bar{q}\bar{c}}, \quad \psi_{[s=0]}^{qc} \otimes \psi_{[s=0]}^{\bar{q}\bar{c}}. \quad (2.3)$$

The explicit spin wave functions  $\psi_{(S(qc)\otimes S(\bar{q}\bar{c}))}^{S(qc\bar{q}\bar{c})}$  of  $qc\bar{q}\bar{c}$  tetraquark states are listed as follows:

$$\begin{aligned} \psi_{(1\otimes 1)}^{S=2} &= \uparrow\uparrow \bar{\uparrow}\bar{\uparrow}, \\ \psi_{(1\otimes 1)}^{S=1} &= \frac{1}{2}(\uparrow\uparrow \bar{\uparrow}\bar{\downarrow} + \uparrow\uparrow \bar{\downarrow}\bar{\uparrow} - \uparrow\downarrow \bar{\uparrow}\bar{\uparrow} - \downarrow\uparrow \bar{\uparrow}\bar{\uparrow}), \\ \psi_{(1\otimes 0)}^{S=1} &= \frac{1}{\sqrt{2}}(\uparrow\uparrow \bar{\uparrow}\bar{\downarrow} - \uparrow\uparrow \bar{\downarrow}\bar{\uparrow}), \\ \psi_{(1\otimes 1)}^{S=0} &= \frac{1}{\sqrt{3}}[\uparrow\uparrow \bar{\downarrow}\bar{\downarrow} - \frac{1}{2}(\uparrow\downarrow \bar{\uparrow}\bar{\downarrow} + \uparrow\downarrow \bar{\downarrow}\bar{\uparrow} + \downarrow\uparrow \bar{\uparrow}\bar{\downarrow} + \downarrow\uparrow \bar{\downarrow}\bar{\uparrow}) + \downarrow\downarrow \bar{\uparrow}\bar{\uparrow}], \\ \psi_{(0\otimes 0)}^{S=0} &= \frac{1}{2}(\uparrow\downarrow \bar{\uparrow}\bar{\downarrow} - \uparrow\downarrow \bar{\downarrow}\bar{\uparrow} - \downarrow\uparrow \bar{\uparrow}\bar{\uparrow} + \downarrow\uparrow \bar{\downarrow}\bar{\downarrow}). \end{aligned} \quad (2.4)$$

Considering that a fully-light ( $qq\bar{q}\bar{q}$ ) and a fully-charm ( $cc\bar{c}\bar{c}$ ) tetraquark state must be a color singlet and antisymmetric simultaneously under any permutation between identical quarks, one gets the spatial-spin-flavor configurations of color  $[2]_6$  and  $[11]_3$  configuration must be  $[11]$  and  $[2]$  states by conjugation for identical cluster, respectively. Considering the identical  $qq$  cluster of a  $qq\bar{q}\bar{q}$  tetraquark state, since the spatial wave function is always symmetric, one gets all the possible color-spatial-spin-flavor configurations of the  $qq$  cluster as follows:

$$\psi_{[2]}^c \psi_{[2]}^o \psi_{[11]}^s \psi_{[2]}^f, \quad \psi_{[2]}^c \psi_{[2]}^o \psi_{[2]}^s \psi_{[11]}^f, \quad (2.5)$$

for  $\psi_{[2]}^c \psi_{[11]}^{osf}$ , and

$$\psi_{[11]}^c \psi_{[2]}^o \psi_{[11]}^s \psi_{[11]}^f, \psi_{[11]}^c \psi_{[2]}^o \psi_{[2]}^s \psi_{[2]}^f, \quad (2.6)$$

for  $\psi_{[11]}^c \psi_{[2]}^{osf}$ .

The possible spin combinations are  $\left[ \psi_{[s=1]}^{qq} \otimes \psi_{[s=1]}^{\bar{q}\bar{q}} \right]_{S=0,1,2}$ ,  $\psi_{[s=1]}^{qq} \otimes \psi_{[s=0]}^{\bar{q}\bar{q}}$ , and  $\psi_{[s=0]}^{qq} \otimes \psi_{[s=0]}^{\bar{q}\bar{q}}$ .

The explicit spin wave functions  $\psi_{(S(qq) \otimes S(\bar{q}\bar{q}))}^{S(qq\bar{q}\bar{q})}$  of  $qq\bar{q}\bar{q}$  tetraquark states are listed as follows:

$$\begin{aligned} \psi_{(1 \otimes 1)}^{S=2} &= \uparrow\uparrow \bar{\uparrow}\bar{\uparrow}, \\ \psi_{(1 \otimes 1)}^{S=1} &= \frac{1}{2}(\uparrow\uparrow \bar{\uparrow}\bar{\downarrow} + \uparrow\uparrow \bar{\downarrow}\bar{\uparrow} - \uparrow\downarrow \bar{\uparrow}\bar{\uparrow} - \downarrow\uparrow \bar{\uparrow}\bar{\uparrow}), \\ \psi_{(1 \otimes 0)}^{S=1} &= \frac{1}{\sqrt{2}}(\uparrow\uparrow \bar{\uparrow}\bar{\downarrow} - \uparrow\uparrow \bar{\downarrow}\bar{\uparrow}), \\ \psi_{(1 \otimes 1)}^{S=0} &= \frac{1}{\sqrt{3}}[\uparrow\uparrow \bar{\downarrow}\bar{\downarrow} - \frac{1}{2}(\uparrow\downarrow \bar{\uparrow}\bar{\downarrow} + \uparrow\downarrow \bar{\downarrow}\bar{\uparrow} + \downarrow\uparrow \bar{\uparrow}\bar{\downarrow} + \downarrow\uparrow \bar{\downarrow}\bar{\uparrow}) + \downarrow\downarrow \bar{\uparrow}\bar{\uparrow}], \\ \psi_{(0 \otimes 0)}^{S=0} &= \frac{1}{2}(\uparrow\downarrow \bar{\uparrow}\bar{\downarrow} - \uparrow\downarrow \bar{\downarrow}\bar{\uparrow} - \downarrow\uparrow \bar{\uparrow}\bar{\downarrow} + \downarrow\uparrow \bar{\downarrow}\bar{\uparrow}). \end{aligned} \quad (2.7)$$

For  $cc\bar{c}\bar{c}$  tetraquarks, since the flavor wave function for  $cc$  is always symmetric, the spin wave functions for  $cc$  must be symmetric and antisymmetric are for  $[11]_{\bar{3}}$  and  $[2]_6$  color configurations, respectively. Thus, the possible color-spatial-spin-flavor configurations of the  $cc$  cluster are  $\psi_{[2]}^c \psi_{[2]}^o \psi_{[11]}^s \psi_{[2]}^f$  for  $\psi_{[2]}^c \psi_{[11]}^{osf}$ , and  $\psi_{[11]}^c \psi_{[2]}^o \psi_{[2]}^s \psi_{[2]}^f$  for  $\psi_{[11]}^c \psi_{[2]}^{osf}$ .

The explicit spin wave function  $\psi_{(S(cc) \otimes S(\bar{c}\bar{c}))}^{S(cc\bar{c}\bar{c})}$  of  $cc\bar{c}\bar{c}$   $[2](c_1 c_2) \otimes [22](\bar{c}_3 \bar{c}_4)$  configuration is listed as follows:

$$\psi_{(0 \otimes 0)}^{S=0} = \frac{1}{2}(\uparrow\downarrow \bar{\uparrow}\bar{\downarrow} - \uparrow\downarrow \bar{\downarrow}\bar{\uparrow} - \downarrow\uparrow \bar{\uparrow}\bar{\downarrow} + \downarrow\uparrow \bar{\downarrow}\bar{\uparrow}). \quad (2.8)$$

The explicit spin wave functions  $\psi_{(S(cc) \otimes S(\bar{c}\bar{c}))}^{S(cc\bar{c}\bar{c})}$  of  $cc\bar{c}\bar{c}$   $[11](c_1 c_2) \otimes [211](\bar{c}_3 \bar{c}_4)$

configuration are listed as follows:

$$\begin{aligned}
 \psi_{(1\otimes 1)}^{S=2} &= \uparrow\uparrow \bar{\uparrow}\bar{\uparrow}, \\
 \psi_{(1\otimes 1)}^{S=1} &= \frac{1}{2}(\uparrow\uparrow \bar{\uparrow}\bar{\downarrow} + \uparrow\uparrow \bar{\downarrow}\bar{\uparrow} - \uparrow\downarrow \bar{\uparrow}\bar{\uparrow} - \downarrow\uparrow \bar{\uparrow}\bar{\uparrow}), \\
 \psi_{(1\otimes 1)}^{S=0} &= \frac{1}{\sqrt{3}}[\uparrow\uparrow \bar{\downarrow}\bar{\downarrow} - \frac{1}{2}(\uparrow\downarrow \bar{\uparrow}\bar{\downarrow} + \uparrow\downarrow \bar{\downarrow}\bar{\uparrow} + \downarrow\uparrow \bar{\uparrow}\bar{\downarrow} + \downarrow\uparrow \bar{\downarrow}\bar{\uparrow}) + \downarrow\downarrow \bar{\uparrow}\bar{\uparrow}].
 \end{aligned} \tag{2.9}$$

### 2.3 Spatial Wave Function

Here we introduce Jacobi coordinates, a complete basis may be constructed with  $q\bar{q}$  systems in the harmonic oscillator interaction.

$$H = \frac{p_\rho^2}{2m} + \frac{1}{2}C(\rho^2) \tag{2.10}$$

where

$$\vec{\rho} = \frac{1}{\sqrt{2}}(\vec{r}_1 - \vec{r}_2) \tag{2.11}$$

In the center of mass system, with  $\vec{R} = 1/2(\vec{r}_1 + \vec{r}_2)$ , we have:

$$r_{12} = \sqrt{2}\rho \tag{2.12}$$

The spatial wave functions of the  $q\bar{q}$  take the general form,

$$\psi_{NLM} = \sum_{\{n_\rho, l_\rho\}} A(n_\rho, l_\rho) \times \psi_{n_\rho l_\rho}(\vec{\rho}), \tag{2.13}$$

where  $A(n_\rho, l_\rho)$  are coupling constants, and  $N = 2n_\rho + l_\rho$ .  $\psi_{n_r l_r m_r}(r)$  are harmonic oscillator wave functions with the form,  $\psi_{n_r l_r m_r}(r) = R_{n_r l_r}(r)Y_{l_r m_r}(\hat{r})$ .  $Y_{l_r m_r}$  denotes spherical harmonics. The state function  $R_{n_r l_r}(r)$  reads,

$$R_{nl}(r) = \left[ \frac{2\alpha^3 n!}{\Sigma(n+l+3/2)} \right]^{1/2} (\alpha r)^l e^{-\frac{1}{2}\alpha^2 r^2} L_n^{l+1/2}(\alpha^2 r^2) \tag{2.14}$$

where  $L_n^{l+1/2}$  are the associated Laguerre polynomials.

The complete bases for tetraquark system are constructed by using the harmonic oscillator wave function. The antisymmetric property of identical particles is guaranteed by enforcing the corresponding symmetries of the spatial wave functions. The Jacobi coordinates and the corresponding momenta are defined as

$$\begin{aligned}
\vec{x}_1 &= \frac{1}{\sqrt{2}}(\vec{r}_1 - \vec{r}_3), \\
\vec{x}_2 &= \frac{1}{\sqrt{2}}(\vec{r}_2 - \vec{r}_4), \\
\vec{x}_3 &= \frac{m_1\vec{r}_1 + m_3\vec{r}_3}{m_1 + m_3} - \frac{m_2\vec{r}_2 + m_4\vec{r}_4}{m_2 + m_4}, \\
\vec{x}_0 &= \frac{m_1\vec{r}_1 + m_2\vec{r}_2 + m_3\vec{r}_3 + m_4\vec{r}_4}{m_1 + m_2 + m_3 + m_4}, \\
\vec{p}_i &= u_i \frac{d\vec{x}_i}{dt},
\end{aligned} \tag{2.15}$$

where  $\vec{r}_j$  and  $m_j$  are the coordinate and mass of the  $j$ th quark.  $u_i$  are the reduced quark masses defined as:

$$u_1 = \frac{2m_1m_3}{m_1 + m_3}, \quad u_2 = \frac{2m_2m_4}{m_2 + m_4}, \quad u_3 = \frac{(m_1 + m_3)(m_2 + m_4)}{m_1 + m_2 + m_3 + m_4}. \tag{2.16}$$

For the  $qc\bar{q}\bar{c}$ ,  $cc\bar{c}\bar{c}$ , and  $qq\bar{q}\bar{q}$  tetraquark states, we have:

$$\begin{aligned}
r_{12}^{\vec{r}} &= \frac{\vec{x}_1}{\sqrt{2}} - \frac{\vec{x}_2}{\sqrt{2}} + \vec{x}_3, \quad r_{13}^{\vec{r}} = \sqrt{2}\vec{x}_1, \quad r_{23}^{\vec{r}} = \frac{\vec{x}_1}{\sqrt{2}} + \frac{\vec{x}_2}{\sqrt{2}} - \vec{x}_3 \\
r_{14}^{\vec{r}} &= \frac{\vec{x}_1}{\sqrt{2}} + \frac{\vec{x}_2}{\sqrt{2}} + \vec{x}_3, \quad r_{24}^{\vec{r}} = \sqrt{2}\vec{x}_2, \quad r_{34}^{\vec{r}} = -\frac{\vec{x}_1}{\sqrt{2}} + \frac{\vec{x}_2}{\sqrt{2}} + \vec{x}_3.
\end{aligned} \tag{2.17}$$

The total spatial wave function of tetraquark may be expanded in the complete basis formed by the function,

$$\begin{aligned}
\psi_{NL} &= \sum_{\{n_i, l_i\}} A(n_1, n_2, n_3, l_1, l_2, l_3) \\
&\times \psi_{n_1 l_1}(\vec{x}_1) \otimes \psi_{n_2 l_2}(\vec{x}_2) \otimes \psi_{n_3 l_3}(\vec{x}_3)
\end{aligned} \tag{2.18}$$

where  $\psi_{n_i l_i}$  are harmonic oscillator wave functions and the sum  $\{n_i, l_i\}$  is over  $n_1, n_2, n_3, l_1, l_2, l_3$ .  $N$  and  $L$  are the total principle quantum number and orbital angular momentum number of the tetraquark respectively. One has  $N = (2n_1 + l_1) + (2n_2 + l_2) + (2n_3 + l_3)$ . The spatial wave functions  $\psi_{NL}$  are employed as complete bases to study tetraquark states, and the bases size is  $N = 14$  in the calculation. The best eigenvalue is from adjusting the length parameter of harmonic oscillator wave functions.

The complete bases of the tetraquarks are listed in Appendix C Table C. 1, up to  $N = 14$ , where  $l_1, l_2$ , and  $l_3$  are limited to 0 only.



## CHAPTER III

### THEORETICAL MODEL ESTABLISHMENT

#### 3.1 Constituent quark model

The  $q\bar{q}$  and  $qq\bar{q}\bar{q}$  systems are studied in the nonrelativistic Hamiltonian,

$$H = H_0 + H_{hyp}^{OGE},$$

$$H_0 = \sum_{k=1}^N \left( \frac{1}{2} M_k^{ave} + \frac{p_k^2}{2m_k} \right) + \sum_{i<j}^N \left( -\frac{3}{16} \vec{\lambda}_i \cdot \vec{\lambda}_j \right) \left( A_{ij} r_{ij} - \frac{B_{ij}}{r_{ij}} \right), \quad (3.1)$$

$$H_{hyp} = \sum_{i<j} C_{ij} \vec{\lambda}_i \cdot \vec{\lambda}_j \vec{\sigma}_i \cdot \vec{\sigma}_j,$$

where  $m_k$  denotes the constituent quark masses.  $M_k^{ave}$  are the spin-averaged masses taking the form  $\frac{1}{4}M_{PS} + \frac{3}{4}M_V$  (except for  $s\bar{s}$  and  $q\bar{q}$ ), where  $M_{PS}$  and  $M_V$  are the ground state masses of pseudoscalar and vector mesons from experimental data. For each kind of mesons, the spin-averaged masses  $M_k^{ave}$  are listed in Table 3.1, with units in MeV. To avoid the Goldstone bosons of the chiral symmetry breaking (Brambilla et al., 2020), the spin-averaged masses  $M_k^{ave}$  for  $s\bar{s}$  and  $q\bar{q}$  are fitted by experimental data.

**Table 3.1** Spin-averaged masses  $M_k^{ave}$  for various kinds of mesons.

Meson	$b\bar{b} (\eta_b, \Upsilon)$	$c\bar{c} (\eta_c, \psi)$	$s\bar{b} (B_s)$	$q\bar{b} (B)$	$s\bar{c} (D_s)$	$q\bar{c} (D)$	$s\bar{s} (\phi)$	$q\bar{q} (\rho)$
$M_k^{ave}$	9445	3069	5404	5314	2076	1972	952	675

In studies of lattice QCD and quark model, the Cornell potential,

$$V(r) = Ar - \frac{B}{r}, \quad (3.2)$$

has been widely employed while fitting the string tension coefficient  $A$  and Coulomb coefficient  $B$  with experimental data. Each kind of hadrons has a set of model

parameters in quark model and lattice QCD studies (Kawanai and Sasaki, 2011; Ikeda and Iida, 2012).

The Cornell potential predicts that the average velocity of large quark mass will saturate at the value  $\langle v^2 \rangle = B^2$ , where  $B$  denotes the Coulomb coefficient in Eq. (3.2).  $\langle v^2 \rangle_{\Upsilon} / \langle v^2 \rangle_{J/\psi} \approx m_c / m_b$  is expected based on the approximate equality of  $b\bar{b}$  and  $c\bar{c}$  level splittings. For large quark masses, the Coulomb coefficients  $B$  are mass-dependent with the form  $B_{\Upsilon} = B_{J/\psi} \sqrt{m_c / m_b}$ .

For heavy quarkonia in lattice QCD, interquark potentials ( $V_{q\bar{q}}$ ) at finite quark mass are studied (Kawanai and Sasaki, 2011). For fitting the data, the Cornell potential is employed. With finite quark masses ( $m_i$ ) ranging from 1.0 to 3.6 GeV, the Coulomb coefficient  $B$  fit results are mass-dependent with the form  $B = B_0 \sqrt{1/m_i}$ .

Later, in a quenched lattice QCD, interquark potential study for  $q\bar{q}$  is carried out (Ikeda and Iida, 2012). Cornell-type fitting functions,  $V(r) = Ar - B/r + C$ , are one of the fitting functions.  $B$  are mass-dependent while constant quark masses  $m_q$  ranging from 0.52 to 1.275 GeV and determined by half of vector meson masses  $M_V$ , i.e.,  $m_q = M_V/2$ , according to the fitting results. The  $B = B_0 \sqrt{1/m_q}$  is the form of the Coulomb coefficient. Meanwhile, with the form  $A = a + b m_q$ , the string tension coefficient is linearly mass-dependent.

In accordance with the previous studies discussed above, we propose that  $A_{ij}$  and  $B_{ij}$  are mass-dependent coupling parameters, having the form,

$$A_{ij} = a + b m_{ij}, \quad B_{ij} = B_0 \sqrt{\frac{1}{m_{ij}}}. \quad (3.3)$$

where  $a$ ,  $b$ , and  $B_0$  are constants.  $m_{ij}$  are the  $i$ th and  $j$ th quark reduced masses which are defined as  $m_{ij} = \frac{2m_i m_j}{m_i + m_j}$ .

The hyperfine and Coulomb-like interactions coming from the same route of one gluon exchange are assumed. The mass-dependent hyperfine coefficient  $C_{ij}$  is denoted by the form,

$$C_{ij} = C_0 \sqrt{\frac{1}{m_{ij}}}. \quad (3.4)$$

Here,  $C_0$  is a constant. The quark color and spin operator are represented by  $\vec{\lambda}_i$

and  $\vec{\sigma}_i$  in Eq. (3.1) respectively. The color matrix elements are listed in Table 3.2.

**Table 3.2** Color matrix elements of tetraquarks.

$\hat{O}$	$\langle \psi_{6-\bar{6}}^c   \hat{O}   \psi_{6-\bar{6}}^c \rangle$	$\langle \psi_{3-\bar{3}}^c   \hat{O}   \psi_{3-\bar{3}}^c \rangle$
$\vec{\lambda}_1 \cdot \vec{\lambda}_2$	4/3	-8/3
$\vec{\lambda}_1 \cdot \vec{\lambda}_3$	-10/3	-4/3
$\vec{\lambda}_1 \cdot \vec{\lambda}_4$	-10/3	-4/3
$\vec{\lambda}_2 \cdot \vec{\lambda}_3$	-10/3	-4/3
$\vec{\lambda}_2 \cdot \vec{\lambda}_4$	-10/3	-4/3
$\vec{\lambda}_3 \cdot \vec{\lambda}_4$	4/3	-8/3
$\sum \vec{\lambda}_i \cdot \vec{\lambda}_j$	-32/3	-32/3

**Table 3.3** Spin matrix elements of  $qc\bar{q}\bar{c}$  and  $qq\bar{q}\bar{q}$  tetraquark states.

$\hat{O}$	$\psi_{0\otimes 0}^{S=0}$	$\psi_{1\otimes 1}^{S=0}$	$\psi_{1\otimes 0}^{S=1}$	$\psi_{1\otimes 1}^{S=1}$	$\psi_{1\otimes 1}^{S=2}$
$\vec{\sigma}_1 \cdot \vec{\sigma}_2$	-3	1	1	1	1
$\vec{\sigma}_1 \cdot \vec{\sigma}_3$	0	-2	0	-1	1
$\vec{\sigma}_1 \cdot \vec{\sigma}_4$	0	-2	0	-1	1
$\vec{\sigma}_2 \cdot \vec{\sigma}_3$	0	-2	0	-1	1
$\vec{\sigma}_2 \cdot \vec{\sigma}_4$	0	-2	0	-1	1
$\vec{\sigma}_3 \cdot \vec{\sigma}_4$	-3	1	-3	1	1
$\sum \vec{\sigma}_i \cdot \vec{\sigma}_j$	-6	-6	-2	-2	6

Tables 3.3 and 3.4 summarize the spin matrix elements for the spin combinations of  $qc\bar{q}\bar{c}$  and  $qq\bar{q}\bar{q}$  states, as listed in Eqs. (2.4) and (2.7), and the spin combinations of  $cc\bar{c}\bar{c}$  states, as listed in Eqs. (2.8) and (2.9), respectively.

### 3.2 Fixing model parameters

The light, charmed and bottom mesons mass spectra are evaluated in the Hamiltonian in Eq. (3.1), which are believed and treated as conventional  $q\bar{q}$  states. The comparison of the theoretical results and experimental data is listed in Table 3.5 with units in MeV. The deviation between the theoretical and experimental mean values,  $D = 100 \cdot (M^{exp} - M^{cal}) / M^{exp}$ , is listed in the last column, and  $M^{exp}$  is taken from PDG (Zyla et al., 2020).

**Table 3.4** Spin matrix elements of  $cc\bar{c}\bar{c}$  tetraquark states.

$\hat{O}$	$\psi_{(6\otimes\bar{6})(0\otimes 0)}^{C,S=0}$	$\psi_{(3\otimes\bar{3})(1\otimes 1)}^{C,S=0}$	$\psi_{(3\otimes\bar{3})(1\otimes 1)}^{C,S=1}$	$\psi_{(3\otimes\bar{3})(1\otimes 1)}^{C,S=2}$
$\vec{\sigma}_1 \cdot \vec{\sigma}_2$	-3	1	1	1
$\vec{\sigma}_1 \cdot \vec{\sigma}_3$	0	-2	-1	1
$\vec{\sigma}_1 \cdot \vec{\sigma}_4$	0	-2	-1	1
$\vec{\sigma}_2 \cdot \vec{\sigma}_3$	0	-2	-1	1
$\vec{\sigma}_2 \cdot \vec{\sigma}_4$	0	-2	-1	1
$\vec{\sigma}_3 \cdot \vec{\sigma}_4$	-3	1	1	1
$\sum \vec{\sigma}_i \cdot \vec{\sigma}_j$	-6	-6	-2	6

**Table 3.5** Meson states applied to fit the model parameters.

Meson	$M^{exp}$	$M^{cal}$	D(%)
$\Upsilon(1S)$	9460	9467	-0.07
$\Upsilon(2S)$	10023	10063	-0.40
$\eta_b$	9399	9404	-0.05
$\eta_b(2S)$	9999	10001	-0.02
$J/\psi$	3097	3092	0.16
$\psi(2S)$	3686	3674	0.32
$\psi(3S)$	4040	4048	-0.20
$\eta_c$	2984	2979	0.16
$\eta_c(2S)$	3638	3561	2.12
$B_s^*$	5415	5438	-0.42
$B_s^0$	5367	5309	1.08
$B^*$	5325	5371	-0.86
$B^0$	5279	5218	1.16
$D_s^*$	2112	2125	-0.61
$D_{s1}^*(2700)$	2708	2730	-0.81
$D_s$	1968	1980	-0.61
$D^*(2010)^0$	2010	2043	-1.64
$D^0$	1870	1876	-0.32
$\phi(1020)$	1020	1027	-0.69
$\phi(1680)$	1680	1658	1.31

Table 3.5 (Continued)

Meson	$M^{exp}$	$M^{cal}$	D(%)
$\rho(770)$	770	788	2.34
$\rho(1450)$	1450	1455	-0.34

The fitting results of four model coupling parameters and four constituent quark masses are as follows:

$$\begin{aligned}
 a &= 67413 \text{ MeV}^2, \quad b = 35 \text{ MeV}, \\
 B_0 &= 31.7 \text{ MeV}^{1/2}, \quad C_0 = -188.8 \text{ MeV}^{3/2}, \\
 m_{u,d} &= 380 \text{ MeV}, \quad m_s = 550 \text{ MeV}, \\
 m_c &= 1270 \text{ MeV}, \quad m_b = 4180 \text{ MeV}.
 \end{aligned} \tag{3.5}$$

The Hamiltonian in Eq. (3.1) is applied to predict the tetraquark masses with the predetermined as well as imported parameters .

## CHAPTER IV

### PREDICTION OF TETRAQUARK MASSES

The mass spectra of the 1S, 2S, and 3S fully-charm  $cc\bar{c}\bar{c}$  tetraquarks, as well as the 1S and 2S charmonium-like  $qc\bar{q}\bar{c}$  and light  $qq\bar{q}\bar{q}$  tetraquarks, are evaluated in Eq. (3.1). The complete bases defined in Chapter II are applied. Model parameters are predetermined in Chapter III. The hyperfine interaction  $H_{hyp}$  in Eq. (3.1) may mix up different color-spin configurations due to the cross terms,

$$\begin{aligned} \langle \psi_{3\otimes 3}^c \psi_{(0\otimes 0)}^{S=0} | \vec{\lambda}_i \cdot \vec{\lambda}_j \vec{\sigma}_i \cdot \vec{\sigma}_j | \psi_{6\otimes 6}^c \psi_{(1\otimes 1)}^{S=0} \rangle &= 8\sqrt{6}, \\ \langle \psi_{3\otimes 3}^c \psi_{(1\otimes 1)}^{S=0} | \vec{\lambda}_i \cdot \vec{\lambda}_j \vec{\sigma}_i \cdot \vec{\sigma}_j | \psi_{6\otimes 6}^c \psi_{(0\otimes 0)}^{S=0} \rangle &= 8\sqrt{6}. \end{aligned} \quad (4.1)$$

Eigenstates of the Hamiltonian are linear combinations of  $\psi_{3\otimes 3}^c \psi_{(0\otimes 0)}^{S=0}$  and  $\psi_{6\otimes 6}^c \psi_{(1\otimes 1)}^{S=0}$  as well as  $\psi_{3\otimes 3}^c \psi_{(1\otimes 1)}^{S=0}$  and  $\psi_{6\otimes 6}^c \psi_{(0\otimes 0)}^{S=0}$ . Thus, mixed states  $|\psi_{3\otimes 3}^c \psi_{(0\otimes 0)}^{S=0}, \psi_{6\otimes 6}^c \psi_{(1\otimes 1)}^{S=0}\rangle$  and  $|\psi_{3\otimes 3}^c \psi_{(1\otimes 1)}^{S=0}, \psi_{6\otimes 6}^c \psi_{(0\otimes 0)}^{S=0}\rangle$  are considered.

Listed in Tables 4.1, 4.2, and 4.3 are the theoretical results including mixed states for charmonium-like, light, and fully-charm tetraquarks of various quark configurations, respectively.

**Table 4.1** 1S and 2S  $qc\bar{q}\bar{c}$  tetraquark masses.

$J$	$qc\bar{q}\bar{c}$ configurations	M(1S)	M(2S)		
$J = 0$	$ \psi_{3\otimes 3}^c \psi_{(0\otimes 0)}^{S=0}, \psi_{6\otimes 6}^c \psi_{(1\otimes 1)}^{S=0}\rangle$	3824	4119	4232	4275
	$ \psi_{3\otimes 3}^c \psi_{(1\otimes 1)}^{S=0}, \psi_{6\otimes 6}^c \psi_{(0\otimes 0)}^{S=0}\rangle$	4012	4305	4419	4504
$J = 1$	$ \psi_{6\otimes 6}^c \psi_{(1\otimes 0)}^{S=1}\rangle$	4169	4539		
	$ \psi_{3\otimes 3}^c \psi_{(1\otimes 0)}^{S=1}\rangle$	4117	4512		
	$ \psi_{6\otimes 6}^c \psi_{(1\otimes 1)}^{S=1}\rangle$	4026	4395		
	$ \psi_{3\otimes 3}^c \psi_{(1\otimes 1)}^{S=1}\rangle$	4159	4554		
$J = 2$	$ \psi_{6\otimes 6}^c \psi_{(1\otimes 1)}^{S=2}\rangle$	4230	4599		
	$ \psi_{3\otimes 3}^c \psi_{(1\otimes 1)}^{S=2}\rangle$	4241	4636		

All the possible color-spatial-spin-flavor configurations of the  $qq$  cluster for  $\psi_{[2]}^c \psi_{[11]}^{osf}$  are listed in Eq. (2.5) and Eq. (2.6). All the possible isospins of the

**Table 4.2** 1S and 2S  $qq\bar{q}\bar{q}$  tetraquark masses.

$J$	$qq\bar{q}\bar{q}$ configurations	M(1S)		M(2S)	
$J = 0$	$ \psi_{3\otimes 3}^c \psi_{(0\otimes 0)}^{S=0}, \psi_{6\otimes 6}^c \psi_{(1\otimes 1)}^{S=0}\rangle$	1431	1812	1886	1986
	$ \psi_{3\otimes 3}^c \psi_{(1\otimes 1)}^{S=0}, \psi_{6\otimes 6}^c \psi_{(0\otimes 0)}^{S=0}\rangle$	1676	2041	2141	2252
$J = 1$	$ \psi_{6\otimes 6}^c \psi_{(1\otimes 0)}^{S=1}\rangle$	1858		2262	
	$ \psi_{3\otimes 3}^c \psi_{(1\otimes 0)}^{S=1}\rangle$	1823		2280	
	$ \psi_{6\otimes 6}^c \psi_{(1\otimes 1)}^{S=1}\rangle$	1678		2081	
	$ \psi_{3\otimes 3}^c \psi_{(1\otimes 1)}^{S=1}\rangle$	1875		2331	
$J = 2$	$ \psi_{6\otimes 6}^c \psi_{(1\otimes 1)}^{S=2}\rangle$	1936		2339	
	$ \psi_{3\otimes 3}^c \psi_{(1\otimes 1)}^{S=2}\rangle$	1978		2435	

**Table 4.3** 1S, 2S, and 3S  $cc\bar{c}\bar{c}$  tetraquark masses.

$J$	$cc\bar{c}\bar{c}$ configurations	M(1S)		M(2S)		M(3S)	
$J = 0$	$ \psi_{3\otimes 3}^c \psi_{(1\otimes 1)}^{S=0}, \psi_{6\otimes 6}^c \psi_{(0\otimes 0)}^{S=0}\rangle$	6389	6591	6785	6865	7088	7106
$J = 1$	$ \psi_{3\otimes 3}^c \psi_{(1\otimes 1)}^{S=1}\rangle$	6491		6907		7248	
$J = 2$	$ \psi_{3\otimes 3}^c \psi_{(1\otimes 1)}^{S=2}\rangle$	6548		6964		7305	

light tetraquark  $qq\bar{q}\bar{q}$  configurations are listed as follows:

For  $|\psi_{3\otimes 3}^c \psi_{(0\otimes 0)}^{S=0}, \psi_{6\otimes 6}^c \psi_{(1\otimes 1)}^{S=0}\rangle$ , since the configurations of  $qq$  cluster must be  $\psi_{[11]}^c \psi_{[2]}^o \psi_{[11]}^s \psi_{[11]}^f$  and  $\psi_{[2]}^c \psi_{[2]}^o \psi_{[2]}^s \psi_{[11]}^f$ , the isospin  $I = 0$ .

For  $|\psi_{3\otimes 3}^c \psi_{(1\otimes 1)}^{S=0}, \psi_{6\otimes 6}^c \psi_{(0\otimes 0)}^{S=0}\rangle$ , since the configurations of  $qq$  cluster must be  $\psi_{[11]}^c \psi_{[2]}^o \psi_{[2]}^s \psi_{[2]}^f$  and  $\psi_{[2]}^c \psi_{[2]}^o \psi_{[11]}^s \psi_{[2]}^f$ , the isospin  $I = 0, 1, 2$ .

For  $|\psi_{3\otimes 3}^c \psi_{(1\otimes 0)}^{S=1}\rangle$  and  $|\psi_{6\otimes 6}^c \psi_{(1\otimes 0)}^{S=1}\rangle$ , since the total flavor configurations must be  $\psi_{[2]}^f \otimes \psi_{[11]}^f$ , the isospin  $I = 1$ .

For  $|\psi_{6\otimes 6}^c \psi_{(1\otimes 1)}^{S=1}\rangle$  and  $|\psi_{6\otimes 6}^c \psi_{(1\otimes 1)}^{S=2}\rangle$ , since the total flavor configurations must be  $\psi_{[11]}^f \otimes \psi_{[11]}^f$ , the isospin  $I = 0$ .

For  $|\psi_{3\otimes 3}^c \psi_{(1\otimes 1)}^{S=1}\rangle$  and  $|\psi_{3\otimes 3}^c \psi_{(1\otimes 1)}^{S=2}\rangle$ , since the total flavor configurations must be  $\psi_{[2]}^f \otimes \psi_{[2]}^f$ , the isospin  $I = 0, 1, 2$ .

The possible color-spatial-spin-flavor configurations of the  $cc$  cluster are  $\psi_{[2]}^c \psi_{[2]}^o \psi_{[11]}^s \psi_{[2]}^f$  for  $\psi_{[2]}^c \psi_{[11]}^{osf}$ , and  $\psi_{[11]}^c \psi_{[2]}^o \psi_{[2]}^s \psi_{[2]}^f$  for  $\psi_{[11]}^c \psi_{[2]}^{osf}$ . Thus, the total flavor configurations must be  $\psi_{[2]}^f \otimes \psi_{[2]}^f$ , and the isospin  $I = 0, 1, 2$  for all fully-charm tetraquark  $cc\bar{c}\bar{c}$  configurations.

Since color-spatial-spin-flavor configurations are not considered for

charmonium-like tetraquark  $qc\bar{q}\bar{c}$  states due to the inexistence of identical quarks, the isospin can not be identified.



# CHAPTER V

## ASSIGNMENTS OF TETRAQUARK STATES

### 5.1 Tentative assignments of $qc\bar{q}\bar{c}$ tetraquark

Recent years in hadron physics is a revolutionary period due to the discovery of a number of exotic states. Charged charmonium-like mesons, which have a charmonium-like mass but are electrically charged, may be the most intriguing of the exotic particles (Albuquerque et al., 2019). Because of carrying one charge, the charged charmonium-like states are likely  $c\bar{c}u\bar{d}$  tetraquark states, which are beyond the normal  $c\bar{c}$  meson image. These exotic charmonium-like states are listed in Table 5.1. Throughout this discussion, we will refer to neutral states and charged states with hidden charm as  $X$  and  $Z_c$ , respectively.

$Z_c(4050)$  and  $Z_c(4250)$  have been observed together by Belle in the process  $\bar{B}^0 \rightarrow K^-(\pi^+\chi_{c1})$  (Mizuk et al., 2008). Tetraquark interpretations of the  $Z_c(4050)$  and  $Z_c(4250)$  are widely studied in various models.

In a non-relativistic quark model with a Cornell-like potential, the  $Z_c(4050)$  is studied as a molecular-like tetraquark states in the cluster of  $Q\bar{q}$  and  $\bar{Q}q$  (Patel et al., 2014). In the theoretical results,  $Z_c(4050)$  is associated with two predicted states. One state is with mass 4046 MeV and with quantum number  $J^{PC} = 2^{+-}$ , and another state is with mass 4054 MeV and with quantum number  $J^{PC} = 3^{++}$ . In a color flux-tube model, the  $Z_c(4050)$  is assigned to be a tetraquark  $(cu)(\bar{c}\bar{d})$  state in diquark-antidiquark picture with  $J^P = 1^-$ . The  $Z_c(4250)$  is also interpreted as a  $(cu)(\bar{c}\bar{d})$  tetraquark state with a different quantum number  $J^P = 1^+$  (Deng et al., 2015). The  $Z_c(4250)$  is also interpreted as a tetraquark state in a relativistic quark model, but there is no tetraquark candidate being found for the  $Z_c(4050)$  (Ebert et al., 2008).

Since both  $Z_c(4050)$  and  $Z_c(4250)$  are observed in the process  $\bar{B}^0 \rightarrow K^-\pi^+\chi_{c1}$  (Mizuk et al., 2008), supported by the present predictions, the  $Z_c(4050)$  and  $Z_c(4250)$  are assigned to be the tetraquark 1S states  $J = 0$  of the  $|\psi_{\bar{3}\otimes\bar{3}}^c\psi_{(1\otimes 1)}^{S=0}, \psi_{6\otimes\bar{6}}^c\psi_{(0\otimes 0)}^{S=0}\rangle$  mixed configuration, respectively.

$Z_c^+(4200)$  is observed by Belle in the  $\bar{B}^0 \rightarrow K^-(\pi^+J/\psi)$  decay process

**Table 5.1** Masses, widths and  $J^{PC}$  of  $X$  and  $Z_c$  states in the  $c\bar{c}$  region.

States	Mass (MeV)	Width (MeV)	$J^{PC}$	Process	Experiment
$X(3860)$	$3862^{+26+40}_{-32-13}$	$201^{+154+88}_{-67-82}$	$0^{++}$	$e^+e^- \rightarrow J/\psi(D\bar{D})$	Belle (Chilikin et al., 2017)
$X(3915)$	$3918.4 \pm 1.9$	$20 \pm 5$	$0/2^{++}$	$B \rightarrow K(J/\psi\omega)$	Belle (Choi et al., 2005)
$X(3940)$	$3942^{+7}_{-6} \pm 6$	$37^{+26}_{-15} \pm 18$	???	$e^+e^- \rightarrow J/\psi(D\bar{D}^*)$	Belle (Adachi et al., 2008)
$X(4160)$	$4156^{+25}_{-20} \pm 15$	$139^{+111}_{-61} \pm 21$	???	$e^+e^- \rightarrow J/\psi(D^*\bar{D}^*)$	Belle (Adachi et al., 2008)
$X(4350)$	$4350.6^{+4.6}_{-5.1} \pm 0.7$	$13^{+18}_{-9} \pm 4$	??+	$\gamma\gamma \rightarrow \phi J/\psi$	Belle (Shen et al., 2010)
$Z_c(3900)$	$3881 \pm 4 \pm 53$	$52 \pm 5 \pm 36$	$1^{+-}$	$e^+e^- \rightarrow (J/\psi\pi^+)\pi^-$	BESIII (Ablikim et al., 2017b)
$Z_c(4020)$	$4024.1 \pm 1.9$	$13 \pm 5$	??-	$e^+e^- \rightarrow \pi^-(\pi^+h_c)$	BESIII (Ablikim et al., 2013c)
$Z_c(4050)$	$4051^{+24}_{-40}$	$82^{+50}_{-28}$	??+	$\bar{B}^0 \rightarrow K^-(\pi^+\chi_{c1})$	Belle (Mizuk et al., 2008)
$Z_c(4055)$	$4054 \pm 3.2$	$45 \pm 13$	??-	$e^+e^- \rightarrow \pi^-(\pi^+\psi(2S))$	Belle (Wang et al., 2015)
	$4032.1 \pm 2.4$	$26.1 \pm 5.3$	??-	$e^+e^- \rightarrow \pi^+\pi^-\psi(2S)$	BESIII (Ablikim et al., 2017a)
$Z_c(4100)$	$4096 \pm 28$	$152^{+80}_{-70}$	$0^{++}/1^{+-}$	$B^0 \rightarrow K^+(\pi^-\eta_c)$	LHCb (Aaij et al., 2018)
$Z_c(4200)$	$4196^{+35}_{-32}$	$370^{+100}_{-150}$	$1^{+-}$	$\bar{B}^0 \rightarrow K^-(\pi^+J/\psi)$	Belle (Chilikin et al., 2014)
$Z_c(4250)$	$4248^{+190}_{-50}$	$177^{+320}_{-70}$	??+	$\bar{B}^0 \rightarrow K^-(\pi^+\chi_{c1})$	Belle (Mizuk et al., 2008)
$Z_c(4430)$	$4478^{+15}_{-18}$	$181 \pm 31$	$1^{+-}$	$\bar{B}^0 \rightarrow K^-(\pi^+J/\psi)$	Belle (Chilikin et al., 2014)

Table 5.2 Tentative assignments of 1S and 2S  $qc\bar{q}\bar{c}$  tetraquark states.

$J = 0$		$ \psi_{3\otimes 3}^c \psi_{(0\otimes 0)}^{S=0}, \psi_{6\otimes 6}^c \psi_{(1\otimes 1)}^{S=0}\rangle$	$ \psi_{3\otimes 3}^c \psi_{(1\otimes 1)}^{S=0}, \psi_{6\otimes 6}^c \psi_{(0\otimes 0)}^{S=0}\rangle$		
	The work	3824	4119	4232 4275	4012 4305 4419 4504
	Data	$X(3860)$	$Z_c(4100)$	... ..	$Z_c(4050)$ $Z_c(4250)$ ... ..
$J = 1$		$ \psi_{6\otimes 6}^c \psi_{(1\otimes 0)}^{S=1}\rangle$	$ \psi_{3\otimes 3}^c \psi_{(1\otimes 0)}^{S=1}\rangle$	$ \psi_{6\otimes 6}^c \psi_{(1\otimes 1)}^{S=1}\rangle$	$ \psi_{3\otimes 3}^c \psi_{(1\otimes 1)}^{S=1}\rangle$
	The work	4169	4539	4117 4512	4026 4395 4159 4554
	Data	$Z_c(4200)$	$Z_c(4430)$	... ..	$Z_c(4020)/Z_c(4055)$ ... .. $X(4160)$ ... ..
$J = 2$		$ \psi_{6\otimes 6}^c \psi_{(1\otimes 1)}^{S=2}\rangle$	$ \psi_{3\otimes 3}^c \psi_{(1\otimes 1)}^{S=2}\rangle$		
	The work	4230	4599	4241 4636	
	Data	...	...	...	...

with a significance of  $6.2\sigma$  while the quantum number  $J^P$  is assigned as  $1^+$  (Chilikin et al., 2014). Meanwhile, the evidence of  $Z^+(4430) \rightarrow \pi^+ J/\psi$  is found during studying the same process.

The  $Z_c^+(4430)$  is first observed by the Belle in  $B \rightarrow K(\pi^+\psi(2S))$  decay process in 2007 with a significance of  $6.5\sigma$  (Choi et al., 2008). A year later, a signal for  $Z_c^+(4430) \rightarrow \pi^+\psi(2S)$  is also observed during performing a Dalitz plot analysis of  $B^+ \rightarrow K\pi^+\psi(2S)$  by Belle (Mizuk et al., 2009). The existence of  $Z_c^-(4430)$  is confirmed by LHCb in  $B \rightarrow K^+\pi^-\psi(2S)$  decays with a model-independent approach with the quantum number  $J^P = 1^+$  determined unambiguously (Aaij et al., 2014; Aaij et al., 2015).

Tetraquark interpretations of the  $Z_c(4200)$  and  $Z_c(4430)$  are suggested in several model calculations. A  $(cu)(\bar{c}\bar{d})$  tetraquark state associated with  $Z_c(4200)$  with  $J^P = 1^+$  is predicted in a color flux-tube model. The interactions of quark-quark are considered through  $\sigma$  exchange, one boson exchange and one gluon exchange (Deng et al., 2018). The  $Z_c^+(4430)$  is widely interpreted as the 2S tetraquark state with a quark content  $cu\bar{c}\bar{d}$  (Ebert et al., 2008; Patel et al., 2014; Wang, 2015; Goerke et al., 2016; Agaev et al., 2017).

In a chromomagnetic model based on color magnetic interactions, both of the  $Z_c(4200)$  and  $Z_c(4430)$  are described as an tetraquark states with  $J^P = 1^+$  (Zhao et al., 2014a). In a light-front holographic QCD framework, a soft-wall model is generalized with a generic dilaton profile. Both of the  $Z_c(4200)$  and  $Z_c(4430)$  are categorized into tetraquark states with  $J = 1$ , and preferred having a generic dilaton profile (Guo et al., 2016).

Considering both  $Z_c(4200)$  and  $Z_c(4430)$  are observed while studying the process  $\bar{B}^0 \rightarrow K^-(\pi^+ J/\psi)$  with the same order decay widths (Chilikin et al., 2014), the  $Z_c(4200)$  and  $Z_c(4430)$  are naturally paired together. Therefore, the  $Z_c(4200)$  and  $Z_c(4430)$  may be assigned to be the 1S and 2S states, with  $J = 1$ , of the  $(6_c \otimes \bar{6}_c)(1_s \otimes 0_s)_{S=1}$  configuration, respectively.

The  $Z_c(4025)$  and  $Z_c(4020)$  are considered to be a same state nowadays in PDG (Zyla et al., 2020). The quantum numbers of the  $X(4020)$  except for the parity are not well determined. The quantum number assignment  $J^{PC} = 1^{+-}$  is assumed in all the experimental analyses from BESIII (Ablikim et al., 2013c; Ablikim et al., 2014c; Ablikim et al., 2014a; Ablikim et al., 2015b).

Tetraquark states in the diquark-antidiquark configuration are studied in a

color flux tube model, and the  $Z_c^+(4025)$  is assigned to be a tetraquark state with quantum number  $J^P = 2^+$  (Deng et al., 2014; Deng et al., 2015). However, more works support that the  $Z_c^+(4025)$  is a tetraquark state with quantum numbers  $1^{+-}$ . In a nonrelativistic quark model study with a Cornell-type potential, a tetraquark state of  $Q\bar{q}-\bar{Q}q$  with  $J^{PC} = 1^{+-}$  is predicted around 4036 MeV, which is associated with the  $Z_c(4025)$  (Patel et al., 2014).

The process  $e^+e^- \rightarrow \pi^+\pi^-h_c$  is studied by BESIII at c.m. energies from 3.90 to 4.42 GeV (Ablikim et al., 2013c). At 4.02 GeV, a distinct structure is observed in the  $\pi^\pm h_c$  mass spectrum, which is referred to the  $Z_c(4020)$ . The mass and width are measured to be  $(4022.9 \pm 0.8 \pm 2.7)$  MeV and  $(7.9 \pm 2.7 \pm 2.6)$  MeV for the  $Z_c(4020)$ , where the first errors are statistical and the second systematic.

Belle studies the process  $e^+e^- \rightarrow \pi^+\pi^-\psi(2S)$  via initial state radiation (ISR) using the 980  $fb^{-1}$  full data sample (Wang et al., 2015). In Fig. 5.1, the  $M_{max}[\pi^\pm\psi(2S)]$  distribution is showed, a structure at around 4.05 GeV can be seen. The mass and width are fitted to be  $(4054 \pm 3 \pm 1)$  MeV and  $(45 \pm 11 \pm 6)$  MeV with a significance of the signal  $3.5\sigma$ .

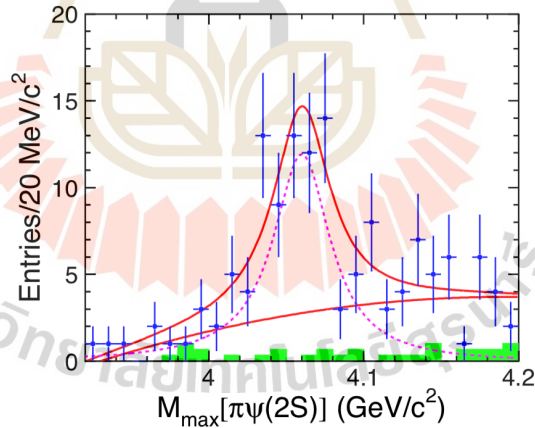


**Figure 5.1** The distributions of  $M_{max}[\pi^\pm\psi(2S)]$  from Belle (Wang et al., 2015).

Later, the same process  $e^+e^- \rightarrow \pi^+\pi^-\psi(2S)$  is studied by BESIII at c.m. energies from 4.0 to 4.6 GeV (Ablikim et al., 2017a). As shown in Fig.5.2, a narrow structure was observed around 4030 MeV in the  $M[\pi^\pm\psi(2S)]$  spectrum. The mass and width are measured to be  $(4032.1 \pm 2.4)$  MeV and  $(26.1 \pm 5.3)$  MeV with a much higher significance than Belle of  $9.2\sigma$ .

At the Charm 2018 meeting, a work (Bondar, 2018) of preliminary partial wave analysis (PWA) on the process  $e^+e^- \rightarrow \pi^+\pi^-\psi(2S)$  are reported by using BESIII

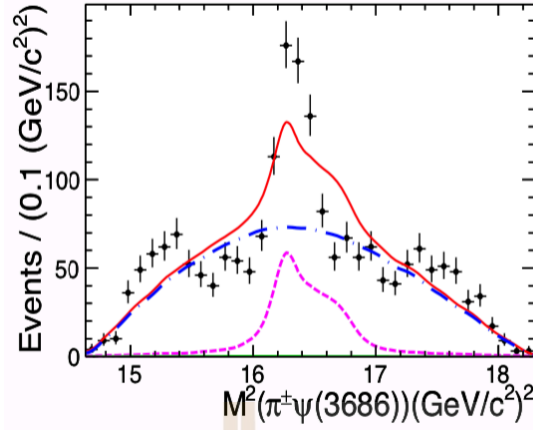


**Figure 5.2** The distributions of  $M[\pi^\pm\psi(2S)]$  at  $\sqrt{s} = 4.416$  GeV from BESIII (Ablikim et al., 2017a).

published results (Ablikim et al., 2017a) where the fit quality is much improved. The structure can be described well with a charged state, and the mass and width are fitted to be  $(4019.0 \pm 1.9)$  MeV and  $(29 \pm 4)$  MeV respectively, which is close to the mass of the  $Z_c(4020)$  state observed in the  $\pi^+\pi^-h_c$  final state (Ablikim et al., 2013c). Another decay mode of the  $Z_c(4020)$ ,  $Z_c(4020) \rightarrow \pi^+\psi(2S)$ , may be argued when such PWA results are identified later. Moreover,  $Z_c(4020)$  and  $Z_c(4055)$  might be the same state. Thus, both  $\pi^+\pi^-h_c$  and  $\pi^+\pi^-\psi(2S)$  final states need to be further investigated in order to fully understand the intermediate structures.

At this moment, we may just assign either  $Z_c(4020)$  or  $Z_c(4055)$ , if they are not the same particle, to be the  $(6_c \otimes \bar{6}_c)(1_s \otimes 1_s)_{s=1}$  configuration tetraquark 1S states with  $J = 1$ .

The  $Z_c^-(4100)$  is observed in the  $\eta_c(1S)\pi^-$  invariant mass distribution in  $B^0 \rightarrow \eta_c(1S)K^+\pi^-$  decay process with a significance  $3.4\sigma$  by LHCb (Aaij et al., 2018). The mass splitting among tetraquark states including  $Z_c(4100)$  is studied in a simple chromomagnetic model (Wu et al., 2019). The model is based on the idea that the chromomagnetic interaction term in the one gluon exchange potential give the mainly contribution to the mass splitting among the same quark content hadron states. The  $Z_c(4100)$  is assigned to be a  $0^{++}(c\bar{q})(\bar{c}q)$  tetraquark state.

In our assignments,  $Z_c(4100)$  is assigned to be tetraquark 1S state, with  $J = 0$ , of the  $|\psi_{3\otimes 3}^c \psi_{(0\otimes 0)}^{S=0}, \psi_{6\otimes \bar{6}}^c \psi_{(1\otimes 1)}^{S=0}\rangle$  mixed configuration.

In the present model, there is no room for the  $Z_c(3900)$  in the scenario of tetraquark states. The  $Z_c^+(3900)$  state can be explained in two ways: as a

charged diquark-antidiquark  $(cu)(\bar{c}\bar{d})$  state or as a  $D\bar{D}^*$  molecular state. In the molecular-like tetraquark studies (Zhao et al., 2014b; He, 2014; Prelovsek and Leskovec, 2013; Chen et al., 2014), the  $Z_c^+(3900)$  can not be accommodated as a  $J^P = 1^+ D\bar{D}^*$  molecule state. In the works (Wang and Huang, 2014; Aceti et al., 2014; Ke and Li, 2016), however, a  $D\bar{D}^*$  molecular state interpretation is compatible with the  $Z_c(3900)$  and the  $Z_c(3900)$  can be interpreted as a axial vector moleculelike state with  $J^{PC} = 1^{+-}$ .

Except the assignments discussed above, the  $X(3860)$  is tentatively assigned to be the  $|\psi_{\bar{3}\otimes\bar{3}}^c \psi_{(0\otimes 0)}^{S=0}, \psi_{6\otimes\bar{6}}^c \psi_{(1\otimes 1)}^{S=0}\rangle$  mixed configuration tetraquark 1S state with  $J = 0$ , and the  $X(4160)$  is tentatively assigned to be the  $(\bar{3}_c \otimes 3_c)(1_s \otimes 1_s)_{S=1}$  configuration tetraquark ground state with  $J = 1$ , due to the mass matching.

Here, in Table 5.2, the work has assigned seven in eight charged charmonium-like tetraquark states observed by experimental collaborations. To make unambiguous assignments, more theoretical works and experimental data are required. Furthermore, in the present tetraquark state scenario, there is no room for the  $X(3915)$ ,  $X(3940)$ , and  $X(4350)$  in the 1S and 2S states.

## 5.2 Tentative assignments of $qq\bar{q}\bar{q}$ tetraquark

The meson mass spectrum has been studied by using the quark model for more than a half century. Especially, the heavy (c and b) flavor sector is well described by the NQM, and the predictions of NQM are accurate even for higher excited states. However, in the light meson region, the problem of understanding some exotic light mesons, firstly  $f_0$  states, has puzzled people for many years. Listed in Table 5.3 are the masses, widths,  $J^{PC}$ , and decay processes of these exotic mesons which are going to be reviewed and discussed separately in this section.

For the states with  $J^{PC} = 0^{++}$ , three isoscalar resonances: the  $f_0(1370)$ ,  $f_0(1500)$ , and  $f_0(1710)$  which are likely non- $q\bar{q}$  candidates are mainly reviewed in (Zyla et al., 2020). One conclusion reached is that none of the proposed  $q\bar{q}$  ordering schemes in scalar multiplets is completely satisfactory. The  $f_0(1370)$  and  $f_0(1500)$  decay mostly into pions ( $2\pi$  and  $4\pi$ ), and the  $f_0(1710)$  decays mainly into  $K\bar{K}$  final states. Naively, one implies an  $n\bar{n}(=u\bar{u} + d\bar{d})$  structure for the  $f_0(1370)$  and  $f_0(1500)$ , and an  $s\bar{s}$  structure for the  $f_0(1710)$ .

However, the  $1^3P_0$  state is always the lightest state in the three  $1^3P_J$

**Table 5.3** Masses, widths and  $J^{PC}$  of the  $qq\bar{q}\bar{q}$  tetraquark candidates.

States	M(MeV)	$\Gamma$	$J^{PC}$	Process	Experiment
$f_0(1500)$	$1473 \pm 5$	$108 \pm 9$	$0^{++}$	$p\bar{p} \rightarrow (\eta\eta)\pi$	E835(Uman et al., 2006)
$f_0(1710)$	$1759 \pm 6_{-25}^{+14}$	$172 \pm 10_{-16}^{+32}$	$0^{++}$	$J/\psi \rightarrow \gamma(\eta\eta)$	BESIII(Ablikim et al., 2013b)
		$125 \pm 25_{-15}^{+10}$	$0^{++}$	$\psi(2s) \rightarrow \gamma\pi^+\pi^-(K^+K^-)$	BES(Ablikim et al., 2005b)
$X(1840)$	$1842 \pm 4_{-3}^{+7}$	$83 \pm 14 \pm 11$	???	$J/\psi \rightarrow \gamma\mathcal{B}(\pi^+\pi^-)$	BESIII(Ablikim et al., 2013d)
$f_0(2020)$	$2037 \pm 8$	$296 \pm 17$	$0^{++}$	$p\bar{p} \rightarrow (\eta\eta)\pi$	E835(Uman et al., 2006)
$f_0(2100)$	$2081 \pm 13_{-36}^{+24}$	$273_{-24-23}^{+27+70}$	$0^{++}$	$J/\psi \rightarrow \gamma(\eta\eta)$	BESIII(Ablikim et al., 2013b)
$f_0(2200)$	$2170 \pm 20_{-15}^{+10}$	$220 \pm 60_{-45}^{+40}$	$0^{++}$	$\psi(2s) \rightarrow \gamma\pi^+\pi^-(K^+K^-)$	BES(Ablikim et al., 2005b)
$h_1(1595)$	$1594 \pm 15_{-60}^{+10}$	$384 \pm 60_{-100}^{+70}$	$1^{+-}$	$\pi^-p \rightarrow (\omega\eta)n$	BNL-E852(Eugenio et al., 2001)
$b_1(1960)$	$1960 \pm 35$	$230 \pm 50$	$1^{+-}$	$p\bar{p} \rightarrow \omega\pi^0, \omega\eta\pi^0, \pi^+\pi^-$	SPEC(Anisovich et al., 2002a)
$h_1(1965)$	$1965 \pm 45$	$345 \pm 75$	$1^{+-}$	$p\bar{p} \rightarrow \omega\eta, \omega\pi^0\pi^0$	SPEC(Anisovich et al., 2002b)
$b_1(2240)$	$2240 \pm 35$	$320 \pm 85$	$1^{+-}$	$p\bar{p} \rightarrow \omega\pi^0, \omega\eta\pi^0, \pi^+\pi^-$	SPEC(Anisovich et al., 2002a)
$X_2(1930)$	$1930 \pm 25$	$450 \pm 50$	$2^{++}$	$\pi^-p \rightarrow (\eta\eta)n$	GAMS(Binon et al., 2005)
$X_2(1980)$	$1980 \pm 2 \pm 14$	$297 \pm 12 \pm 6$	$2^{++}$	$\gamma\gamma \rightarrow (K^+K^-)$	BELL(Abe et al., 2003)
$f_2(2300)$	$2327 \pm 9 \pm 6$	$275 \pm 36 \pm 20$	$2^{++}$	$\gamma\gamma \rightarrow (K^+K^-)$	BELL(Abe et al., 2003)
$f_2(2340)$	$2362_{-30-63}^{+31+140}$	$334_{-54-100}^{+62+165}$	$2^{++}$	$J/\psi \rightarrow \gamma(\eta\eta)$	BESIII(Ablikim et al., 2013b)

**Table 5.4** Tentative assignments of 1S and 2S  $q\bar{q}q\bar{q}$  tetraquark states.

$J = 0$	The work	1431	1812	1886	1986	1676	2041	2141	2252
	Data	$f_0(1500)$	...	...	$f_0(2020)$	$f_0(1710)$	$f_0(2020)$	$f_0(2100)$	$f_0(2200)$
$J = 1$	The work	1858	2262	1823	2280	1678	2081	1875	2331
	Data	$b_1(1960)$	$b_1(2240)$	...	...	$h_1(1595)$	$h_1(1965)$	...	...
$J = 2$	The work	1936	2339	1978	2435				
	Data	$X_2(1930)$	$f_2(2340)$	$X_2(1980)$	$f_2(2300)$				

states ( $J = 0, 1, 2$ ) in potential model studies (Godfrey and Isgur, 1985; Vijande et al., 2005; Ebert et al., 2009; Xiao et al., 2019; Li et al., 2021), which is confirmed in the observation of the  $\chi_{cJ}(1P)$  and  $\chi_{bJ}(1P)$  for charmonium and bottomonium mesons respectively. Since the mass splitting between  $\chi_{c0}(1P)$  and  $\chi_{c2}(1P)$  is around 150 MeV, and the mass splitting between  $\chi_{b0}(1P)$  and  $\chi_{b2}(1P)$  is around 50 MeV (Zyla et al., 2020), one may conclude that the  $1^3P_0$   $n\bar{n}$  and  $s\bar{s}$  states should be obviously lighter than  $1^3P_2$   $n\bar{n}$  and  $s\bar{s}$  states which are widely accepted as the  $f_2(1270)$  and  $f_2'(1525)$  respectively (Amsler and Tornqvist, 2004). Thus, the  $f_0(1500)$  and  $f_0(1710)$  are too heavy to be accommodated as conventional mesons.

In  $\gamma\gamma$  collisions, both of the  $f_0(1500)$  and  $f_0(1710)$  are not observed by ALEPH in  $\gamma\gamma \rightarrow \pi^+\pi^-$  (Barate et al., 2000), and the  $f_0(1500)$  is also not observed by Belle in  $\gamma\gamma \rightarrow \pi^0\pi^0$  (Uehara et al., 2008), which does not favor an  $n\bar{n}$  interpretation for the  $f_0(1500)$ . Several glueball interpretations are proposed: the  $f_0(1370)$  is mainly  $n\bar{n}$ , the  $f_0(1500)$  mainly glueball, the  $f_0(1710)$  dominantly  $s\bar{s}$  (Amsler and Close, 1996; Close and Kirk, 2001), or the  $f_0(1710)$  as the glueball (Janowski et al., 2014; Br unner and Rebhan, 2015).

The  $f_0(1710)$  and  $f_2(2200)$  are observed by Belle in  $\gamma\gamma \rightarrow K_S^0 K_S^0$  (Uehara et al., 2013). The mass, total width, and decay branching fraction to the  $K\bar{K}$  state  $\Gamma_{\gamma\gamma} B(K\bar{K})$  are measured. One conclusion is that the  $f_0(1710)$  and  $f_2(2200)$  are unlikely to be glueballs because their total widths and  $\Gamma_{\gamma\gamma} B(K\bar{K})$  values are much larger than those expected for a pure glueball state. The  $f_0(1500)$  is observed by BESII in  $J/\psi \rightarrow \gamma\pi\pi$  (Ablikim et al., 2006) and by BESIII in  $J/\psi \rightarrow \gamma\eta\eta$  (Ablikim et al., 2013b) with a much smaller rate than for the  $f_0(1710)$ , which speaks against a glueball interpretation of the  $f_0(1500)$ . Recently, the  $f_0(1500)$  is studied in the framework of supersymmetric light front holographic QCD (LFHQCD) and identified as a isoscalar tetraquark (Zou et al., 2019).

As the review and discussion above, neither a conventional meson nor a glueball interpretation for the  $f_0(1500)$  and  $f_0(1710)$  is completely satisfactory.

The  $f_0(1370)$  is assigned to be the  $1^3P_0$   $s\bar{s}$  state by a recently quark model study of  $s\bar{s}$  meson mass spectrum (Li et al., 2021), which is consistent with quark model mass spectrum studies (Xiao et al., 2019; Vijande et al., 2005; Ebert et al., 2009) but conflicts with the experimental conclusion that the  $f_0(1370)$  decays mostly into pions. Actually, since the average mass of the  $f_0(1370)$  is from 1200 MeV to 1500 MeV (Zyla et al., 2020), the broad  $f_0(1370)$  resonance may

correspond to two different states, each with the  $n\bar{n}$  or  $s\bar{s}$  content. Therefore, some resonances around 1370 MeV observed in the  $K\bar{K}$  channel might be good candidates for the  $1^3P_0$   $s\bar{s}$  state (Li et al., 2021).

Since both the  $f_0(1500)$  and  $f_0(2020)$  were observed by E835 in the process  $p\bar{p} \rightarrow (\eta\eta)\pi$  (Uman et al., 2006), we may group the  $f_0(1500)$  and  $f_0(2020)$  to be the 1S and 2S states respectively, with  $J = 0$ , of the  $|\psi_{3\otimes 3}^c \psi_{(0\otimes 0)}^{S=0}, \psi_{6\otimes 6}^c \psi_{(1\otimes 1)}^{S=0}\rangle$  mixed configuration.

Considering that both the  $f_0(1710)$  and  $f_0(2100)$  were observed by BESIII in the process  $J/\psi \rightarrow \gamma(\eta\eta)$  (Ablikim et al., 2013b), and the  $f_0(2020)$  was observed by E835 in the process  $p\bar{p} \rightarrow (\eta\eta)\pi$  and their decay widths are in the same order (Uman et al., 2006), and both the  $f_0(1710)$  and  $f_0(2200)$  were observed by BES in the process  $\psi(2s) \rightarrow \gamma\pi^+\pi^-(K^+K^-)$  with the same order decay widths (Ablikim et al., 2005b), we may assign the  $f_0(1710)$  and  $f_0(2020)$  to be the 1S states, the  $f_0(2100)$  and  $f_0(2200)$  to be the 2S state with  $J = 0$  of the  $|\psi_{3\otimes 3}^c \psi_{(1\otimes 1)}^{S=0}, \psi_{6\otimes 6}^c \psi_{(0\otimes 0)}^{S=0}\rangle$  mixed configuration, respectively.

Two states with masses 1815 and 1890 MeV are predicted in the calculation, which are close to  $X(1835)$  and  $X(1840)$ . The  $X(1835)$  is interpreted as a baryonium (Wang, 2011; Deng et al., 2012; Deng et al., 2013) or the second radial excited state of  $\eta'(958)$  (Liu et al., 2010; Yu et al., 2011). The  $X(1835)$  has been observed and confirmed mainly by BESIII since 2005 (Ablikim et al., 2005a; Ablikim et al., 2012; Ablikim et al., 2013d; Ablikim et al., 2015a; Ablikim et al., 2016), with the mass determined ranging from 1825 to 1910 MeV in various decay processes. The  $X(1840)$  listed in Table 5.3 is observed in the decay process  $J/\psi \rightarrow \gamma 3(\pi^+\pi^-)$  (Ablikim et al., 2013d), and can theoretically take the  $0^{++}$  quantum numbers. More experimental data in the 1800 – 1900 MeV region are essential to reveal whether there might be more resonances in the mass region.

Two well established  $2^{++}$  states, the  $f_2(1270)$  and  $f_2'(1525)$ , are widely accepted as the isoscalar  $1^3P_2$  mesons for  $n\bar{n}$  and  $s\bar{s}$  structure respectively (Amsler and Tornqvist, 2004), which is consistent with the theoretical predictions of mesons (Godfrey and Isgur, 1985; Vijande et al., 2005; Ebert et al., 2009; Xiao et al., 2019; Li et al., 2021). At higher masses, the  $f_2(1950)$  and  $f_2(2010)$  appear to be solid (Zyla et al., 2020), and the  $f_2(2010)$  is assigned to be the  $2^3P_2$   $s\bar{s}$  state while the  $f_2(1950)$  does not fit into quark model spectrum easily (Ebert et al., 2009; Li et al., 2021). Another two established tensor states, the  $f_2(2300)$  and  $f_2(2340)$ , do

not fit into quark model spectrum either.

The broad  $f_2(1950)$  has been observed in several processes decaying to  $4\pi$  (Barberis et al., 2000),  $\eta\eta$  (Binon et al., 2005), and  $K^+K^-$  (Abe et al., 2003). Based on assuming that the  $\eta\eta$  and the  $K^+K^-$  are the dominant decay modes of the  $f_2(1950)$ , the  $f_2(1950)$  is unlikely to be  $n\bar{n}$  state. And it may not be a  $s\bar{s}$  state too since the  $2^3P_2$   $s\bar{s}$  state is occupied by the  $f_2(2010)$  (Li et al., 2021). Meanwhile, the big mass difference of the two  $f_2(1950)$  determined in the two processes  $\pi^-p \rightarrow (\eta\eta)n$  (Binon et al., 2005) and  $\gamma\gamma \rightarrow (K^+K^-)$  (Abe et al., 2003) leads us to propose that they are likely two different states. We may use the  $X_2(1930)$  and  $X_2(1980)$  to represent the states of  $\eta\eta$  and  $K^+K^-$  decay modes respectively.

Since both the  $X_2(1980)$  and  $f_2(2300)$  are observed in the process  $\gamma\gamma \rightarrow (K^+K^-)$  with the similar decay widths (Abe et al., 2003), one may naturally pair the  $X_2(1980)$  and  $f_0(2300)$  together. Therefore, we may assign the  $X_2(1980)$  and  $f_0(2300)$  to be the 1S and 2S states, with  $J = 2$ , of the  $(6_c \otimes \bar{6}_c)(1_s \otimes 1_s)_{S=2}$  configuration, respectively.

Since both the  $X_2(1930)$  and  $f_2(2340)$  can decay to  $\eta\eta$  and their decay widths are in the same order, we may group the  $X_2(1930)$  and  $f_2(2340)$  to be the 1S and 2S tetraquark states respectively, with  $J = 2$ , of the  $(\bar{3}_c \otimes 3_c)(1_s \otimes 1_s)_{S=2}$  configuration.

With  $J^{PC} = 1^{+-}$ , the  $h_1(1170)$  and  $h_1(1415)$  are convinced ground states of  $n\bar{n}$  and  $s\bar{s}$  isoscalar mesons respectively, and the  $b_1(1235)$  is the ground state of isovector mesons in quark model (Godfrey and Isgur, 1985; Li et al., 2021; Zyla et al., 2020). However, the  $h_1(1595)$  observed by BNL-E852 in the  $\pi^-p \rightarrow (\omega\eta)n$  process (Eugenio et al., 2001), the  $h_1(1965)$  with a mainly decay channel  $\omega\eta$  (Anisovich et al., 2002b), and the  $b_1(1960)$  and  $b_1(2240)$  observed in the process  $p\bar{p} \rightarrow \omega\pi^0, \omega\eta\pi^0, \pi^+\pi^-$  (Anisovich et al., 2002a) do not fit into the  $q\bar{q}$  meson mass spectrum.

The main decay channel of the  $h_1(1595)$  and  $h_1(1965)$ ,  $\omega\eta$ , is observed for neither the  $h_1(1170)$  nor  $h_1(1415)$  while the decay widths of the  $h_1(1595)$  and  $h_1(1965)$  are in the same order, one may tentatively pair the  $h_1(1595)$  and  $h_1(1965)$  together and separate them from conventional mesons. We may group the  $h_1(1595)$  and  $h_1(1965)$  to be the 1S and 2S states respectively, with  $J = 1$ , of the  $(6_c \otimes \bar{6}_c)(1_s \otimes 1_s)_{S=1}$  configuration.

We may tentatively assign the  $b_1(1960)$  and  $b_1(2240)$  to be the 1S and 2S states, with  $J = 1$ , of the  $(6_c \otimes \bar{6}_c)(1_s \otimes 0_s)_{S=1}$  configuration, respectively. The  $b_1(1960)$  and  $b_1(2240)$  are paired since they are observed in the process  $p\bar{p} \rightarrow \omega\pi^0, \omega\eta\pi^0, \pi^+\pi^-$  (Anisovich et al., 2002a) and their decay widths are in the same order. There are very rare experimental data for  $b_1$  states except for the established  $b_1(1235)$ , and the  $b_1(1960)$  and  $b_1(2240)$  are not established states in PDG (Zyla et al., 2020). More experimental data for  $b_1$  states are required to make more unambiguous assignments.

As shown in Table 5.4, the 1S and 2S  $0^{++}$ ,  $1^{+-}$ , and  $2^{++}$  light tetraquark states predicted in the work have been tentatively matched with experimental data in pairs. We have provided in the work a possible tetraquark interpretation for exotic meson states. For the interpretation that those exotic particles might be the mixture of  $q\bar{q}$  meson, glueball, and tetraquark, one may refer to (Klempt, 2021; Sarantsev et al., 2021).

### 5.3 The first $cc\bar{c}\bar{c}$ tetraquark candidate: $X(6900)$

The LHCb collaboration has reported evidence for at least one resonance in the  $J/\psi$ -pair spectrum around 6900 MeV (Aaij et al., 2020). As illustrated in Figure 5.3 adapted from figure S3 in (Aaij et al., 2020), the data also revealed a broader structure centered about 6500 MeV. Such states have the valence-quark content  $cc\bar{c}\bar{c}$ , making them the first all-heavy multiquark exotic candidates reported in the experimental literature to date. The mass and width of the resonance around 6900 MeV are measured to be:

$$M[X(6900)] = 6905 \pm 11 \pm 7, \quad (5.1)$$

$$\Gamma[X(6900)] = 80 \pm 19 \pm 33,$$

and in the second fitting model,

$$M[X(6900)] = 6886 \pm 11 \pm 11, \quad (5.2)$$

$$\Gamma[X(6900)] = 168 \pm 33 \pm 69.$$

The theoretical predictions, as given in Table 4.3, support assigning the  $X(6900)$  to be the 2S fully-charm tetraquark state in the  $\bar{3}_c \otimes 3_c$  configuration, with

$J = 1$ . Meanwhile, with  $J = 1$ , the 1S and 3S states of fully-charm tetraquarks are about 6491 and 7248 MeV, respectively, in the  $\bar{3}_c \otimes 3_c$  configuration, which is consistent with the experimental data in Figure 5.3.

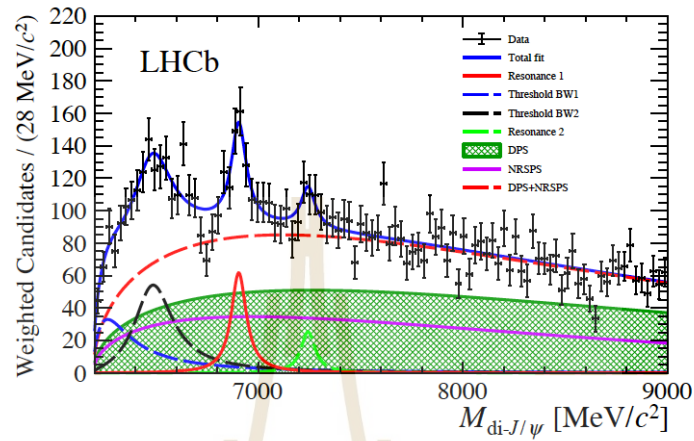


**Figure 5.3** Invariant mass spectra of weighted di- $J/\psi$  candidates (Aaij et al., 2020).

For comparison, our numerical results and some typical results of other works are collected in Table 5.5 with units in MeV. Including our results, the predictions from non-relativistic quark models which consider both confining and OGE Coulomb-like potentials are compatible (Wang et al., 2019; Liu et al., 2019; Ader et al., 1982; Lloyd and Vary, 2004). Similar results are given in a QCD sum rules work (Chen et al., 2020). Without considering color configurations, the works (Barnea et al., 2006; Berezhnoy et al., 2012; Wang, 2017; Wang and Di, 2019; Debastiani and Navarra, 2019) give smaller masses.

**Table 5.5** Present predictions of 1S state  $c\bar{c}c\bar{c}$  tetraquark masses compared with others.

$c\bar{c}c\bar{c}$	$J = 0$			$J = 1$	$J = 2$
	$ \psi_{3\otimes 3}^c, \psi_{(1\otimes 1)}^{S=0}\rangle,  \psi_{6\otimes 6}^c, \psi_{(0\otimes 0)}^{S=0}\rangle$	$ \psi_{3\otimes 3}^c, \psi_{(1\otimes 1)}^{S=1}\rangle$	$ \psi_{3\otimes 3}^c, \psi_{(1\otimes 1)}^{S=2}\rangle$		
Ours	(6389, 6591)	6491		6548	
(Wang et al., 2019)	6383-6421	6420-6436	6425-6450	6432-6479	
(Liu et al., 2019)	6518	6487	6500	6524	
(Lloyd and Vary, 2004)	6695	6477	6528	6573	
(Ader et al., 1982)	6383	6437	6437	6437	
(Chen et al., 2020)	6440-6820	6460-6470	6370-6510	6370-6510	
(Barnea et al., 2006)		6038-6115	6101-6176	6172-6216	
(Berezhnoy et al., 2012)		5966	6051	6223	
(Wang, 2017; Wang and Di, 2019)		5990	6050	6090	
(Debastiani and Navarra, 2019)		5969	6021	6115	

## CHAPTER VI

### CONCLUSIONS

We compared the experimental data and theoretical results of light, charmed, and bottom mesons to fit the model parameters. The predetermined model parameters are applied to calculate the  $qc\bar{q}\bar{c}$  and  $qq\bar{q}\bar{q}$  tetraquark masses of 1S and 2S states, as well as the  $cc\bar{c}\bar{c}$  tetraquark masses of 1S, 2S, and 3S states.

The predicted 1S and 2S  $qc\bar{q}\bar{c}$  tetraquark states and the  $X$  and  $Z_c$  particles have been tentatively matched. Some charmonium-like  $qc\bar{q}\bar{c}$  tetraquark states predicted in this work can not be matched with observed particles. Experimental searchings in the processes  $e^+e^- \rightarrow \pi^\mp(\pi^\pm h_c), \pi^\mp(\pi^\pm \psi(2S))$  for higher mass resonances, most likely the first radial excited states of  $Z_c(4020)$ , and  $Z_c(4055)$ , might be suggested.

The  $X(6900)$  detected by LHCb is likely the 2S  $cc\bar{c}\bar{c}$  tetraquark state in the  $\bar{3}_c \otimes 3_c$  color configuration, with  $J = 1$ . The  $cc\bar{c}\bar{c}$  tetraquarks in the  $J = 1$   $\bar{3}_c \otimes 3_c$  color configuration may have 1S and 3S states of 6491 MeV and 7248 MeV, respectively.

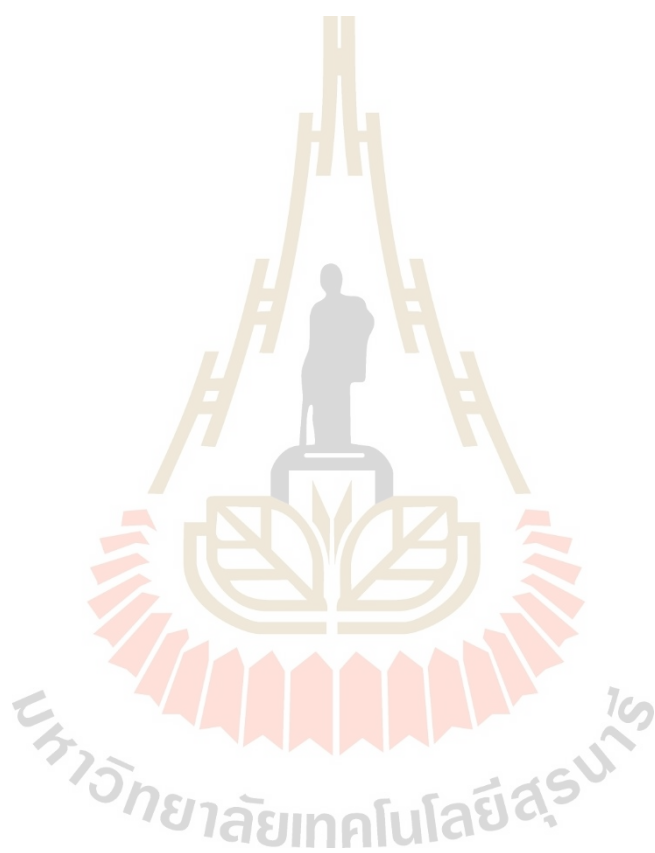
A tentative matching has been made between the predicted 1S and 2S light tetraquark states and the believed exotic mesons.

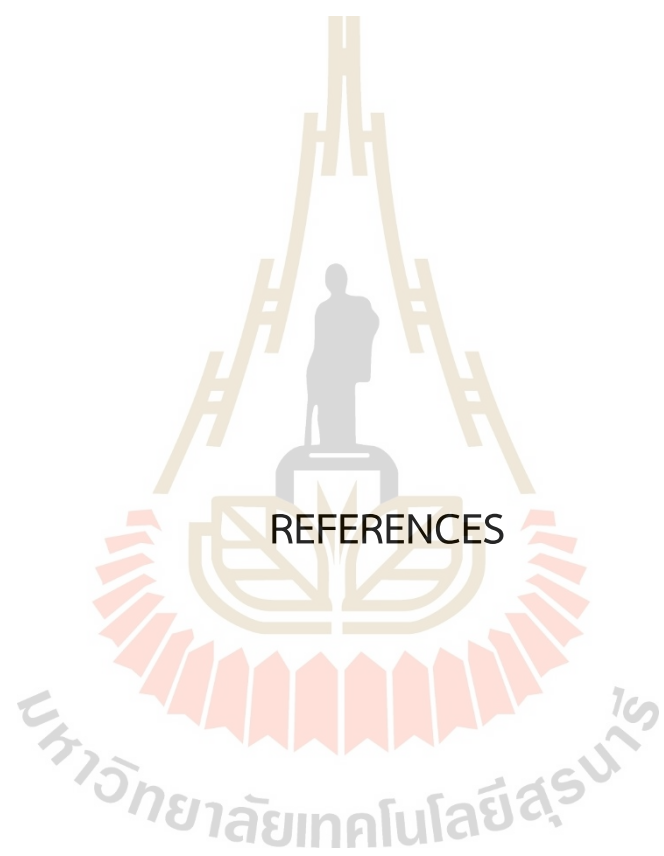
For  $J = 0$  states, the work suggests that the  $f_0(1500)$  and  $f_0(2200)$  might be the 1S and 2S states respectively of the  $|\psi_{\bar{3}\otimes\bar{3}}^c \psi_{(0\otimes 0)}^{S=0}, \psi_{6\otimes\bar{6}}^c \psi_{(1\otimes 1)}^{S=0}\rangle$  mixed configuration, and that the  $f_0(1710)$ , and the  $f_0(2020)$  and  $f_0(2100)$  might be the 1S and 2S states of the  $|\psi_{\bar{3}\otimes\bar{3}}^c \psi_{(1\otimes 1)}^{S=0}, \psi_{6\otimes\bar{6}}^c \psi_{(0\otimes 0)}^{S=0}\rangle$  mixed configuration, respectively.

For  $J = 2$  states, we first assume that the  $f_2(1950)$  may represent two different resonances because of the large mass difference of the  $f_2(1950)$  determined in the two processes  $\pi^-p \rightarrow (\eta\eta)n$  (Binon et al., 2005) and  $\gamma\gamma \rightarrow (K^+K^-)$  (Abe et al., 2003). Then we have tentatively assigned the  $X_2(1980)$  and  $f_0(2300)$  to be the 1S and 2S states of the  $(6_c \otimes \bar{6}_c)(1_s \otimes 1_s)_{S=2}$  configuration, respectively, and the  $X_2(1930)$  and  $f_2(2340)$  to be the 1S and 2S tetraquark states respectively of the  $(\bar{3}_c \otimes 3_c)(1_s \otimes 1_s)_{S=2}$  configuration.

For  $J = 1$  states, the work supports that the  $h_1(1595)$  might be the 1S light tetraquark state of the  $(6_c \otimes \bar{6}_c)(1_s \otimes 1_s)_{S=1}$  configuration, and the  $h_1(1965)$

might be the 2S state of the  $h_1(1595)$ . The assignment of the  $b_1(1960)$  and  $b_1(2240)$  is rather ambiguous in the work, that is, the  $b_1(1960)$  and  $b_1(2240)$  may be paired to be the 1S and 2S states respectively of the  $(6_c \otimes \bar{6}_c)(1_s \otimes 0_s)_{S=1}$  configuration.





REFERENCES

## REFERENCES

- Aaij, R., Adeva, B., Adinolfi, M., Affolder, A., Ajaltouni, Z., Akar, S., Albrecht, J., Alessio, F., Alexander, M., Ali, S., Alkhazov, G., Cartelle, P. A., Jr, A. A., Amato, S., Amerio, S., et al. (2015). Model-independent confirmation of the  $Z(4430)^-$  state. *Physical Review D*, 92(11), 112009.
- Aaij, R., Adeva, B., Adinolfi, M., Affolder, A., Ajaltouni, Z., Albrecht, J., Alessio, F., Alexander, M., Ali, S., Alkhazov, G., Cartelle, P. A., Jr, A. A., Amato, S., Amerio, S., Amhis, Y., et al. (2014). Observation of the resonant character of the  $Z(4430)^-$  state. *Physical Review Letters*, 112(22), 222002.
- Aaij, R., Beteta, C. A., Ackernley, T., Adeva, B., Adinolfi, M., Afsharnia, H., Aidala, C., Aiola, S., Ajaltouni, Z., Akar, S., Albrecht, J., Alessio, F., Alexander, M., Albero, A. A., Aliouche, Z., et al. (2020). Observation of structure in the  $J/\psi$ -pair mass spectrum. *Science Bulletin*, 65(23), 1983–1993.
- Aaij, R., Beteta, C. A., Ackernley, T., Adeva, B., Adinolfi, M., Afsharnia, H., Aidala, C., Aiola, S., Ajaltouni, Z., Akar, S., Albrecht, J., Alessio, F., Alexander, M., Albero, A. A., Aliouche, Z., et al. (2021). Observation of New Resonances Decaying to  $J/\psi K^{++}$  and  $J/\psi \phi$ . *Physical Review Letters*, 127(8), 082001.
- Aaij, R., Beteta, C. A., Adeva, B., Adinolfi, M., Aidala, C., Ajaltouni, Z., Akar, S., Albicocco, P., Albrecht, J., Alessio, F., Alexander, M., Albero, A. A., Alkhazov, G., Cartelle, P. A., Jr, A. A., et al. (2018). Evidence for an  $\eta_c(1S)\pi^-$  resonance in  $B^0 \rightarrow \eta_c(1S)K^+\pi^-$  decays. *The European Physical Journal C*, 78(12), 1019.
- Abe, K., Abe, K., Abe, T., Adachi, I., Aihara, H., Akatsu, M., Asano, Y., Aso, T., Aulchenko, V., Aushev, T., Bakich, A. M., Bay, A., Bedny, I., Bizjak, I., Bozek, A., et al. (2003). Measurement of  $K^+ K^-$  production in two photon collisions in the resonant mass region. *The European Physical Journal C*, 32, 323–336.
- Ablikim, M., Achasov, M. N., Adlarson, P., Ahmed, S., Albrecht, M., Aliberti, R., Amoroso, A., An, Q., Anita, Bai, X. H., Bai, Y., Bakina, O., Ferroli, R. B., Balossino, I., Ban, Y., et al. (2021). Observation of a Near-Threshold Structure in the  $K^+$

Recoil-Mass Spectra in  $e^+e^- \rightarrow K^+(D_s^- D^{*0} + D_s^{*-} D^0)$ . *Physical Review Letters*, 126(10), 102001.

Ablikim, M., Achasov, M. N., Adlarson, P., Ahmed, S., Albrecht, M., Amoroso, A., An, Q., Anita, Bai, Y., Bakina, O., Ferroli, R. B., Balossino, I., Ban, Y., Begzsuren, K., Bennett, J. V., et al. (2020). Study of the process  $e^+e^- \rightarrow \pi^0\pi^0 J/\psi$  and neutral charmonium-like state  $Z_c(3900)^0$ . *Physical Review D*, 102(1), 012009.

Ablikim, M., Achasov, M. N., Ahmed, S., Ai, X. C., Albayrak, O., Albrecht, M., Ambrose, D. J., Amoroso, A., An, F. F., An, Q., Bai, J. Z., Bakina, O., Ferroli, R. B., Ban, Y., Bennett, D. W., et al. (2017a). Measurement of  $e^+e^- \rightarrow \pi^+\pi^-\psi(3686)$  from 4.008 to 4.600 GeV and observation of a charged structure in the  $\pi^\pm\psi(3686)$  mass spectrum. *Physical Review D*, 96(3), 032004.

Ablikim, M., Achasov, M. N., Ahmed, S., Ai, X. C., Albayrak, O., Albrecht, M., Ambrose, D. J., Amoroso, A., An, F. F., An, Q., Bai, J. Z., Ferroli, R. B., Ban, Y., Bennett, D. W., Bennett, J. V., et al. (2016). Observation of an anomalous line shape of the  $\eta'\pi^+\pi^-$  mass spectrum near the  $p\bar{p}$  mass threshold in  $J/\psi \rightarrow \gamma\eta'\pi^+\pi^-$ . *Physical Review Letters*, 117(4), 042002.

Ablikim, M., Achasov, M. N., Ahmed, S., Albrecht, M., Amoroso, A., An, F. F., An, Q., J. Z. Bai, O. B., Ferroli, R. B., Ban, Y., Bennett, D. W., Bennett, J. V., Berger, N., Bertani, M., et al. (2018). Measurement of  $e^+e^- \rightarrow \pi^0\pi^0\psi(3686)$  at  $\sqrt{s}$  from 4.009 to 4.600 GeV and observation of a neutral charmoniumlike structure. *Physical Review D*, 97(5), 052001.

Ablikim, M., Achasov, M. N., Ai, X. C., Albayrak, O., Albrecht, M., Ambrose, D. J., Amoroso, A., An, F. F., An, Q., Bai, J. Z., Ferroli, R. B., Ban, Y., Bennett, D. W., Bennett, J. V., Bertani, M., et al. (2014a). Observation of  $e^+e^- \rightarrow \pi^0\pi^0 h_c$  and a Neutral Charmoniumlike Structure  $Z_c(4020)^0$ . *Physical Review Letters*, 113(21), 212002.

Ablikim, M., Achasov, M. N., Ai, X. C., Albayrak, O., Albrecht, M., Ambrose, D. J., Amoroso, A., An, F. F., An, Q., Bai, J. Z., Ferroli, R. B., Ban, Y., Bennett, D. W., Bennett, J. V., Bertani, M., et al. (2015a). Observation and Spin-Parity Determination of the X(1835) in  $J/\psi \rightarrow \gamma K_S^0 K_S^0 \eta$ . *Physical Review Letters*, 115(9), 091803.

Ablikim, M., Achasov, M. N., Ai, X. C., Albayrak, O., Albrecht, M., Ambrose, D. J., Amoroso, A., An, F. F., An, Q., Bai, J. Z., Ferroli, R. B., Ban, Y., Bennett, D. W., Bennett, J. V., Bertani, M., et al. (2015b). Observation of a neutral charmoniumlike state  $Z_c(4025)^0$  in  $e^+e^- \rightarrow (D^*\bar{D}^*)^0\pi^0$ . *Physical Review Letters*, 115(18), 182002.

Ablikim, M., Achasov, M. N., Ai, X. C., Albayrak, O., Albrecht, M., Ambrose, D. J., Amoroso, A., An, F. F., An, Q., Bai, J. Z., Ferroli, R. B., Ban, Y., Bennett, D. W., Bennett, J. V., Bertani, M., et al. (2015c). Observation of a Neutral Structure near the  $D\bar{D}^*$  Mass Threshold in  $e^+e^- \rightarrow (D\bar{D}^*)^0\pi^0$  at  $\sqrt{s} = 4.226$  and  $4.257$  GeV. *Physical Review Letters*, 115(22), 222002.

Ablikim, M., Achasov, M. N., Ai, X. C., Albayrak, O., Albrecht, M., Ambrose, D. J., Amoroso, A., An, F. F., An, Q., Bai, J. Z., Ferroli, R. B., Ban, Y., Bennett, D. W., Bennett, J. V., Bertani, M., et al. (2017b). Determination of the Spin and Parity of the  $Z_c(3900)$ . *Physical Review Letters*, 119(7), 072001.

Ablikim, M., Achasov, M. N., Ai, X. C., Albayrak, O., Ambrose, D. J., An, F. F., An, Q., Bai, J. Z., Ferroli, R. B., Ban, Y., Becker, J., Bennett, J. V., Bertani, M., Bian, J. M., Boger, E., et al. (2013a). Observation of a Charged Charmoniumlike Structure in  $e^+e^- \rightarrow \pi^+\pi^-J/\psi$  at  $\sqrt{s} = 4.26$  GeV. *Physical Review Letters*, 110, 252001.

Ablikim, M., Achasov, M. N., Albayrak, O., Ambrose, D. J., An, F. F., An, Q., Bai, J. Z., Ferroli, R. B., Ban, Y., Becker, J., Bennett, J. V., Berger, N., Bertani, M., Bian, J. M., Boger, E., et al. (2013b). Partial wave analysis of  $J/\psi \rightarrow \gamma\eta\eta$ . *Physical Review D*, 87(9), 092009.

Ablikim, M., Achasov, M. N., Albayrak, O., Ambrose, D. J., An, F. F., An, Q., Bai, J. Z., Ferroli, R. B., Ban, Y., Becker, J., Bennett, J. V., Bertani, M., Bian, J. M., Boger, E., Bondarenko, O., et al. (2013c). Observation of a Charged Charmoniumlike Structure  $Z_c(4020)$  and Search for the  $Z_c(3900)$  in  $e^+e^- \rightarrow \pi^+\pi^-h_c$ . *Physical Review Letters*, 111, 242001.

Ablikim, M., Achasov, M. N., Albayrak, O., Ambrose, D. J., An, F. F., An, Q., Bai, J. Z., Ferroli, R. B., Ban, Y., Becker, J., Bennett, J. V., Bertani, M., Bian, J. M., Boger, E., Bondarenko, O., et al. (2013d). Observation of a structure at  $1.84 \text{ GeV}/c^2$

in the  $3(\pi^+\pi^-)$  mass spectrum in  $J/\psi \rightarrow \gamma 3(\pi^+\pi^-)$  decays. *Physical Review D*, 88(9), 091502.

Ablikim, M., Achasov, M. N., Albayrak, O., Ambrose, D. J., An, F. F., An, Q., Bai, J. Z., Ferroli, R. B., Ban, Y., Becker, J., Bennett, J. V., Bertani, M., Bian, J. M., Boger, E., Bondarenko, O., et al. (2014b). Observation of a charged  $(D\bar{D}^*)^\pm$  mass peak in  $e^+e^- \rightarrow \pi D\bar{D}^*$  at  $\sqrt{s} = 4.26$  GeV. *Physical Review Letters*, 112(2), 022001.

Ablikim, M., Achasov, M. N., Albayrak, O., Ambrose, D. J., F. F. An and, Q. A., Bai, J. Z., Ferroli, R. B., Ban, Y., Becker, J., Bennett, J. V., Bertani, M., Bian, J. M., Boger, E., Bondarenko, O., et al. (2014c). Observation of a charged charmoniumlike structure in  $e^+e^- \rightarrow (D^*\bar{D}^*)^\pm\pi^\mp$  at  $\sqrt{s} = 4.26$  GeV. *Physical Review Letters*, 112(13), 132001.

Ablikim, M., Achasov, M. N., Alberto, D., Ambrose, D., An, F. F., An, Q., An, Z. H., Bai, J. Z., Ferroli, R. B. F. B., Ban, Y., Becker, J., Berger, N., Bertani, M. B., Bian, J. M., Boger, E., et al. (2012). Spin-Parity Analysis of  $p\bar{p}$  Mass Threshold Structure in  $J/\psi$  and  $\psi'$  Radiative Decays. *Physical Review Letters*, 108, 112003.

Ablikim, M., Bai, J. Z., Ban, Y., Bian, J. G., Cai, X., Chen, H. F., Chen, H. S., Chen, H. X., Chen, J. C., Chen, J., Chen, Y. B., Chi, S. P., Chu, Y. P., Cui, X. Z., Dai, Y. S., et al. (2005a). Observation of a resonance  $X(1835)$  in  $J/\psi \rightarrow \gamma\pi^+\pi^-\eta'$ . *Physical Review Letters*, 95, 262001.

Ablikim, M., Bai, J. Z., Ban, Y., Bian, J. G., Cai, X., Chen, H. F., Chen, H. S., Chen, H. X., Chen, J. C., Chen, J., Chen, Y. B., Chi, S. P., Chu, Y. P., Cui, X. Z., Dai, Y. S., et al. (2005b). Partial wave analysis of  $\chi_{c0} \rightarrow \pi^+\pi^-K^+K^-$ . *Physical Review D*, 72, 092002.

Ablikim, M., Bai, J. Z., Ban, Y., Bian, J. G., Cai, X., Chen, H. F., Chen, H. S., Chen, H. X., Chen, J. C., Chen, J., Chen, Y. B., Chi, S. P., Chu, Y. P., Cui, X. Z., Dai, Y. S., et al. (2006). Partial wave analyses of  $J/\psi \rightarrow \gamma\pi^+\pi^-$  and  $\gamma\pi^0\pi^0$ . *Physics Letters B*, 642, 441–448.

Aceti, F., Bayar, M., Oset, E., Martinez Torres, A., Khemchandani, K. P., Dias, J. M., Navarra, F. S., and Nielsen, M. (2014). Prediction of an  $I = 1$   $D\bar{D}^*$  state and relationship to the claimed  $Z_c(3900)$ ,  $Z_c(3885)$ . *Physical Review D*, 90(1), 016003.

- Adachi, I., Aihara, H., Arinstein, K., Aushev, T., Aziz, T., Bakich, A. M., Balagura, V., Barberio, E., Bedny, I., Belous, K., Bhardwaj, V., Bitenc, U., Bondar, A., Bozek, A., Brăcko, M., et al. (2008). Production of New Charmoniumlike States in  $e^+e^- \rightarrow J/\psi D^{(*)} \bar{D}^{(*)}$  at  $\sqrt{s} \approx 10.6$  GeV. *Physical Review Letters*, 100, 202001.
- Ader, J. P., Richard, J. M., and Taxil, P. (1982). Do narrow heavy multi-quark states exist? *Physical Review D*, 252370.
- Agaev, S. S., Azizi, K., and Sundu, H. (2017). Treating  $Z_c(3900)$  and  $Z(4430)$  as the ground-state and first radially excited tetraquarks. *Physical Review D*, 96(3), 034026.
- Albaladejo, M. and Oller, J. A. (2008). Identification of a Scalar Glueball. *Physical Review Letters*, 101, 252002.
- Albuquerque, R. M., Dias, J. M., Khemchandani, K. P., Martínez Torres, A., Navarra, F. S., Nielsen, M., and Zanetti, C. M. (2019). QCD sum rules approach to the  $X$ ,  $Y$  and  $Z$  states. *Journal of Physics G*, 46, 093002.
- Amsler, C. and Close, F. E. (1996). Is  $f_0(1500)$  a scalar glueball? *Physical Review D*, 53, 295–311.
- Amsler, C. and Tornqvist, N. A. (2004). Mesons beyond the naive quark model. *Physics Reports*, 389, 61–117.
- Anisovich, A. V., Baker, C. A., Batty, C. J., Bugg, D. V., Montanet, L., Nikonov, V. A., Sarantsev, A. V., Sarantsev, V. V., and Zou, B. S. (2002a). Combined analysis of meson channels with  $I = 0$ ,  $C = -1$  from 1940 to 2410 MeV. *Physics Letters B*, 542, 8–18.
- Anisovich, A. V., Baker, C. A., Batty, C. J., Bugg, D. V., Montanet, L., Nikonov, V. A., Sarantsev, A. V., Sarantsev, V. V., and Zou, B. S. (2002b).  $I = 0$ ,  $C = -1$  mesons from 1940 to 2410 MeV. *Physics Letters B*, 542, 19–28.
- Anwar, M. N., Ferretti, J., Guo, F.-K., Santopinto, E., and Zou, B.-S. (2018a). Spectroscopy and decays of the fully-heavy tetraquarks. *The European Physical Journal C*, 78(8), 647.

- Anwar, M. N., Ferretti, J., and Santopinto, E. (2018b). Spectroscopy of the hidden-charm  $[qc][\bar{q}\bar{c}]$  and  $[sc][\bar{s}\bar{c}]$  tetraquarks in the relativized diquark model. *Physical Review D*, 98(9), 094015.
- Barate, R., Decamp, D., Ghez, P., Goy, C., Lees, J.-P., Merle, E., Minard, M.-N., Pietrzyk, B., Alemany, R., Bravo, S., Casado, M., Chmeissani, M., Crespo, J., Fernandez, E., Fernandez-Bosman, M., et al. (2000). Search for the glueball candidates  $f_0(1500)$  and  $f_J(1710)$  in  $\gamma\gamma$  collisions. *Physics Letters B*, 472, 189–199.
- Barberis, D., Binon, F., Close, F., Danielsen, K., Donskov, S., Earl, B., Evans, D., French, B., Hino, T., Inaba, S., Jacholkowski, A., Jacobsen, T., Khaustov, G., Kinson, J., Kirk, A., et al. (2000). A Spin analysis of the  $4\pi$  channels produced in central  $pp$  interactions at 450 GeV/c. *Physics Letters B*, 471, 440–448.
- Barnea, N., Vijande, J., and Valcarce, A. (2006). Four-quark spectroscopy within the hyperspherical formalism. *Physical Review D*, 73, 054004.
- Berezhnoy, A. V., Luchinsky, A. V., and Novoselov, A. A. (2012). Tetraquarks Composed of 4 Heavy Quarks. *Physical Review D*, 86, 034004.
- Binon, F., A.M.Blik, Donskov, S. V., Inaba, S., Kolosov, V. N., Lednev, A. A., Lishin, V. A., Mikhailov, Y. V., Peigneux, J. P., Polyakov, V. A., Sadovsky, S. A., Samoilenko, V. D., Sobol, A. ., Stroot, J. P., gonyaev, V., et al. (2005). Investigation of the eta eta system in  $\pi^-p$  interactions at a momentum of 32.5 GeV/c at the GAMS-4 $\pi$  spectrometer. *Physics of Atomic Nuclei*, 68, 960–973.
- Bondar, A. (2018). Complementarity of the beauty and charm hadron physics. talk at the 9th international workshop on charm physics, may 21 to 25, 2018, novosibirsk, russia.
- Brambilla, N., Eidelman, S., Hanhart, C., Nefediev, A., Shen, C.-P., Thomas, C. E., Vairo, A., and Yuan, C.-Z. (2020). The  $XYZ$  states: experimental and theoretical status and perspectives. *Physics Reports*, 873, 1–154.
- Brüner, F. and Rebhan, A. (2015). Nonchiral enhancement of scalar glueball decay in the Witten-Sakai-Sugimoto model. *Physical Review Letters*, 115(13), 131601.

- Chen, H.-X., Chen, W., Liu, X., and Zhu, S.-L. (2020). Strong decays of fully-charm tetraquarks into di-charmonia. *Science Bulletin*, *65*, 1994–2000.
- Chen, Y., Alexandru, A., Dong, S., Draper, T., Horváth, I., Lee, F., Liu, K., Mathur, N., Morningstar, C., Peardon, M., Tamhankar, S., Young, B., and Zhang, J. (2006). Glueball spectrum and matrix elements on anisotropic lattices. *Physical Review D*, *73*, 014516.
- Chen, Y., Gong, M., Lei, Y.-H., Li, N., Liang, J., Liu, C., Liu, H., Liu, J.-L., Liu, L., Liu, Y.-F., Liu, Y.-B., Liu, Z., Ma, J.-P., Wang, Z.-L., Yang, Y.-B., et al. (2014). Low-energy scattering of the  $(D\bar{D}^*)^\pm$  system and the resonance-like structure  $Z_c(3900)$ . *Physical Review D*, *89*(9), 094506.
- Chilikin, K., Adachi, I., Aihara, H., Said, S. A., Asner, D. M., Aulchenko, V., Ayad, R., Babu, V., Badhrees, I., Bakich, A. M., Bansal, V., Barberio, E., Besson, D., Bhardwaj, V., Bhuyan, B., et al. (2017). Observation of an alternative  $\chi_{c0}(2P)$  candidate in  $e^+e^- \rightarrow J/\psi D\bar{D}$ . *Physical Review D*, *95*, 112003.
- Chilikin, K., Mizuk, R., Adachi, I., Aihara, H., Arinstein, K., Asner, D. M., Aulchenko, V., Aushev, T., Aziz, T., Bakich, A. M., Bala, A., Bhardwaj, V., Bhuyan, B., Bondar, A., Bonvicini, G., et al. (2013). Experimental constraints on the spin and parity of the  $Z(4430)^+$ . *Physical Review D*, *88*(7), 074026.
- Chilikin, K., Mizuk, R., Adachi, I., Aihara, H., Said, S. A., Arinstein, K., Asner, D. M., Aulchenko, V., Aushev, T., Ayad, R., Aziz, T., Bakich, A. M., Bansal, V., Bondar, A., Bonvicini, G., et al. (2014). Observation of a new charged charmoniumlike state in  $\bar{B}^0 \rightarrow J/\psi K^- \pi^+$  decays. *Physical Review D*, *90*(11), 112009.
- Choi, S.-K., Olsen, S. L., Abe, K., Abe, K., Adachi, I., Aihara, H., Asano, Y., Bahinipati, S., Bakich, A. M., Ban, Y., Bedny, I., Bitenc, U., Bizjak, I., Bondar, A., Bozek, A., et al. (2005). Observation of a near-threshold omega  $J/\psi$  mass enhancement in exclusive  $B \rightarrow K\omega J/\psi$  decays. *Physical Review Letters*, *94*, 182002, page .
- Choi, S.-K., Olsen, S. L., Abe, K., Abe, T., Adachi, I., Ahn, B. S., Aihara, H., Akai, K., Akatsu, M., Akemoto, M., Asano, Y., Aso, T., Aulchenko, V., Aushev, T., Bakich, A. M., et al. (2003). Observation of a narrow charmonium-like state in exclusive  $B^\pm \rightarrow K^\pm \pi^+ \pi^- J/\psi$  decays. *Physical Review Letters*, *91*, 262001.

- Choi, S.-K., Olsen, S. L., Adachi, I., Aihara, H., Aulchenko, V., Aushev, T., Aziz, T., Bakich, A. M., Balagura, V., Bedny, I., Bitenc, U., Bondar, A., Bozek, A., Brücko, M., Brodzicka, J., et al. (2008). Observation of a resonance-like structure in the  $\pi^\pm\psi'$  mass distribution in exclusive  $B \rightarrow K\pi^\pm\psi'$  decays. *Physical Review Letters*, 100, 142001.
- Close, F. E. and Kirk, A. (2001). Scalar glueball- $q\bar{q}$  mixing above 1 GeV and implications for lattice QCD. *The European Physical Journal C*, 21, 531–543.
- Debastiani, V. R. and Navarra, F. S. (2019). A non-relativistic model for the  $[cc][\bar{c}\bar{c}]$  tetraquark. *Chinese Physics C*, 43(1), 013105.
- Deng, C., Ping, J., Huang, H., and Wang, F. (2015). Systematic study of  $Z_c^+$  family from a multiquark color flux-tube model. *Physical Review D*, 92(3), 034027.
- Deng, C., Ping, J., Huang, H., and Wang, F. (2018). Hidden charmed states and multibody color flux-tube dynamics. *Physical Review D*, 98(1), 014026.
- Deng, C., Ping, J., and Wang, F. (2014). Interpreting  $Z_c(3900)$  and  $Z_c(4025)/Z_c(4020)$  as charged tetraquark states. *Physical Review D*, 90, 054009.
- Deng, C., Ping, J., Yang, Y., and Wang, F. (2012).  $X(1835)$ ,  $X(2120)$  and  $X(2370)$  in a flux tube model. *Physical Review D*, 86014008.
- Deng, C., Ping, J., Yang, Y., and Wang, F. (2013). Baryonia and near-threshold enhancements. *Physical Review D*, 88(7), 074007.
- Ebert, D., Faustov, R. N., and Galkin, V. O. (2008). Excited heavy tetraquarks with hidden charm. *The European Physical Journal C*, 58, 399–405.
- Ebert, D., Faustov, R. N., and Galkin, V. O. (2009). Mass spectra and Regge trajectories of light mesons in the relativistic quark model. *Physical Review D*, 79, 114029.
- Eugenio, P., Adams, G. S., Adams, T., Bar-Yam, Z., Bishop, J. M., Bodyagin, V. A., Brabson, B. B., Brown, D. S., Cason, N. M., Chung, S. U., Crittenden, R. R., Cummings, J. P., Demianov, A. I., Denisov, S., Dorofeev, V., et al. (2001). Observation of a new  $J^{PC} = 1^{+-}$  isoscalar state in the reaction  $\pi^-p \rightarrow \omega\eta\eta$  at 18 GeV/c. *Physics Letters B*, 497, 190–198.

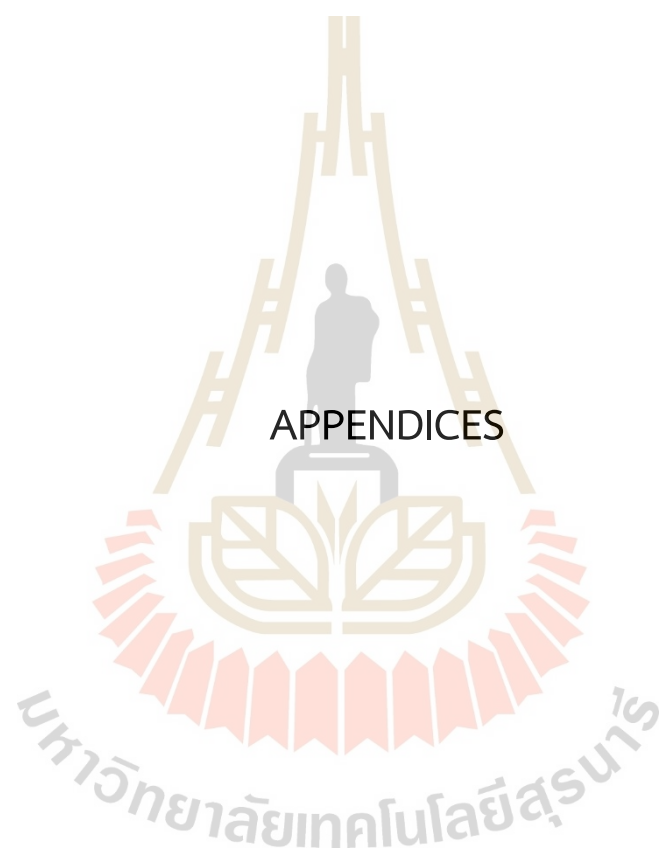
- Gaspero, M. (1993). Evidence for the dominance of an  $I^G J^{PC} = 0^+0^{++}$  resonance in  $\bar{p}n \rightarrow 2\pi^+3\pi^-$  annihilation at rest. *Nuclear Physics A*, 562, 407–445.
- Gell-Mann, M. (1964). A Schematic Model of Baryons and Mesons. *Physics Letters*, 8, 214–215.
- Godfrey, S. and Isgur, N. (1985). Mesons in a Relativized Quark Model with Chromodynamics. *Physical Review D*, 32, 189–231.
- Goerke, F., Gutsche, T., Ivanov, M. A., Korner, J. G., Lyubovitskij, V. E., and Santorelli, P. (2016). Four-quark structure of  $Z_c(3900)$ ,  $Z(4430)$  and  $X_b(5568)$  states. *Physical Review D*, 94(9), 094017.
- Guo, Z., Liu, T., and Ma, B.-Q. (2016). Light-front holographic QCD with generic dilaton profile. *Physical Review D*, 93(7), 076010.
- Hagiwara, K., Hikasa, K., Nakamura, K., Tanabashi, M., Aguilar-Benitez, M., Amsler, C., Barnett, R., Burchat, P., Carone, C., Caso, C., Conforto, G., Dahl, O., Doser, M., Eidelman, S., Feng, J., et al. (2002). Review of particle physics. Particle Data Group. *Physical Review D*, 66, 010001.
- He, J. (2014). Study of the  $B\bar{B}^*/D\bar{D}^*$  bound states in a Bethe-Salpeter approach. *Physical Review D*, 90(7), 076008.
- Ikeda, Y. and Iida, H. (2012). Quark-anti-quark potentials from Nambu-Bethe-Salpeter amplitudes on lattice. *Progress of Theoretical Physics*, 128, 941–954.
- Janowski, S., Giacosa, F., and Rischke, D. H. (2014). Is  $f_0(1710)$  a glueball? *Physical Review D*, 90(11), 114005.
- Kawanai, T. and Sasaki, S. (2011). Interquark potential with finite quark mass from lattice QCD. *Physical Review Letters*, 107, 091601.
- Ke, H.-W. and Li, X.-Q. (2016). Study on decays of  $Z_c(4020)$  and  $Z_c(3900)$  into  $h_c + \pi$ . *The European Physical Journal C*, 76(6), 334.
- Klempt, E. (2021). Scalar mesons and the fragmented glueball. *Physics Letters B*, 820, 136512.

- Klempt, E. and Zaitsev, A. (2007). Glueballs, Hybrids, Multiquarks. Experimental facts versus QCD inspired concepts. *Physics Reports*, 454, 1–202.
- Li, Q., Gui, L.-C., Liu, M.-S., Lü, Q.-F., and Zhong, X.-H. (2021). Mass spectrum and strong decays of strangeonium in a constituent quark model. *Chinese Physics C*, 45(2), 023116.
- Liu, J.-F., Ding, G.-J., and Yan, M.-L. (2010). X(1835) and the New Resonances X(2120) and X(2370) Observed by the BES Collaboration. *Physical Review D*, 82, 074026.
- Liu, M.-S., Lü, Q.-F., Zhong, X.-H., and Zhao, Q. (2019). All-heavy tetraquarks. *Physical Review D*, 100(1), 016006.
- Liu, Z. Q., Shen, C. P., Yuan, C. Z., Adachi, I., Aihara, H., Asner, D. M., Aulchenko, V., Aushev, T., Aziz, T., Bakich, A. M., Bala, A., Belous, K., Bhardwaj, V., Bhuyan, B., Bischofberger, M., et al. (2013). Study of  $e^+e^- \rightarrow \pi^+\pi^-J/\psi$  and Observation of a Charged Charmoniumlike State at Belle. *Physical Review Letters*, 110, 252002.
- Lloyd, R. J. and Vary, J. P. (2004). All charm tetraquarks. *Physical Review D*, 70, 014009.
- Maiani, L., Piccinini, F., Polosa, A. D., and Riquer, V. (2005). Diquark-antidiquarks with hidden or open charm and the nature of X(3872). *Physical Review D*, 71, 014028.
- Maiani, L., Piccinini, F., Polosa, A. D., and Riquer, V. (2014). The Z(4430) and a New Paradigm for Spin Interactions in Tetraquarks. *Physical Review D*, 89, 114010.
- Maiani, L., Riquer, V., Faccini, R., Piccinini, F., Pilloni, A., and Polosa, A. D. (2013). A  $J^{PG} = 1^{++}$  Charged Resonance in the  $Y(4260) \rightarrow \pi^+\pi^-J/\psi$  Decay? *Physical Review D*, 87(11), 111102.
- Mizuk, R., Adachi, I., Aihara, H., Arinstein, K., Aushev, T., Bakich, A. M., Balagura, V., Barberio, E., Bay, A., Belous, K., Bhardwaj, V., Bozek, A., Brăcko, M., Browder, T. E., Chang, M.-C., et al. (2009). Dalitz analysis of  $B \rightarrow K\pi^+\psi'$  decays and the  $Z(4430)^+$ . *Physical Review D*, 80, 031104.

- Mizuk, R., Chistov, R., Adachi, I., Aihara, H., Arinstein, K., Aulchenko, V., Aushev, T., Bakich, A. M., Balagura, V., Barberio, E., Bay, A., Bhardwaj, V., Bitenc, U., Bondar, A., Bozek, A., et al. (2008). Observation of two resonance-like structures in the  $\pi^+\chi_{c1}$  mass distribution in exclusive  $\bar{B}^0 \rightarrow K^-\pi^+\chi_{c1}$  decays. *Physical Review D*, 78, 072004.
- Ochs, W. (2013). The Status of Glueballs. *Journal of Physics G*, 40, 043001.
- Olsen, S. L. (2015). XYZ Meson Spectroscopy. *Proceeding of science, Bormio2015*, 050.
- Patel, S., Shah, M., and Vinodkumar, P. C. (2014). Mass spectra of four-quark states in the hidden charm sector. *The European Physical Journal A*, 50, 131.
- Prelovsek, S. and Leskovec, L. (2013). Search for  $Z_c^+(3900)$  in the  $1^{+-}$  Channel on the Lattice. *Physics Letters B*, 727, 172–176.
- Sarantsev, A. V., Denisenko, I., Thoma, U., and Klempt, E. (2021). Scalar isoscalar mesons and the scalar glueball from radiative  $J/\psi$  decays. *Physics Letters B*, 816, 136227.
- Shen, C. P., Yuan, C. Z., Aihara, H., Arinstein, K., Aushev, T., Bakich, A. M., Balagura, V., Barberio, E., Bay, A., Belous, K., Bhardwaj, V., Bischofberger, M., Brăcko, M., Browder, T. E., Chang, M.-C., et al. (2010). Evidence for a new resonance and search for the  $Y(4140)$  in the  $\gamma\gamma \rightarrow \phi J/\psi$  process. *Physical Review Letters*, 104, 112004.
- Silvestre-Brac, B. (1996). Spectrum and static properties of heavy baryons. *Few-Body Systems*, 20, 1–25.
- Silvestre-Brac, B. and Semay, C. (1993). Systematics of  $L = 0$   $q^2\bar{q}^2$  systems. *Zeitschrift für Physik C*, 57, 273–282.
- Uehara, S., Watanabe, Y., Adachi, I., Aihara, H., Arinstein, K., Bakich, A. M., Balagura, V., Barberio, E., Bay, A., Bedny, I., Belous, K., Bhardwaj, V., Bitenc, U., Bondar, A., Brăcko, M., et al. (2008). High-statistics measurement of neutral pion-pair production in two-photon collisions. *Physical Review D*, 78, 052004.

- Uehara, S., Watanabe, Y., Nakazawa, H., Adachi, I., Aihara, H., Asner, D. M., Aulchenko, V., Aushev, T., Bakich, A. M., Bala, A., Bhardwaj, V., Bhuyan, B., Bondar, A., Bonvicini, G., Bozek, A., et al. (2013). High-statistics study of  $K_S^0$  pair production in two-photon collisions. *Progress of Theoretical and Experimental Physics*, 2013(12), 123C01.
- Uman, I., Joffe, D., Metreveli, Z., Seth, K. K., Tomaradze, A., and Zweber, P. K. (2006). Light quark resonances in  $p\bar{p}$  annihilations at 5.2 GeV/c. *Physical Review D*, 73, 052009.
- Vijande, J., Fernandez, F., and Valcarce, A. (2005). Constituent quark model study of the meson spectra. *Journal of Physics G*, 31, 481.
- Wang, G.-J., Meng, L., and Zhu, S.-L. (2019). Spectrum of the fully-heavy tetraquark state  $QQ\bar{Q}'\bar{Q}'$ . *Physical Review D*, 100(9), 096013.
- Wang, X. L., Yuan, C. Z., Shen, C. P., Wang, P., Abdesselam, A., Adachi, I., Aihara, H., Said, S. A., Arinstein, K., Asner, D. M., Ayad, R., Bakich, A. M., Bansal, V., Bhuyan, B., Bobrov, A., et al. (2015). Measurement of  $e^+e^- \rightarrow \pi^+\pi^-\psi(2S)$  via Initial State Radiation at Belle. *Physical Review D*, 91, 112007.
- Wang, Z.-G. (2011). Analysis of the  $X(1835)$  and related baryonium states with Bethe-Salpeter equation. *The European Physical Journal A*, 47, 71.
- Wang, Z.-G. (2015). Analysis of the  $Z(4430)$  as the first radial excitation of the  $Z_c(3900)$ . *Communications in Theoretical Physics*, 63(3), 325–330.
- Wang, Z.-G. (2017). Analysis of the  $QQ\bar{Q}\bar{Q}$  tetraquark states with QCD sum rules. *The European Physical Journal C*, 77(7), 432.
- Wang, Z.-G. and Di, Z.-Y. (2019). Analysis of the vector and axialvector  $QQ\bar{Q}\bar{Q}$  tetraquark states with QCD sum rules. *Acta Physica Polonica B*, 50, 1335.
- Wang, Z.-G. and Huang, T. (2014). Possible assignments of the  $X(3872)$ ,  $Z_c(3900)$  and  $Z_b(10610)$  as axial-vector molecular states. *The European Physical Journal C*, 74(5), 2891.
- Wong, C.-Y., Swanson, E. S., and Barnes, T. (2002). Heavy quarkonium dissociation cross-sections in relativistic heavy ion collisions. *Physical Review C*, 65, 014903.

- Wu, J., Liu, X., Liu, Y.-R., and Zhu, S.-L. (2019). Systematic studies of charmonium-, bottomonium-, and  $B_c$ -like tetraquark states. *Physical Review D*, 99(1), 014037.
- Wu, J., Liu, Y.-R., Chen, K., Liu, X., and Zhu, S.-L. (2018). Heavy-flavored tetraquark states with the  $QQ\bar{Q}\bar{Q}$  configuration. *Physical Review D*, 97(9), 094015.
- Xiao, L.-Y., Weng, X.-Z., Zhong, X.-H., and Zhu, S.-L. (2019). A possible explanation of the threshold enhancement in the process  $e^+e^- \rightarrow \Lambda\bar{\Lambda}$ . *Chinese Physics C*, 43(11), 113105.
- Xiao, T., Dobbs, S., Tomaradze, A., and Seth, K. K. (2013). Observation of the Charged Hadron  $Z_c^\pm(3900)$  and Evidence for the Neutral  $Z_c^0(3900)$  in  $e^+e^- \rightarrow \pi\pi J/\psi$  at  $\sqrt{s} = 4170$  MeV. *Physics Letters B*, 727, 366–370.
- Yu, J.-S., Sun, Z.-F., Liu, X., and Zhao, Q. (2011). Categorizing resonances X(1835), X(2120) and X(2370) in the pseudoscalar meson family. *Physical Review D*, 83, 114007.
- Zhao, L., Deng, W.-Z., and Zhu, S.-L. (2014a). Hidden-Charm Tetraquarks and Charged  $Z_c$  States. *Physical Review D*, 90(9), 094031.
- Zhao, L., Ma, L., and Zhu, S.-L. (2014b). Spin-orbit force, recoil corrections, and possible  $B\bar{B}^*$  and  $D\bar{D}^*$  molecular states. *Physical Review D*, 89(9), 094026.
- Zou, L., Dosch, H. G., De Téramond, G. F., and Brodsky, S. J. (2019). Isoscalar mesons and exotic states in light front holographic QCD. *Physical Review D*, 99(11), 114024.
- Zyla, P., Barnett, R., Beringer, J., Bonventre, R., Dahl, O., Dwyer, D., Groom, D., Lin, C.-J., Lugovsky, K., Pianori, E., Robinson, D., Wohl, C., Yao, W.-M., Agashe, K., Aielli, G., et al. (2020). Review of Particle Physics. *Progress of Theoretical and Experimental Physics*, 2020, 083C01.



APPENDICES

## APPENDIX A

### GROUP THEORY APPROACH

Tetraquark states consist of two quarks and two antiquarks,  $qq\bar{q}\bar{q}$ . The contributions of the spatial degrees of freedom as well as the internal degrees of freedom of color, flavor, and spin are included in tetraquark wave functions. The two light flavors  $u$  and  $d$  with spin  $s = 1/2$  and three potential colors  $r, g$  and  $b$  are assumed to be the internal degrees of freedom.

The quark and antiquark transform under the fundamental representation of  $SU(n)$  and the conjugate representation of  $SU(n)$ , respectively, with  $n = 2, 2, 3$  for the spin, flavor, color degree of freedom. The spin, flavor, and color algebras,  $SU_f(2) \otimes SU_s(2) \otimes SU_c(3)$ , make up the algebraic structure of the multi-quark state.

The construction of tetraquark  $q_1q_2\bar{q}_3\bar{q}_4$  states follows two rules. One is that a  $q_1q_2\bar{q}_3\bar{q}_4$  state must be a color singlet. Another is that the wave function of the identical quark cluster must be antisymmetric under any permutation between identical quarks. In the language of group theory, the permutation symmetry of the quark-quark configuration  $qq$  is characterized by the  $S_2$  Young tabloids [2], and [11].

The rule that a tetraquark state must be a color singlet, which means that the tetraquark color wave function must be a  $[222]_1$  singlet of the  $SU_c(3)$  group, is followed while constructing tetraquark states. Since the color part of the quark-quark cluster ( $q_1q_2$ ) in tetraquark states are a  $[2]_6$  sextet and a  $[11]_3$  antitriplet as follows,

$$\psi_{[2]}^c(q_1q_2) = \square\square, \quad \psi_{[11]}^c(q_1q_2) = \begin{array}{|c|} \hline \square \\ \hline \end{array}, \quad (\text{A.1})$$

the color part of the two antiquarks cluster ( $\bar{q}_3\bar{q}_4$ ) must be a  $[22]_6$  antisextet and  $[211]_3$  triplet respectively as follows,

$$\psi_{[22]}^c(\bar{q}_3\bar{q}_4) = \begin{array}{|c|c|} \hline \square & \square \\ \hline \end{array}, \quad \psi_{[211]}^c(\bar{q}_3\bar{q}_4) = \begin{array}{|c|c|} \hline \square & \square \\ \hline \square & \\ \hline \end{array}. \quad (\text{A.2})$$

The identical quark cluster  $q^2$  must be antisymmetric under any permutation between identical quarks, which implies that the spatial-spin-flavour part must

be a [11] and [2] states for color part  $[2]_6$  and  $[11]_3$  states, respectively,

$$\psi_{[11]}^{osf}(q_1q_2) = \begin{array}{|c|} \hline \square \\ \hline \square \\ \hline \end{array}, \quad \psi_{[2]}^{osf}(q_1q_2) = \begin{array}{|c|c|} \hline \square & \square \\ \hline \end{array}. \quad (\text{A.3})$$

For the  $q^2$  configuration, the total wave function may be written in the general form,

$$\psi = \psi_{[2]}^c \psi_{[11]}^{osf}, \quad \psi = \psi_{[11]}^c \psi_{[2]}^{osf}. \quad (\text{A.4})$$

Since the spatial wave function is symmetric  $\psi_{[2]}^o$ , all the possible color-spatial-spin-flavor configurations of the  $q_1q_2$  cluster for  $\psi_{[2]}^c \psi_{[11]}^{osf}$  are listed as follows:

$$\psi_{[2]}^c \psi_{[2]}^o \psi_{[11]}^s \psi_{[2]}^f, \quad \psi_{[2]}^c \psi_{[2]}^o \psi_{[2]}^s \psi_{[11]}^f, \quad (\text{A.5})$$

and for  $\psi_{[11]}^c \psi_{[2]}^{osf}$ :

$$\psi_{[11]}^c \psi_{[2]}^o \psi_{[11]}^s \psi_{[11]}^f, \quad \psi_{[11]}^c \psi_{[2]}^o \psi_{[2]}^s \psi_{[2]}^f. \quad (\text{A.6})$$

For  $cc\bar{c}\bar{c}$  tetraquarks, the flavor wave functions for  $cc$  and  $\bar{c}\bar{c}$  must be symmetric  $\psi_{[2]}^f$ . Thus, the possible color-spatial-spin-flavor configurations of the  $cc$  cluster are  $\psi_{[2]}^c \psi_{[2]}^o \psi_{[11]}^s \psi_{[2]}^f$  for  $\psi_{[2]}^c \psi_{[11]}^{osf}$ , and  $\psi_{[11]}^c \psi_{[2]}^o \psi_{[2]}^s \psi_{[2]}^f$  for  $\psi_{[11]}^c \psi_{[2]}^{osf}$ .

## APPENDIX B

### COLOR-SPIN WAVE FUNCTIONS

For  $q^2$  system, according to Young tableaux of symmetric (S), and anti-symmetric (A) types, the projection operators of  $\begin{array}{|c|} \hline \square \\ \hline \end{array}$ , and  $\begin{array}{|c|c|} \hline \square & \square \\ \hline \end{array}$  are as follows:

$$\begin{aligned} P_{[2]_S} &= 1 + (12), \\ P_{[11]_A} &= 1 - (12). \end{aligned} \tag{B.1}$$

$q^2$  color wave functions can be derived by applying the symmetric (S), and anti-symmetric (A) type projection operators of the  $S_2$   $IR[2]$  and  $IR[11]$  in Yamanouchi basis respectively,

$$\begin{aligned} |\begin{array}{|c|} \hline \underline{12} \\ \hline \end{array}, \underline{RR}\rangle &= P_{[2]_S}(RR) \implies \psi_{[2]_S}^c(RR) : RR, \\ |\begin{array}{|c|} \hline \underline{12} \\ \hline \end{array}, \underline{GG}\rangle &= P_{[2]_S}(GG) \implies \psi_{[2]_S}^c(GG) : GG, \\ |\begin{array}{|c|} \hline \underline{12} \\ \hline \end{array}, \underline{BB}\rangle &= P_{[2]_S}(BB) \implies \psi_{[2]_S}^c(BB) : BB, \\ |\begin{array}{|c|} \hline \underline{12} \\ \hline \end{array}, \underline{RG}\rangle &= P_{[2]_S}(RG) \implies \psi_{[2]_S}^c(RG) : \frac{1}{\sqrt{2}}(RG + GR), \\ |\begin{array}{|c|} \hline \underline{12} \\ \hline \end{array}, \underline{GB}\rangle &= P_{[2]_S}(GB) \implies \psi_{[2]_S}^c(GB) : \frac{1}{\sqrt{2}}(GB + BG), \\ |\begin{array}{|c|} \hline \underline{12} \\ \hline \end{array}, \underline{BR}\rangle &= P_{[2]_S}(BR) \implies \psi_{[2]_S}^c(BR) : \frac{1}{\sqrt{2}}(BR + RB), \\ |\begin{array}{|c|} \hline \underline{1} \\ \hline \underline{2} \end{array}, \begin{array}{|c|} \hline \underline{R} \\ \hline \underline{G} \end{array}\rangle &= P_{[11]_A}(RG) \implies \psi_{[11]_A}^c(RG) : \frac{1}{\sqrt{2}}(RG - GR), \\ |\begin{array}{|c|} \hline \underline{1} \\ \hline \underline{2} \end{array}, \begin{array}{|c|} \hline \underline{G} \\ \hline \underline{B} \end{array}\rangle &= P_{[11]_A}(GB) \implies \psi_{[11]_A}^c(GB) : \frac{1}{\sqrt{2}}(GB - BG), \\ |\begin{array}{|c|} \hline \underline{1} \\ \hline \underline{2} \end{array}, \begin{array}{|c|} \hline \underline{B} \\ \hline \underline{R} \end{array}\rangle &= P_{[11]_A}(BR) \implies \psi_{[11]_A}^c(BR) : \frac{1}{\sqrt{2}}(BR - RB). \end{aligned}$$

$\bar{q}^2$  color wave functions take same form with  $q^2$  color wave functions,

$$\psi_{[22]}^c(\bar{R}\bar{R}) : \bar{R}\bar{R},$$

$$\psi_{[22]}^c(\bar{G}\bar{G}) : \bar{G}\bar{G},$$

$$\psi_{[22]}^c(\bar{B}\bar{B}) : \bar{B}\bar{B},$$

$$\psi_{[22]}^c(\bar{R}\bar{G}) : \frac{1}{\sqrt{2}}(\bar{R}\bar{G} + \bar{G}\bar{R}),$$

$$\psi_{[22]}^c(\bar{G}\bar{B}) : \frac{1}{\sqrt{2}}(\bar{G}\bar{B} + \bar{B}\bar{G}),$$

$$\psi_{[22]}^c(\bar{B}\bar{R}) : \frac{1}{\sqrt{2}}(\bar{B}\bar{R} + \bar{R}\bar{B}),$$

$$\psi_{[211]}^c(\bar{R}\bar{G}) : \frac{1}{\sqrt{2}}(\bar{R}\bar{G} - \bar{G}\bar{R}),$$

$$\psi_{[211]}^c(\bar{G}\bar{B}) : \frac{1}{\sqrt{2}}(\bar{G}\bar{B} - \bar{B}\bar{G}),$$

$$\psi_{[211]}^c(\bar{B}\bar{R}) : \frac{1}{\sqrt{2}}(\bar{B}\bar{R} - \bar{R}\bar{B}).$$

The singlet color wave functions  $\psi_{[2]_6^c[22]_6^c}$  and  $\psi_{[11]_3^c[211]_3^c}$  of tetraquarks are given by:

$$\psi_{[2]_6^c[22]_6^c}^{q_1 q_2 \bar{q}_3 \bar{q}_4} = \frac{1}{\sqrt{6}} \sum_{i=1}^6 \psi_{[2]_6^c}^{q_1 q_2} \psi_{[22]_6^c}^{\bar{q}_3 \bar{q}_4},$$

$$\psi_{[11]_3^c[211]_3^c}^{q_1 q_2 \bar{q}_3 \bar{q}_4} = \frac{1}{\sqrt{3}} \sum_{i=1}^3 \psi_{[11]_3^c}^{q_1 q_2} \psi_{[211]_3^c}^{\bar{q}_3 \bar{q}_4}.$$

The explicit color wave functions are listed as follows, and the terms without subscripts are using the quark order  $q_1 q_2 \bar{q}_3 \bar{q}_4$ :

$$\psi_{[2]_6^c[22]_6^c}^{q_1 q_2 \bar{q}_3 \bar{q}_4} = \frac{1}{\sqrt{6}} [R_1 R_2 \bar{R}_3 \bar{R}_4 + G_1 G_2 \bar{G}_3 \bar{G}_4 + B_1 B_2 \bar{B}_3 \bar{B}_4$$

$$\begin{aligned}
& +\frac{1}{2}(R_1G_2 + G_1R_2)(\bar{R}_3\bar{G}_4 + \bar{G}_3\bar{R}_4) \\
& +\frac{1}{2}(B_1R_2 + R_1B_2)(\bar{B}_3\bar{R}_4 + \bar{R}_3\bar{B}_4) \\
& +\frac{1}{2}(G_1B_2 + B_1G_2)(\bar{G}_3\bar{B}_4 + \bar{B}_3\bar{G}_4)] \\
= & \frac{1}{\sqrt{6}}[RR\bar{R}\bar{R} + GG\bar{G}\bar{G} + BB\bar{B}\bar{B} \\
& +\frac{1}{2}(RG\bar{R}\bar{G} + GR\bar{R}\bar{G} + RG\bar{G}\bar{R} + GR\bar{G}\bar{R}) \\
& +\frac{1}{2}(BR\bar{B}\bar{R} + RB\bar{B}\bar{R} + BR\bar{R}\bar{B} + RB\bar{R}\bar{B}) \\
& +\frac{1}{2}(GB\bar{G}\bar{B} + BG\bar{G}\bar{B} + GB\bar{B}\bar{G} + BG\bar{B}\bar{G})], \\
\psi_{[11]_3^c [211]_3^c}^{q_1q_2\bar{q}_3\bar{q}_4} = & \frac{1}{\sqrt{3}}\left[\frac{1}{2}(R_1G_2 - G_1R_2)(\bar{R}_3\bar{G}_4 - \bar{G}_3\bar{R}_4) \right. \\
& +\frac{1}{2}(B_1R_2 - R_1B_2)(\bar{B}_3\bar{R}_4 - \bar{R}_3\bar{B}_4) \\
& \left. +\frac{1}{2}(G_1B_2 - B_1G_2)(\bar{G}_3\bar{B}_4 - \bar{B}_3\bar{G}_4)\right] \\
= & \frac{1}{\sqrt{3}}\left[\frac{1}{2}(RG\bar{R}\bar{G} - GR\bar{R}\bar{G} - RG\bar{G}\bar{R} + GR\bar{G}\bar{R}) \right. \\
& +\frac{1}{2}(BR\bar{B}\bar{R} - RB\bar{B}\bar{R} - BR\bar{R}\bar{B} + RB\bar{R}\bar{B}) \\
& \left. +\frac{1}{2}(GB\bar{G}\bar{B} - BG\bar{G}\bar{B} - GB\bar{B}\bar{G} + BG\bar{B}\bar{G})\right].
\end{aligned}$$

The possible spin combinations are  $[\psi_{[s=1]}^{q_1q_2} \otimes \psi_{[s=1]}^{\bar{q}_3\bar{q}_4}]_{S=0,1,2}$ ,  $\psi_{[s=1]}^{q_1q_2} \otimes \psi_{[s=0]}^{\bar{q}_3\bar{q}_4}$ ,

$\psi_{[s=0]}^{q_1 q_2} \otimes \psi_{[s=1]}^{\bar{q}_3 \bar{q}_4}$ , and  $\psi_{[s=0]}^{q_1 q_2} \otimes \psi_{[s=0]}^{\bar{q}_3 \bar{q}_4}$  for charmonium-like ( $qc\bar{q}\bar{c}$ ) and light ( $qq\bar{q}\bar{q}$ ) tetraquark states. For fully-charm ( $cc\bar{c}\bar{c}$ ) tetraquark states, the possible spin combinations are  $\left[ \psi_{[s=1]}^{q_1 q_2} \otimes \psi_{[s=1]}^{\bar{q}_3 \bar{q}_4} \right]_{S=0,1,2}$  for  $\psi_{[11]_3[211]_3}^c$  color configuration, and  $\psi_{[s=0]}^{q_1 q_2} \otimes \psi_{[s=0]}^{\bar{q}_3 \bar{q}_4}$  for  $\psi_{[2]_6[22]_6}^c$  color configuration while the possible color-spatial-spin-flavor configurations of the  $cc$  cluster are  $\psi_{[2]}^c \psi_{[2]}^o \psi_{[11]}^s \psi_{[2]}^f$  for  $\psi_{[2]}^c \psi_{[11]}^{osf}$ , and  $\psi_{[11]}^c \psi_{[2]}^o \psi_{[2]}^s \psi_{[2]}^f$  for  $\psi_{[11]}^c \psi_{[2]}^{osf}$ .

The spin of tetraquark state is the coupling of the  $q^2$  and  $\bar{q}^2$  spin with corresponding Clebsch-Gordan coefficients. The tetraquark spin wave functions  $\psi^S(S, S_z)$  with the symmetry [2] of  $q^2$  and [2] of  $\bar{q}^2$  are formed as follows for the spin combination  $\left[ \psi_{[s=1]}^{q_1 q_2} \otimes \psi_{[s=1]}^{\bar{q}_3 \bar{q}_4} \right]_{S=0,1,2}$ :

$$\begin{aligned} \psi^S(2, 2) &= P_{[2]_S} | \uparrow\uparrow \rangle P_{[2]_S} | \bar{\uparrow}\bar{\uparrow} \rangle, \\ \psi^S(2, 1) &= \sqrt{\frac{1}{2}} P_{[2]_S} | \uparrow\uparrow \rangle P_{[2]_S} | \bar{\uparrow}\bar{\downarrow} \rangle + \sqrt{\frac{1}{2}} P_{[2]_S} | \uparrow\downarrow \rangle P_{[2]_S} | \bar{\uparrow}\bar{\uparrow} \rangle, \\ \psi^S(2, 0) &= \sqrt{\frac{1}{6}} P_{[2]_S} | \uparrow\uparrow \rangle P_{[2]_S} | \bar{\downarrow}\bar{\downarrow} \rangle + \sqrt{\frac{2}{3}} P_{[2]_S} | \uparrow\downarrow \rangle P_{[2]_S} | \bar{\uparrow}\bar{\downarrow} \rangle \\ &\quad + \sqrt{\frac{1}{6}} P_{[2]_S} | \downarrow\downarrow \rangle P_{[2]_S} | \bar{\uparrow}\bar{\uparrow} \rangle, \\ \psi^S(2, -1) &= \sqrt{\frac{1}{2}} P_{[2]_S} | \uparrow\downarrow \rangle P_{[2]_S} | \bar{\downarrow}\bar{\downarrow} \rangle + \sqrt{\frac{1}{2}} P_{[2]_S} | \downarrow\downarrow \rangle P_{[2]_S} | \bar{\uparrow}\bar{\downarrow} \rangle, \\ \psi^S(2, -2) &= P_{[2]_S} | \downarrow\downarrow \rangle P_{[2]_S} | \bar{\downarrow}\bar{\downarrow} \rangle, \\ \psi^S(1, 1) &= \sqrt{\frac{1}{2}} P_{[2]_S} | \uparrow\uparrow \rangle P_{[2]_S} | \bar{\uparrow}\bar{\downarrow} \rangle - \sqrt{\frac{1}{2}} P_{[2]_S} | \uparrow\downarrow \rangle P_{[2]_S} | \bar{\uparrow}\bar{\uparrow} \rangle, \\ \psi^S(1, 0) &= \sqrt{\frac{1}{2}} P_{[2]_S} | \uparrow\uparrow \rangle P_{[2]_S} | \bar{\downarrow}\bar{\downarrow} \rangle - \sqrt{\frac{1}{2}} P_{[2]_S} | \downarrow\downarrow \rangle P_{[2]_S} | \bar{\uparrow}\bar{\uparrow} \rangle, \\ \psi^S(1, -1) &= \sqrt{\frac{1}{2}} P_{[2]_S} | \uparrow\downarrow \rangle P_{[2]_S} | \bar{\downarrow}\bar{\downarrow} \rangle - \sqrt{\frac{1}{2}} P_{[2]_S} | \downarrow\downarrow \rangle P_{[2]_S} | \bar{\uparrow}\bar{\downarrow} \rangle, \\ \psi^S(0, 0) &= \sqrt{\frac{1}{3}} P_{[2]_S} | \uparrow\uparrow \rangle P_{[2]_S} | \bar{\downarrow}\bar{\downarrow} \rangle - \sqrt{\frac{1}{3}} P_{[2]_S} | \uparrow\downarrow \rangle P_{[2]_S} | \bar{\uparrow}\bar{\downarrow} \rangle \end{aligned}$$

$$+\sqrt{\frac{1}{3}}P_{[2]_S|\downarrow\downarrow}\rangle P_{[2]_S|\bar{\uparrow}\bar{\uparrow}}\rangle.$$

The all explicit spin wave functions  $\psi^S(S, S_z)$  of  $[\psi_{[s=1]}^{q_1q_2} \otimes \psi_{[s=1]}^{\bar{q}_3\bar{q}_4}]_{S=0,1,2}$  tetraquark states are listed as follows:

$$\begin{aligned}\psi^S(2, 2) &= \uparrow\uparrow\bar{\uparrow}\bar{\uparrow}, \\ \psi^S(2, 1) &= \frac{1}{2}(\uparrow\uparrow\bar{\uparrow}\bar{\downarrow} + \uparrow\uparrow\bar{\downarrow}\bar{\uparrow} + \uparrow\downarrow\bar{\uparrow}\bar{\uparrow} + \downarrow\uparrow\bar{\uparrow}\bar{\uparrow}), \\ \psi^S(2, 0) &= \frac{1}{\sqrt{6}}(\uparrow\uparrow\bar{\downarrow}\bar{\downarrow} + \downarrow\downarrow\bar{\uparrow}\bar{\uparrow} + \uparrow\downarrow\bar{\uparrow}\bar{\downarrow} + \uparrow\downarrow\bar{\downarrow}\bar{\uparrow} + \downarrow\uparrow\bar{\uparrow}\bar{\downarrow} + \downarrow\uparrow\bar{\downarrow}\bar{\uparrow}), \\ \psi^S(2, -1) &= \frac{1}{2}(\uparrow\downarrow\bar{\downarrow}\bar{\downarrow} + \downarrow\uparrow\bar{\downarrow}\bar{\downarrow} + \downarrow\downarrow\bar{\uparrow}\bar{\downarrow} + \downarrow\downarrow\bar{\downarrow}\bar{\uparrow}), \\ \psi^S(2, -2) &= \downarrow\downarrow\bar{\downarrow}\bar{\downarrow}, \\ \psi^S(1, 1) &= \frac{1}{2}(\uparrow\uparrow\bar{\uparrow}\bar{\downarrow} + \uparrow\uparrow\bar{\downarrow}\bar{\uparrow} - \uparrow\downarrow\bar{\uparrow}\bar{\uparrow} - \downarrow\uparrow\bar{\uparrow}\bar{\uparrow}), \\ \psi^S(1, 0) &= \frac{1}{\sqrt{2}}(\uparrow\uparrow\bar{\downarrow}\bar{\downarrow} - \downarrow\downarrow\bar{\uparrow}\bar{\uparrow}), \\ \psi^S(1, -1) &= \frac{1}{2}(\uparrow\downarrow\bar{\downarrow}\bar{\downarrow} + \downarrow\uparrow\bar{\downarrow}\bar{\downarrow} - \downarrow\downarrow\bar{\uparrow}\bar{\downarrow} - \downarrow\downarrow\bar{\downarrow}\bar{\uparrow}), \\ \psi^S(0, 0) &= \frac{1}{\sqrt{3}}[\uparrow\uparrow\bar{\downarrow}\bar{\downarrow} - \frac{1}{2}(\uparrow\downarrow\bar{\uparrow}\bar{\uparrow} + \uparrow\downarrow\bar{\downarrow}\bar{\uparrow} + \downarrow\uparrow\bar{\uparrow}\bar{\downarrow} + \downarrow\uparrow\bar{\downarrow}\bar{\uparrow}) + \downarrow\downarrow\bar{\uparrow}\bar{\uparrow}].\end{aligned}$$

The tetraquark states of a certain spin and the same  $q^2$  and  $\bar{q}^2$  spins but different spin projection  $m_s$  have the same expectation values. In this work all the spins take the maximum spin projections. The spin combinations  $\psi_{[s=1]}^{q_1q_2} \otimes \psi_{[s=0]}^{\bar{q}_3\bar{q}_4}$  and  $\psi_{[s=0]}^{q_1q_2} \otimes \psi_{[s=1]}^{\bar{q}_3\bar{q}_4}$  give same expectation values. In this work, only  $\psi_{[s=1]}^{q_1q_2} \otimes \psi_{[s=0]}^{\bar{q}_3\bar{q}_4}$  is taken.

The explicit spin wave functions  $\psi_{(S(q_1q_2) \otimes S(\bar{q}_3\bar{q}_4))}^{S(q_1q_2\bar{q}_3\bar{q}_4)}$  of tetraquark states are

listed as follows:

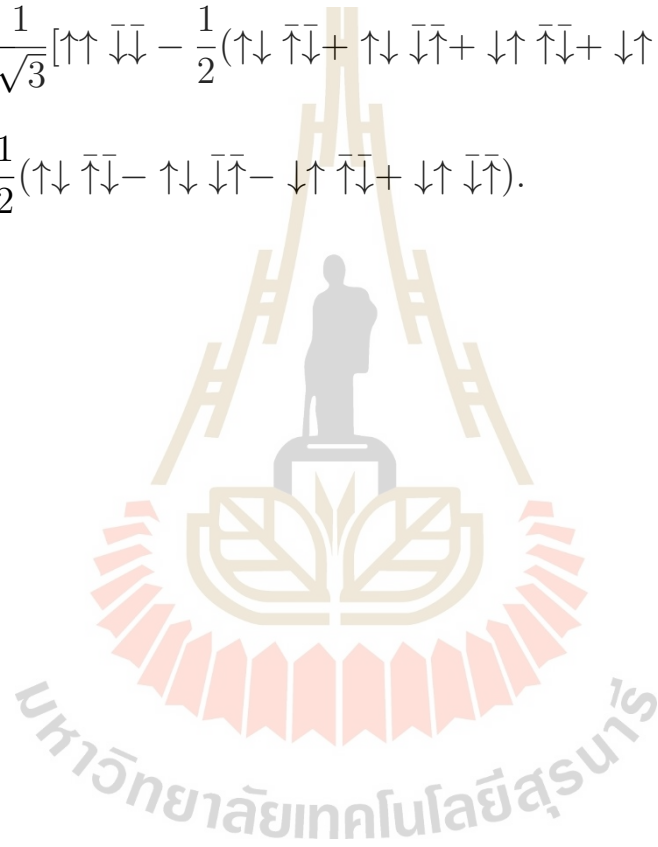
$$\psi_{(1\otimes 1)}^{S=2} = \uparrow\uparrow \bar{\uparrow}\bar{\uparrow},$$

$$\psi_{(1\otimes 1)}^{S=1} = \frac{1}{2}(\uparrow\uparrow \bar{\uparrow}\bar{\downarrow} + \uparrow\uparrow \bar{\downarrow}\bar{\uparrow} - \uparrow\downarrow \bar{\uparrow}\bar{\uparrow} - \downarrow\uparrow \bar{\uparrow}\bar{\uparrow}),$$

$$\psi_{(1\otimes 0)}^{S=1} = \frac{1}{\sqrt{2}}(\uparrow\uparrow \bar{\uparrow}\bar{\downarrow} - \uparrow\uparrow \bar{\downarrow}\bar{\uparrow}), \quad (\text{B.2})$$

$$\psi_{(1\otimes 1)}^{S=0} = \frac{1}{\sqrt{3}}[\uparrow\uparrow \bar{\downarrow}\bar{\downarrow} - \frac{1}{2}(\uparrow\downarrow \bar{\uparrow}\bar{\downarrow} + \uparrow\downarrow \bar{\downarrow}\bar{\uparrow} + \downarrow\uparrow \bar{\uparrow}\bar{\downarrow} + \downarrow\uparrow \bar{\downarrow}\bar{\uparrow}) + \downarrow\downarrow \bar{\uparrow}\bar{\uparrow}],$$

$$\psi_{(0\otimes 0)}^{S=0} = \frac{1}{2}(\uparrow\downarrow \bar{\uparrow}\bar{\downarrow} - \uparrow\downarrow \bar{\downarrow}\bar{\uparrow} - \downarrow\uparrow \bar{\uparrow}\bar{\downarrow} + \downarrow\uparrow \bar{\downarrow}\bar{\uparrow}).$$



## APPENDIX C

### SPATIAL WAVE FUNCTION

In this appendix the spatial wave function of tetraquark in the harmonic oscillator basis are displayed, and the total spatial wave function of tetraquark may be expanded in the complete basis formed by the function,

$$\begin{aligned} \psi_{NL} = & \sum_{\{n_i, l_i\}} A(n_1, n_2, n_3, l_1, l_2, l_3) \\ & \times \psi_{n_1 l_1}(\vec{x}_1) \otimes \psi_{n_2 l_2}(\vec{x}_2) \otimes \psi_{n_3 l_3}(\vec{x}_3) \end{aligned} \quad (\text{C.1})$$

where  $\psi_{n_i l_i}$  are harmonic oscillator wave functions and the sum  $\{n_i, l_i\}$  is over  $n_1, n_2, n_3, l_1, l_2, l_3$ .  $N$  and  $L$  are the total principle quantum number and orbital angular momentum number of the tetraquark respectively. One has  $N = (2n_1 + l_1) + (2n_2 + l_2) + (2n_3 + l_3)$ . We employ the spatial wave functions  $\psi_{NL}$  as complete bases to study tetraquark states with other interactions. The spatial wave functions  $\psi_{NL}$  are employed as complete bases to study tetraquark states, and the bases size is  $N = 14$  in the calculation. The best eigenvalue is from adjusting the length parameter of harmonic oscillator wave functions.

The complete bases of the tetraquarks are listed in Table C.1, up to  $N = 14$ , where  $l_1, l_2$ , and  $l_3$  are limited to 0 only.

**Table C.1** The complete bases of tetraquark with  $N = 2n$ ,  $L = 0$ , and  $N \leq 14$ .

$\psi_{NL}$	$\psi_{n_1, l_1}(\vec{x}_1) \psi_{n_2, l_2}(\vec{x}_2) \psi_{n_3, l_3}(\vec{x}_3)$
$\psi_{00}$	$\psi_{0,0}(\vec{x}_1) \psi_{0,0}(\vec{x}_2) \psi_{0,0}(\vec{x}_3)$ .
$\psi_{20}$	$\psi_{1,0}(\vec{x}_1) \psi_{0,0}(\vec{x}_2) \psi_{0,0}(\vec{x}_3), \psi_{0,0}(\vec{x}_1) \psi_{1,0}(\vec{x}_2) \psi_{0,0}(\vec{x}_3), \psi_{0,0}(\vec{x}_1) \psi_{0,0}(\vec{x}_2) \psi_{1,0}(\vec{x}_3)$ .
$\psi_{40}$	$\psi_{2,0}(\vec{x}_1) \psi_{0,0}(\vec{x}_2) \psi_{0,0}(\vec{x}_3), \psi_{0,0}(\vec{x}_1) \psi_{2,0}(\vec{x}_2) \psi_{0,0}(\vec{x}_3), \psi_{0,0}(\vec{x}_1) \psi_{0,0}(\vec{x}_2) \psi_{2,0}(\vec{x}_3),$ $\psi_{1,0}(\vec{x}_1) \psi_{1,0}(\vec{x}_2) \psi_{0,0}(\vec{x}_3), \psi_{1,0}(\vec{x}_1) \psi_{0,0}(\vec{x}_2) \psi_{1,0}(\vec{x}_3), \psi_{0,0}(\vec{x}_1) \psi_{1,0}(\vec{x}_2) \psi_{1,0}(\vec{x}_3)$ .
$\psi_{60}$	$\psi_{3,0}(\vec{x}_1) \psi_{0,0}(\vec{x}_2) \psi_{0,0}(\vec{x}_3), \psi_{2,0}(\vec{x}_1) \psi_{1,0}(\vec{x}_2) \psi_{0,0}(\vec{x}_3), \psi_{2,0}(\vec{x}_1) \psi_{0,0}(\vec{x}_2) \psi_{1,0}(\vec{x}_3),$ $\psi_{1,0}(\vec{x}_1) \psi_{2,0}(\vec{x}_2) \psi_{0,0}(\vec{x}_3), \psi_{1,0}(\vec{x}_1) \psi_{0,0}(\vec{x}_2) \psi_{2,0}(\vec{x}_3), \psi_{0,0}(\vec{x}_1) \psi_{3,0}(\vec{x}_2) \psi_{0,0}(\vec{x}_3),$ $\psi_{0,0}(\vec{x}_1) \psi_{2,0}(\vec{x}_2) \psi_{1,0}(\vec{x}_3), \psi_{0,0}(\vec{x}_1) \psi_{1,0}(\vec{x}_2) \psi_{2,0}(\vec{x}_3), \psi_{0,0}(\vec{x}_1) \psi_{0,0}(\vec{x}_2) \psi_{3,0}(\vec{x}_3),$ $\psi_{1,0}(\vec{x}_1) \psi_{1,0}(\vec{x}_2) \psi_{1,0}(\vec{x}_3)$ .
$\psi_{80}$	$\psi_{4,0}(\vec{x}_1) \psi_{0,0}(\vec{x}_2) \psi_{0,0}(\vec{x}_3), \psi_{3,0}(\vec{x}_1) \psi_{1,0}(\vec{x}_2) \psi_{0,0}(\vec{x}_3), \psi_{3,0}(\vec{x}_1) \psi_{0,0}(\vec{x}_2) \psi_{1,0}(\vec{x}_3),$



Table C.1 (Continued)

$\psi_{NL}$	$\psi_{n_1, l_1}(\vec{x}_1) \psi_{n_2, l_2}(\vec{x}_2) \psi_{n_3, l_3}(\vec{x}_3)$
	$\psi_{0,0}(\vec{x}_1) \psi_{2,0}(\vec{x}_2) \psi_{5,0}(\vec{x}_3), \psi_{0,0}(\vec{x}_1) \psi_{1,0}(\vec{x}_2) \psi_{6,0}(\vec{x}_3), \psi_{0,0}(\vec{x}_1) \psi_{0,0}(\vec{x}_2) \psi_{7,0}(\vec{x}_3).$



## CURRICULUM VITAE

**NAME:** Zheng Zhao      **GENDER:** Male  
**NATIONALITY:** Chinese      **DATE OF BIRTH:** Oct 22, 1993

### EDUCATIONS:

- B. Sc. School of Applied Physics, Institute of Science, Minzu University of China, China, 2015.

### PUBLICATIONS

- [1] Z. Zhao, K. Xu, A. Kaewsnod, X. Y. Liu, A. Limphirat, and Y. Yan, “**Study of light tetraquark spectroscopy**”, Phys. Rev. D105 (2022), 036001.
- [2] Z. Zhao, K. Xu, A. Kaewsnod, X. Y. Liu, A. Limphirat, and Y. Yan, “**Study of charmoniumlike and fully-charm tetraquark spectroscopy**”, Phys. Rev. D103 (2021), 116027.
- [3] Z. Zhao, K. Xu, A. Kaewsnod, X. Y. Liu, A. Limphirat, and Y. Yan, “**Determination of Parameters of a Potential Model for Tetraquark Study by Studying All S-Wave Mesons**”, Few Body Syst. 62 (2021) 4, 80.
- [4] A. Kaewsnod, K. Xu, Z. Zhao, X. Y. Liu, S. Srisuphaphon, A. Limphirat, and Y. Yan, “**Study of N(1440) structure via  $\gamma^*p \rightarrow N(1440)$  transition**”, Phys. Rev. D105 (2022), 016008.
- [5] K. Xu, A. Kaewsnod, Z. Zhao, X. Y. Liu, S. Srisuphaphon, A. Limphirat, and Y. Yan, “**Pentaquark components in low-lying baryon resonances**”, Phys. Rev. D101 (2020), 076025.